

Abstract

The recent DSM5 and ICD-11 diagnostic manuals include provisional grief disorders, yet mechanisms of complicated grief are still debated. Effective coping with bereavement requires flexible oscillation between mental states, thus perseverative internally-oriented thought processes may interfere with successful integration of loss into ongoing life. However, frequency of these mental shifts and how they occur in the brain is unknown. I test the idea that grief adaptation may be related to large-scale brain network configuration during unconstrained thought, using resting state fMRI and an intranasal oxytocin manipulation. Older widowed adults ($n = 40$) with and without complicated grief participated in two resting state fMRI sessions (oxytocin; placebo) as part of a larger within-subjects crossover study. Group spatial ICA identified resting state functional networks. I examined both static and dynamic functional connectivity between network pairs implicated in my theoretical model. Static functional connectivity between core midline default and cingulo-opercular network components predicted complicated grief symptom scores, controlling for age, sex, and depressive symptoms. Oxytocin increased static connectivity between retrosplenial default network and cingulo-opercular network components for the sample as a whole, but did not differentially impact participants based on complicated grief symptoms. Dynamic functional connectivity analyses identified four cluster centroids (or dynamic “states”) that represent time-varying changes in connections between selected network components. The grief severity x state interaction revealed that participants with higher grief severity spent more time in a dynamic state featuring large positive fluctuations in retrosplenial default network connectivity with right frontoparietal, cingulo-opercular, and midline core default components, indicating that higher-grief participants spent more time in a state characterized by lower network modularity. Grief severity did not predict total number of states or state transitions. Results provide preliminary evidence that in older adults, complicated grief is related to different patterns of static and dynamic functional brain connectivity during periods of unconstrained

38 thought.

39 *Keywords:* complicated grief, bereavement, resting state, functional connectivity,

40 fMRI, oxytocin

41	Contents	
42	Acknowledgements	7
43	Introduction	9
44	Background	9
45	How does complicated grief get “complicated”?	10
46	Attachment	10
47	Maladaptive appraisals	11
48	Past, future, and self	13
49	Dynamics of coping with bereavement	14
50	A network perspective on grief and the brain	15
51	Adding the time dimension: modeling dynamics	18
52	Dynamic functional connectivity	21
53	Application to complicated grief	23
54	Oxytocin	23
55	Effects on attachment behavior	23
56	Effects on constraints over internal thought?	25
57	Effects on functional brain network connectivity	26
58	Specific aims and hypotheses	29
59	Aim 1. To identify whether static and/or dynamic resting state functional	
60	connectivity (FNC/dFNC) differs among widowed older adults who	
61	are adjusting well versus those who are adjusting poorly (i.e., compli-	
62	cated grief).	29
63	Aim 2. To investigate if/how intranasal oxytocin alters static and/or dy-	
64	namic functional network connectivity (FNC/dFNC) in older adults,	
65	and whether effects of oxytocin are moderated by complicated grief	
66	symptoms.	29

67	Method	30
68	Participants	30
69	Design and Procedures	31
70	Resting State	33
71	Materials	33
72	Intranasal spray (oxytocin/placebo)	33
73	Measures	34
74	MRI Data Acquisition and Management	35
75	MRI Data Preprocessing and Analysis	35
76	Quality control	35
77	Preprocessing	36
78	fMRI Analysis	39
79	Results	44
80	Participant characteristics	44
81	Group ICA	46
82	Static FNC	50
83	Effects of oxytocin	52
84	Dynamic FNC	56
85	Effects of oxytocin	57
86	Dwell time	59
87	Number of state transitions	60
88	Discussion	62
89	Summary	62
90	Resting state static and dynamic functional connectivity measures are asso-	
91	ciated with complicated grief symptom severity.	62

92	Complicated grief severity does not influence resting state functional connec-	
93	tivity response to intranasal oxytocin.	63
94	Implications	65
95	Limitations	67
96	Future directions	70
97	Conclusion	73
98	R packages/versions used	74
99	References	75

Acknowledgements

This dissertation reflects the magnitude of support that I have been privileged to receive during my time at the University of Arizona.

Brian Arizmendi played a critical role in designing and executing the parent study in which the resting state data were acquired, and treated me as a genuine collaborator from my day one in the lab. Scott Squire was our intrepid MRI operator, whose generosity and patience with some of the finicky elements of the experiment was invaluable. Dianne Patterson and members of the UA Brain Mapping Workgroup were an important source of knowledge and encouragement. Opportunities to attend extramural trainings, including Neurohackademy, NYAS Science Alliance Leadership Training, and NIBL reproducible fMRI workshop, shaped my professional development and skills.

A special thanks to my dissertation committee Mary-Frances O'Connor, John JB Allen, Jessica Andrews-Hanna, and Elena Plante:

Mary-Frances O'Connor has been a true role model throughout my PhD journey, while encouraging me to draw my own map for a future as a researcher, clinician, mentor, and advocate. I am continually inspired by her scientific ideas, the ways in which her values and humanity inform her academic roles, and her commitment to growth and learning. I cannot imagine a better experience of graduate mentorship.

Even before I came to UA, John Allen's online psychophysiology videos were already making me a better clinical scientist. His mentorship over these past five years has only continued to underscore the importance of precision and deep understanding at all levels.

Jess Andrews-Hanna's work on spontaneous thought, mind-wandering, and brain networks was a major inspiration for my own program of research. Her expertise, thoughtfulness, and thoroughness always brought me back to the important question - *what actual brain process could this observation represent, and how is it meaningful for behavior?*

Elena Plante was instrumental in helping me navigate the world of NIH grantsmanship and develop the project aims. *“You’re an adult, manage your life as you see fit”* is excellent advice that all graduate students should receive.

In my personal life, my family, and in particular my parents, have been incredibly patient and supportive throughout my many different life directions before the PhD, and encouraged my curiosity about the world from the time I was born.

I cannot imagine the past five years without my amazing GLASS labmates and friends in the program – especially Atina Manvelian, Mairead McConnell, Da’Mere Wilson, Eva-Maria Stelzer, Lindsey Knowles, Roman Palitsky, and Deanna Kaplan – thankful for their empathy, guidance, and scientific and clinical acumen. They inspire me on a regular basis.

My friends in New York have also been a wonderful source of support, encouragement, and proper NY bagels. In particular, Mani García has so often been a “secure base”, always empowering me to explore new terrain literally (as I moved across the country), emotionally, and scientifically. *You’re good, you.*

Todd Wilson and the inclusive, welcoming dance community at Breakout Studios helped me find a sense of home in Tucson.

This dissertation is dedicated to all of the participants in this study. Thank you for sharing your personal lives and for your willingness to approach difficult emotions and memories in service of the science. Many of you talked about how you felt deeply personally invested in this line of research. I am so honored that we could be part of your story.

Introduction

Background

By the age of 65, one in four married adults in the United States will have experienced the death of their spouse (US Census Bureau, n.d.). For approximately one in ten bereaved people, the death of a loved one will bring about a chronically painful and disabling disorder known as “complicated grief”, with similar though non-identical grief-related syndromes termed persistent complex bereavement disorder (American Psychiatric Association, 2013) or prolonged grief disorder (Nicotera, Oliviero Rossi, Liveri, & Calandra, 2014). Analogous to, but distinct from post-traumatic stress disorder (e.g., Boelen, Van Den Bout, & De Keijser, 2003; Golden & Dalgleish, 2010; Prigerson & Jacobs, 1999; Williams, Hardt, Henschel, & Eddinger, 2019), complicated grief is considered a disorder of non-recovery: adaptation and healing are, for some reason, unable to proceed, and the bereaved person is unable to integrate the loss into their ongoing life. Complicated grief represents a public health concern given links with excess mortality and morbidity, as well as suicidality and functional impairment (Latham & Prigerson, 2004). Being an older adult is associated with greater risk for complicated grief, perhaps due to factors that often occur in the aging population and may be exacerbated by the death of a partner - such as lower income and more financial stress, or having a more limited social network (Kaplan & Berkman, 2018; Kersting, Brähler, Glaesmer, & Wagner, 2011; Lundorff, Holmgren, Zachariae, Farver-Vestergaard, & O’Connor, 2017; Xiu, Chow, & Tang, 2020; Yi et al., 2018).

Within the past few years, grief-related disorders have seen recognition by major diagnostic entities such as the DSM-5 (American Psychiatric Association, 2013) and ICD-11 (Nicotera et al., 2014). Despite ongoing debate regarding proposed diagnostic criteria (Maciejewski, Maercker, Boelen, & Prigerson, 2016; Prigerson & Maciejewski, 2017; Reynolds, Cozza, & Shear, 2017; Shear et al., 2011), criterion sets appear to agree that

maladaptive or distressing internal thought processes are important symptom. For example, an ICD-11 prolonged grief disorder diagnosis requires at least one of two category A criteria to be met 12 or more months after the death: “Persistent and pervasive preoccupation with the deceased and/or preoccupation with the circumstances of their death” and/or “Persistent and pervasive longing for the deceased”, in addition to “Intense emotional pain”. Yearning and rumination are typical during the acute grief period, but when they become persistent and pervasive, they likely impair a person’s capacity to cognitively, behaviorally, and emotionally integrate the irreparably altered relationship with the deceased (i.e., forming a “continuing bond”) and the fact of their death (Stroebe, Schut, & Boerner, 2010). Prominent inclusion of yearning and rumination in criterion sets reflects our current conceptualizations of disordered grief as involving interrelated motivational/attachment-related, memory, and cognitive-behavioral processes that interfere with adaptation (Boelen, Hout, & Bout, 2006; Eisma, Lang, & Boelen, 2020; Houwen, Stroebe, Schut, Stroebe, & Bout, 2010; Maccallum & Bryant, 2013; Mikulincer & Shaver, 2014; K. Shear & Shair, 2005).

How does complicated grief get “complicated”?

Attachment. Yearning is an “affectively-charged cognitive event” (Robinaugh, LeBlanc, Vuletich, & McNally, 2014), with the emotional impact of yearning the result of a frustrated approach response to an absent attachment figure (e.g., LeRoy, Knee, Derrick, & Fagundes, 2019, @OConnor2014b, @Shear2005a). The role of attachment in complicated grief is supported by one of the first grief fMRI studies, in which O’Connor et al. (2008) observed differential activation in the ventral striatum in bereaved individuals with complicated grief. Self-reported yearning correlated with nucleus accumbens activation, indicating that yearning in complicated grief is indeed a proximity-seeking response to separation distress. A prolonged proximity-seeking response, in a situation like death where the reunion can never be attained, suggests that people with complicated grief could

experience problems in “adaptive disengagement” – giving up on an unlikely or unfulfilling goal in order to adopt new goals e.g., (Carver & Scheier, 2000; Wrosch, Scheier, Miller, Schulz, & Carver, 2003). Although there is little specific research in goal disengagement and bereavement adaptation, people with an anxious attachment style appear have more difficulty with adaptive disengagement (Mikulincer & Shaver, 2014). Theories of self-regulation (Duval & Wicklund, 1972; (Carver & Scheier, 2000) and emotion regulation (Etkin, Büchel, & Gross, 2015) assert that negative affect arises from incongruence between a person’s desired state and their actual state or ability to progress towards the desired state – for example, separation distress and grief elicited by awareness of the discrepancy between the reality of the person’s death vs. one’s intense desire to have them here - underscoring the strong empirical link between distress and yearning in symptom-based network studies (Malgaroli, Maccallum, & Bonanno, 2018, @Robinaugh2014). People vary in how they respond to discrepancy-induced negative affect, but responses generally fall into three major categories: (1) renewed efforts to reduce the incongruence, (2) efforts to escape self-awareness, or (3) switching the goal to an objective that is more attainable (Carver & Scheier, 2000). None of these responses are inherently maladaptive – for example, (1) could involve efforts to develop continuing bonds with the deceased, and (2) could involve temporary distraction from distress in order to replenish one’s capacity to process grief. (3) could involve reorganizing the attachment hierarchy in order to get one’s attachment needs met despite the loss of the formerly primary attachment figure (LeRoy et al., 2019). However, when a response to grief like renewed proximity-seeking or escaping self-awareness is pursued in an inflexible manner, it could impair a person’s ability to cope effectively with grief.

Maladaptive appraisals. Maladaptive internal thought processes in complicated grief (Eisma et al., 2020, 2015; Liu, Taillefer, Tassone, & Vickers, 2019; Wenn, O’Connor, Breen, & Rees, 2019) may illustrate an ironic process in how motivational and cognitive-behavioral aspects of grief can interact to limit a person’s ability to adapt.

Yearning not only involves mental simulation of an anticipated reward (such as being reunited with the deceased loved one), but also highlights the discrepancy between one's current versus desired state (Boddez, 2018; Robinaugh et al., 2016). A person with complicated grief may try to downregulate their distress through avoidance, which can take the form of maladaptive rumination about the death (Eisma & Stroebe, 2017; Wenn et al., 2019). However, avoidance in fact reinforces the emotional salience of deceased-related cues over the long term, which prevents the person from habituating to cues and being able to integrate the loss (Robinaugh et al., 2014). Maladaptive grief-related rumination may involve dwelling on thoughts like “The only thing that can really help me is to have this person back”, “I need this person so much they should not have died”, “This death shouldn't have happened” (from the Typical Beliefs Questionnaire; (Skritskaya et al., 2017)) or “Since [-] is dead, I think I am worthless”, “The world is a bad place, since [-] died”, “I have to mourn otherwise I will forget [-]”, or “My life has no purpose anymore, since [-] died” (Grief Cognitions Questionnaire; (Boelen & Lensvelt-Mulders, 2005)). Bereaved adults with elevated grief symptoms also endorse positive metacognitive beliefs about the benefit of coping strategies that avoid the reality of the death (suppression, rituals) and positive metacognitive beliefs about repetitive negative thinking as helpful, but also negative metacognitive beliefs around grief reactions, such as the belief that repetitive negative thinking is harmful or will become uncontrollable (Wenn et al., 2019).

The interaction of emotion and cognition in grief adaptation are supported by recent network models, which highlight the association between emotional pain and perseverative/intrusive cognitions. Robinaugh et al. (2014) found that distress strongly predicted thoughts of the death (but not thoughts of the deceased) as well as avoidance at 18 months post-loss. Emotional pain also predicted yearning, and yearning in turn predicted thoughts of the deceased (but not the death). In a second study, emotional pain was strongly associated with yearning at three, 14, and 25 months post-loss (Margaroli et al., 2018). Notably, yearning was a strong predictor of preoccupation with the death at

only 14 and 25 months – timepoints at which someone would be eligible for diagnosis of a grief-related disorder – but not at three months, suggesting that yearning is only linked to rumination when yearning is highly distressing for a prolonged period of time. Both authors’ findings could support the idea that maladaptive post-event rumination tends to be intrusive and automatic, in contrast to more adaptive, intentional forms of rumination that focus on understanding and drawing meaning from one’s experience e.g., (Tedeschi & Calhoun, 2004).

Past, future, and self. In addition to yearning and maladaptive appraisals, people with complicated grief show differences in autobiographical memory, prospection, and sense of self. Identity disturbance is central to complicated grief symptom networks (Bellet, Jones, Neimeyer, & McNally, 2018; Malgaroli et al., 2018), and complicated grief severity is associated with reduced self-concept complexity (Bellet et al., 2020) and self-concept clarity (Boelen, Keijsers, & Van Den Hout, 2012). When people with complicated grief imagine the future or remember the past, autobiographical memories or imagined future scenarios appear to be more accessible and detailed when they involve the deceased (Boelen, Huntjens, Deursen, & Hout, 2010; Golden, Dalgleish, & Mackintosh, 2007; Maccallum & Bryant, 2010; MacCallum & Bryant, 2011; Robinaugh & McNally, 2013). The cognitive-attachment model (Maccallum & Bryant, 2013) attributes complicated grief to the persistence of a “merged identity” (the bereaved person and the deceased) that does not accomodate the reality of the loss. A predominance of deceased-related autobiographical memories limit the bereaved person’s ability to access other memories that could help them develop an identity that is no longer merged with the deceased. Both cognitive-attachment (Maccallum & Bryant, 2013) and cognitive-behavioral models (Boelen et al., 2006) emphasize that a major task in grief recovery is for the reality of the loss to become integrated into autobiographical memory. Similarly, the meaning-reconstruction model (Neimeyer, 2016) links distress to a self-narrative that is cannot be reconciled with the event of the death. These studies and

models provide further evidence that how people think about, remember, and imagine themselves and their lives can complicate grief adaptation if these processes are predominantly focused on the deceased and the loss and cannot accomodate the present.

Dynamics of coping with bereavement. Taken together, the research described above supports the idea that a person with complicated grief “gets stuck” in certain mental states that make it more difficult to adapt to their new reality. Considering perseverative thought may be important for efforts to understand the causes and consequences of complicated grief (Kaplan et al., 2019; (O’Connor & Sussman, 2014). For instance, the recognition of repetitive, self-focused, negatively-valenced cognition as a transdiagnostic factor e.g., rumination and worry in depression and anxiety disorders; (Ehring & Watkins, 2008; McEvoy, Moulds, & Mahoney, 2013; McLaughlin & Nolen-Hoeksema, 2011) has led to advances in prevention and treatment e.g., (Mennin & Fresco, 2013; Topper, Emmelkamp, & Ehring, 2010). As described in the previous section, integration of the death is thought to be impaired by perseverative and inflexible grief-related cognitions e.g., (Boelen et al., 2006; Freed, 2007; Houwen et al., 2010; O’Connor & Sussman, 2014; K. Shear & Shair, 2005). From this perspective, the dual process model of coping with bereavement (Schut, Margaret Stroebe, 1999; Stroebe et al., 2010) has been particularly influential on treatment approaches for complicated grief e.g., (K. Shear et al., 2005; Shear et al., 2014). The dual process model asserts that it is, at certain times, useful and adaptive to engage in processing the loss (i.e., focusing on the person, the reality of their death, and its meaning). At other times, individuals must attend to “restoration-oriented” stressors – the secondary stressors of bereavement that represent the task of learning how to live in a world where that important person is no longer present. The dual process model proposes a dynamic routine in which individuals who are coping effectively will, at certain times, confront - and other times, avoid - cognitions focused on loss and restoration stressors. Complicated grief exemplifies a breakdown in these dynamics. Some people who are having difficulty adapting are hypervigilant and go out of their way to avoid all reminders of the

deceased (avoidance of loss-oriented stressors). Others display the opposite pattern, in which their tendency to focus on loss-oriented stressors prevents them from restoring their life. The dual process model captures the clinical picture of complicated grief fairly well. However, the idea of coping with bereavement as an oscillatory process raises a few questions that have yet to be answered empirically: (1) What is the optimal time scale on which the loss-restoration, approach-avoidance oscillations should occur for adaptation to proceed, and relatedly, (2) Does the timescale over which the oscillations occur change over time – for example, between acute vs. later grief – as the need to focus on loss/restoration stressors themselves becomes less frequent, and (3) What is the best way to measure and test oscillatory dynamics of coping (Stroebe et al., 2010)?

A network perspective on grief and the brain

The focus on flexible dynamics of coping with bereavement in the dual process model, rather than linear progress through fixed “stages” of grief, parallels our growing empirical understanding of emotions, emotion regulation, and internal thought as dynamic properties of large-scale brain networks e.g., (Barrett & Satpute, 2013; Sporns, 2011, @Sripada2014) In particular, newer neuroimaging methods such as machine learning, graph-theory models, and dynamic or time-varying functional connectivity have helped us understand how emotion and cognition involve distributed neural systems through which information flows e.g., (Kragel & LaBar, 2016; Najafi, McMenamin, Simon, & Pessoa, 2016; Pessoa & McMenamin, 2017). In the context of grief, neuroimaging offers an avenue to test some of the outstanding questions about the dual process model, as well as generally furthering our understanding of how the grief experience differs in people who are adapting effectively vs. ineffectively. I propose that the tendency for internal thoughts to be intrusive and inflexible in people with complicated grief could be seen in how brain networks interact over time. For example, Schneck et al. (2018) found that bereaved adults with an avoidant grieving style show persistent monitoring for mental representations of the deceased, via a

network of frontotemporoparietal brain regions linked to selective attention to the deceased (identified via multivoxel pattern analysis). Yet avoidant griever reported more deceased-related intrusions during a sustained attention task, suggesting that engaging selective attention in attempt to suppress conscious awareness of deceased-related mental representations might unfortunately reinforce intrusions (Schneck et al., 2017). In contrast, expression of the neural pattern linked to mental representations of the deceased was associated with more adaptive coping when it occurred without conscious awareness (Schneck et al., 2018).

The studies by Schneck and colleagues suggest the relevance of spontaneous thought to grief, including complicated grief. A resting state study in grief found that bereaved parents overall showed decreased connectivity within the default network, and between default and executive control networks, with parents reporting higher avoidance coping tendencies exhibiting greater disruptions in connectivity between nodes (Liu et al., 2015). While most other grief neuroimaging studies have used passive-view or behavioral tasks, overall, results support the idea that interactions in large-scale brain networks may be altered in grief and vary with a person's adaptation or coping. Early neuroimaging studies found that deceased-related stimuli evoked responses in what are typically considered default network areas (posterior cingulate, precuneus, retrosplenial cortex, medial frontal gyrus) involved in autobiographical memory and self-referential processing, as well as salience network areas (dorsal and ventral anterior cingulate [dACC/vACC], anterior insula) typically involved in monitoring and coordinating responses to relevant stimuli (Gündel et al., 2003; (O'Connor et al., 2008). Freed and colleagues (2009) found intrusive thoughts were associated with greater ventral amygdala and rostral ACC reactivity in an emotional Stroop task, and reaction time bias (an index of selective attention) on the task was associated with greater dorsolateral prefrontal cortex (PFC), amygdala, and insula activation. This study involved acutely-bereaved pet owners, so they could not investigate complicated grief given the recency of the death (< three months). However, findings

suggest that even a short time after their loss, people who experience their thoughts as more intrusive and less controllable are more reactive and regulating the impact of attentional bias may be more cognitively demanding (Freed, Yanagihara, Hirsch, & Mann, 2009). Results of a mindfulness-based cognitive therapy intervention for bereaved adults 6-48 months post-loss could corroborate this interpretation. In their pre-post imaging data, decreased reaction time (less interference) on incongruent trials on a numerical Stroop task was associated with reduced frontoparietal network activation, while posterior cingulate and thalamus activation were associated with more intense grief and anxiety symptoms (Huang et al., 2019).

Together, neuroimaging findings in grief and complicated grief indicate the involvement of multiple, distributed brain regions belonging to various large-scale brain networks. Difficulty adapting to grief likely implicates interactions between/within networks, rather than isolated regions of dysfunction. The hypothesis on of network dysfunction in grief is consistent with the “triple network model of psychopathology” (Menon, 2011), and supported by recent large-scale meta-analytic evidence of common hypo- or hyper-connectivity among salience, default, and executive control networks in psychiatric disorders, with grey matter reductions in key network nodes potentially contributing to neurocognitive dysfunction (Sha, Wager, Mechelli, & He, 2019). The triple network model posits that dysfunctional organization of three major brain networks (default, salience, and central executive) and their interconnectivity explain how processes like self-referential thought, salience mapping, and cognitive control can go awry in psychiatric disorders. For example, major depressive disorder may involve overinvolvement of default and salience networks in the context of cognitive control deficits, resulting in difficulty disengaging from self-referential, negative, and emotionally evocative internal thought (Menon, 2011) as evidenced by hyperconnectivity within the default network but hypoconnectivity within the frontoparietal networks, between default and frontoparietal control networks, and between salience and frontoparietal networks (Kaiser,

Andrews-Hanna, Wager, & Pizzagalli, 2015). In generalized anxiety disorder, a condition characterized by persistent, intrusive, and excessive negative future-oriented thought, aberrant functional connectivity between salience and default network regions, coupled with greater compensatory frontoparietal engagement, is hypothesized to contribute to perseverative worry (Fonzo & Etkin, 2017).

Adding the time dimension: modeling dynamics

Using a network perspective is helpful in conceptualizing how grief may become “complicated” in the brain. However, as described in a previous section, we still don’t know how network interactions unfold over time to promote or impede adaptation in bereaved people. A recent dynamic framework for spontaneous thought (Christoff, Irving, Fox, Spreng, & Andrews-Hanna, 2016) offers an avenue to better understand the nature of internal thought processes like yearning and rumination in complicated grief. The framework focuses on how the “flow” of spontaneous thought may be shaped through automatic (i.e., salience of affective or environmental stimuli) or/or deliberate (i.e., cognitive control) constraints over network interactions. Flexible coupling among large-scale brain networks influences spontaneous thought dynamics by (1) exerting varying degrees of constraint, and (2) serving as sources of variability or stability in thought content over time. For example, the frontoparietal (or executive) control network imposes deliberate constraints, which can reinforce or weaken automatic constraints implemented by salience, dorsal attention, or core default mode network regions. In addition, the latter three networks can increase stability over time by inhibiting regions that might introduce variability from sensory input, episodic retrieval, or contextual associative processing (**Figure 1**) (Christoff et al., 2016).

In this dissertation, I use a new model combining the dynamic framework for spontaneous thought (Christoff et al., 2016) and dual process model (Schut, Margaret Stroebe, 1999; Stroebe et al., 2010) to develop and test hypotheses about the role of

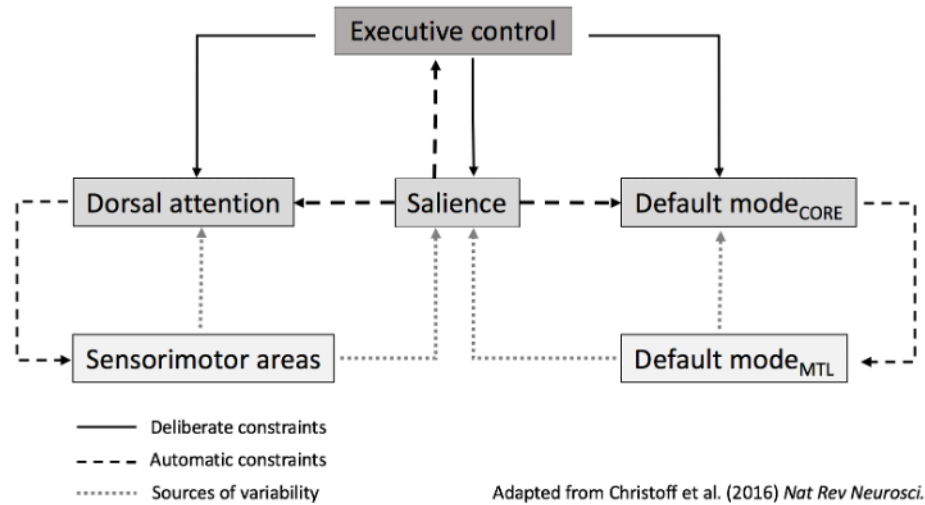
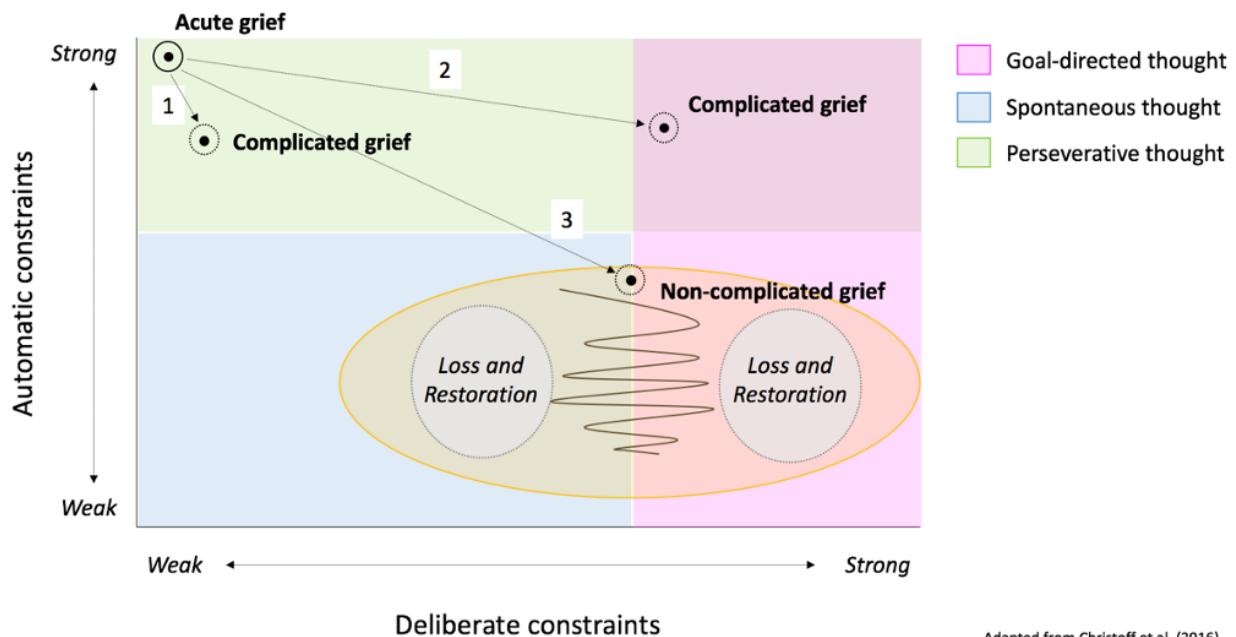


Figure 1. Hypothesized interactions among deliberate constraints, automatic constraints, and sources of variability. Arrows represent network influences on dynamics of spontaneous thought. The executive control network flexibly couples with the dorsal attention network, salience network, or default mode network core subsystem (_{core}) to exert deliberate constraints, reinforcing or weakening the automatic constraints exerted by those networks. Default mode medial temporal subsystem (_{MTL}) and sensorimotor areas contribute variability. Original figure: Christoff et al (2016).

internal thought in grief adaptation and complicated grief (**Figure 2**).

Specifically, I hypothesize that inflexibility in temporal dynamics of thought, as instantiated in large-scale brain networks, might represent a mechanism of grief maladaptation in widowed older adults. The oscillatory coping dynamics described in Stroebe & Schut's (1999; 2010) dual process model are likely supported by the coordinated action of intrinsic brain networks involved in detecting and selecting relevant stimuli (i.e., salience network), internal self-referential thought (i.e., default network), and goal-oriented cognition and behavior (i.e., frontoparietal control network). Thus, in complicated grief we might expect to find more automatically constrained and less variable thought content, hypothetically associated with (a) lesser influence from executive control regions over default network-associated internal thought, (b) greater influence from default network core subsystem regions such as the posterior cingulate and mPFC involved in self-referential thought, and (c) salience network regions that assign greater importance to thoughts and reminders of the deceased (**Figure 3**).



Adapted from Christoff et al. (2016)
and Stroebe & Schut (2010).

Figure 2. Pathways to grief (mal)adaptation. In the acute grief period (i.e., less than 6 months post-loss), the affective salience of the loss exerts high levels of automatic constraints over spontaneous thought in all bereaved individuals, as evidenced by the normative presence of intrusive thoughts and feelings of longing in acute grief. For those with complicated grief, automatic constraints may either fail to gradually decrease over time (Path 1), or are maintained by an increase in deliberate constraints, e.g. maladaptive grief cognitions (Boelen et al., 2003; Nolen-Hoeksema, 2001) (Path 2). In Path 1, continued high levels of automatic constraints may be experienced as either unpleasant or pleasant: intrusive thoughts, images, and yearning for the deceased may provoke serious distress, but counterfactual reveries (i.e., daydreaming) can also be experienced as enjoyable in the short term, until the individual is forced to confront the present reality from which the deceased is absent (Kaplan et al., 2018; Robinaugh et al., 2016). Strong automatic constraints (with or without strong deliberate constraints) impede the capacity for effective coping. In contrast, the gradual decrease in automatic constraints over time (Path 3) in those who do not develop complicated grief allows for oscillation between stronger/weaker deliberate constraints. The capacity for flexible movement between more and less deliberately constrained types of thinking, as well as between loss and restoration-oriented mental representations, may be important for effective coping. In the dual process model, appraisal processes in both loss and restoration orientations encompass what might be construed as more- and less-deliberately constrained types of thought – for example, engaging in rumination, “ventilating dysphoria”, or allowing one’s mind to wander to plans for the future might reflect lower deliberate constraints, while engaging in positive reappraisal or effortful revision of life plans might reflect more a goal-directed manner of thinking. Figure adapted from Christoff et al. (2016) and Stroebe & Schut (2010).

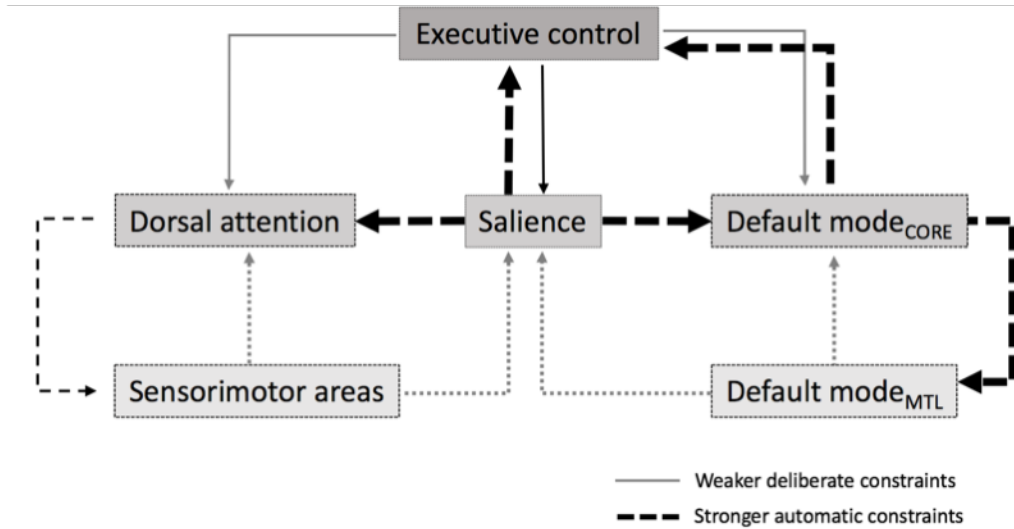


Figure 3. Hypothesized major network interactions in complicated grief, showing the flow and content of spontaneous thought as potentially more automatically constrained and less variable (i.e., intrusive, inflexible, and fixated on the loss) due to (a) lesser influence from executive control regions over default mode influence, (b) greater influence from default mode core subsystem regions, and (c) greater influence of the salience network. Adapted from Christoff et al (2016).

Dynamic functional connectivity

One of the major challenges in studying any dynamic process is how to best capture and test it. Measuring spontaneous (i.e., not stimulus-locked) oscillatory activity in distributed neural ensembles across the whole brain would provide the most direct index of what we want to know about how the brain functions to support internal thought content and variability/stability over time (Kucyi, Tambini, Sadaghiani, Keilholz, & Cohen, 2018). Such a fine-grained view of the human brain is not yet possible. Functional network connectivity (FNC) is typically measured by averaging the correlation between BOLD signals in different brain regions across the scan, termed “static FNC”. Specifically, static FNC is an undirected (i.e., non-causal) estimate based on statistical dependencies between BOLD time series, typically represented by correlation coefficients. Graph theory models get us closer, by allowing us to look at network properties such as modularity, small-worldness (local and global efficiency) and path length that provide information

about how information flows through a network and the relative importance of particular nodes in the network (Farahani, Karwowski, & Lighthall, 2019). Recently, there is increased interest in and use of time-varying, or dynamic FNC (dFNC) methods to examine functional interactions across the scan duration (Kucyi et al., 2018). As described in comprehensive detail by Lurie et al. (2020)’s excellent review describing the “*promises and pitfalls of time-varying functional connectivity*” (Lurie et al., 2020), the “dynamics” of time-resolved FNC can be quantified through either data- or model-driven approaches. In this dissertation, I use the term “dFNC” to refer to changes in statistical dependencies between time series (correlation coefficient strengths between the time series of any two given independent components identified through group ICA; see Method section) as a function of time, using a tapered sliding window approach.

Both static and dynamic FNC have emerged as sensitive and specific markers of mental disorders (Calhoun, Miller, Pearlson, & Adalı, 2014). However, whether dFNC contributes unique information (above and beyond static FNC) is debated (Chiang et al., 2018; Jin et al., 2017). In other resting state studies, variability in network dynamics appear to be linked to flexibility and adaptability (Zhang et al., 2016), including traits like creativity, mindfulness, and well-being e.g. (Beaty, Benedek, Silvia, & Schacter, 2016; Beaty et al., 2018; Karapanagiotidis et al., 2018; Marusak et al., 2018). There are no published studies of dFNC in grief or complicated grief, but other disorders that feature high negative affect and internal thought processes like yearning/craving, intrusions, and rumination could offer some clues. For example, methamphetamine users with more intense craving were less likely to shift a state of greater modularity among default and executive control networks (Soltanian-Zadeh, Hossein-Zadeh, Shahbabaie, & Ekhtiari, 2016). Veterans with PTSD showed more frequent occurrence of EEG microstates dominated by default network activity (Yuan et al., 2018), and patients with major depressive disorder showed higher static FNC and lower dFNC variability both within the default network, lower static connectivity and lower dFNC between the default mode network and

frontoparietal control regions, and greater insula-mPFC FNC associated with higher rumination (Demirtaş et al., 2016; Kaiser et al., 2016) - which might reflect over-assignment of salience to self-referential information and perseveration in depression (Menon, 2011).

Application to complicated grief. Drawing on the “ironic process” hypothesis for how the internal thought processes-emotional pain link could interfere with loss integration (Robinaugh et al., 2014; Schneck et al., 2018) complicated grief could involve over-assignment of salience to mental representations of the deceased or thoughts about their death. In my initial model of internal thought in grief adaptation (**Figure 2**), I hypothesized two pathways through which a person may develop complicated grief. The first depicts a consistently low level of deliberate constraints that does not significantly change from the acute grief period. Pathway 1 might reflect the way in which grief often makes it difficult to focus on a goal-directed activity as it requires the person to implement deliberate constraints and reduce variability. In the second pathway, automatic constraints (emotional salience) remain high in the context of high deliberate constraints. Pathway 2 might reflect cognitive efforts to suppress or avoid reminders of the loss often seen in people with complicated grief, with automatic and deliberate constraints possibly reinforcing each other. The pathways are entirely theoretical and would require tracking grief trajectories and internal thought dynamics over time, but could be tested in a preliminary, cross-sectional way through resting state dFNC. In this dissertation, I aimed to test my prediction that in people with higher complicated grief severity, I would see dFNC patterns reflecting more automatically constrained and less variable spontaneous thought.

Oxytocin

Effects on attachment behavior. One of the mechanisms through which complicated grief is hypothesized to develop is through continued proximity-seeking of the deceased partner as a primary attachment figure (LeRoy et al., 2019), and insecure attachment is implicated in risk for complicated grief e.g., (LeRoy et al., 2020; Lobb et al.,

2010). The neuropeptide oxytocin regulates attachment formation and maintenance through interactions with mesolimbic dopamine pathways and other peptides such as vasopressin and corticotropin-releasing factor (Bosch & Young, 2018; Johnson & Young, 2017; Marlin & Froemke, 2017; Sadino & Donaldson, 2018; Walum & Young, 2018). In the central nervous system, oxytocin has the capacity to travel from its point of synthesis in hypothalamic nuclei, due to its long half-life and capacity for transmission both through direct synaptic or axonal projections and through volume transmission via intracellular fluid (Agnati, Guidolin, Guescini, Genedani, & Fuxe, 2010; Agnati, Zoli, Strömberg, & Fuxe, 1995; Gimpl & Fahrenholz, 2001; Ludwig & Leng, 2006). This means that oxytocin can have widespread effects on diverse areas of the brain regions (as well as on the peripheral nervous system, where it is released into the bloodstream via hypothalamic projections to the pituitary). Oxytocin receptors are broadly distributed in the human brain; however, certain brain regions possess a particularly high receptor density, meaning that oxytocin has an affinity for binding there (Quintana et al., 2019).

Given the centrality of attachment, bonding, and re-forming attachments in grief and bereavement, experiencing the death of a primary attachment figure such as a partner could disrupt normal oxytocin signaling and lead to emotional dysregulation, e.g., (Hurlemann & Scheele, 2016; Pohl, Young, & Bosch, 2018). Much of our knowledge of oxytocin's function in social behavior and attachment comes from translational prairie vole models, given that prairie voles are one of the few species that form selective attachments, or monogamous pair bonds, e.g., (Bosch & Young, 2018). For example, neonatally-isolated prairie voles with greater oxytocin receptor binding in the nucleus accumbens show less impaired adult attachment behavior compared to voles with lower accumbal binding (Barrett, Arambula, & Young, 2015), with the strength of the bond correlated with Ca^{2+} signaling in specific neuronal ensembles in the nucleus accumbens that regulate approach behavior (Scribner et al., 2019).

There is currently little published research showing that oxytocin system signaling

plays a specific role in modulating how people adapt after bereavement. A few candidate gene pilot studies found a genetic variation in OXTR rs2254298 interacts with self-reported behavioral inhibition and separation anxiety to predict complicated grief scores (Schiele et al., 2018), and that circulating (peripheral) oxytocin levels are higher in people with complicated grief (Bui et al., 2019). However, small candidate gene studies may not replicate and these studies were observational. A more direct test of oxytocin's role in complicated grief would be to manipulate central release through intranasal administration of exogenous oxytocin. In behavioral data from the parent study for this dissertation, we found that intranasal oxytocin (vs. placebo) slowed reaction times in an approach-avoidance task. The effect was present across various grief-related, social, and neutral stimuli; however, planned comparisons of the spouse > stranger contrast indicated that oxytocin (vs. placebo) decreased implicit avoidance bias for the spouse in the complicated grief group. Intranasal oxytocin (vs. placebo) had no significant effect on approach/avoidance bias for the spouse in the non-complicated grief group (Arizmendi et al., n.d.). Our behavioral findings corroborate the hypothesis that the oxytocin system may function differently in people who develop complicated grief.

Effects on constraints over internal thought? Oxytocin is colloquially thought of having prosocial effects, such as increased intimacy, bonding, and trust. However, there is robust evidence that oxytocin does not merely have prosocial effects and increase social approach behaviors, as intranasal oxytocin is increasingly used as an experimental paradigm in human subjects research (Bartz, Zaki, Bolger, & Ochsner, 2011). Effects of oxytocin appear to be highly dependent on the context in which they occur (including the context of individual differences). For example, securely-attached men recalled their mother as being more close and caring after intranasal oxytocin administration, but intranasal oxytocin had the opposite effect in anxiously-attached men (Bartz et al., 2010). Context-dependent effects of oxytocin may be explained by the idea that oxytocin increases the salience of social stimuli in general – so depending on what that social information is,

how it is received, increased salience could result in either appetitive or aversive responses, and the response could be either contextually-appropriate or maladaptive (Shamay-Tsoory & Abu-Akel, 2016). In addition to regulating responses to other people, there is some evidence that oxytocin affects self-oriented processing such as encoding and retrieval of self-referential material (Liu, Sheng, Woodcock, & Han, 2013; Liu et al., 2017). Oxytocin might introduce a self-referential processing bias by modulating interoceptive signals and emotional awareness (Hurlemann & Scheele, 2016) and amplifies subjective sensation of social stress (Eckstein et al., 2014). In particular, the study by Eckstein et al. (2014) suggests that in social stress contexts, intranasal oxytocin caused participants to perceive the situation as more stressful, and increased activation in brain regions implicated in self-referential processing and coordinating responses to salient stimuli, such as the precuneus and cingulate cortex. Increased self-referential processing in the context of heightened aversive experience of grief might hinder loss integration in individuals already predisposed to engage in repetitive negative thinking, if the self-referential bias increases unconstructive perseveration on the deceased and/or their death.

The death of a partner is certainly a major social stressor, and the studies described in the previous paragraph support the idea that for the person with complicated grief, the deceased and their death continue to be highly salient (perhaps via oxytocin system dysregulation) and that heightened salience interacts with self-referential processing to perpetuate distress. This still begs the question of exactly how oxytocin signaling is dysregulated in complicated grief in a way that maintains salience and attachment to the deceased. However, based on the premise that oxytocin influences social salience and self-referential processing, we should be able to see a change in the brain's functional interconnectivity given that the large-scale networks involved in regulating salience, social processing, and self-referential thought are fairly well characterized.

Effects on functional brain network connectivity. The final piece of the puzzle is the effect of oxytocin on functional connectivity. The first review on this subject

identified that intranasal oxytocin modulates FNC in task-based fMRI studies, but at the time was unable to establish whether effects were a function of task context, or whether they would be observed during unconstrained thought as well (Bethlehem et al., 2013). To answer this question, I undertook a systematic review of intranasal oxytocin effects on resting state FNC specifically (Seeley, Chou, & O'Connor, 2018). I observed that intranasal oxytocin modulates static FNC even in the absence of explicit tasks - supporting the idea that oxytocin likely reconfigures brain networks in a way that facilitates noticing and responding to socially or affectively-salient stimuli. Also notable was the fact that intranasal oxytocin's effects on FNC were often modulated by symptoms, traits, and early life experiences related to social and emotional functioning.

Intranasal oxytocin studies have often focused on the amygdala as a seed region of particular interest, but a recent ALE meta-analysis of task-related activation in fMRI studies (Grace, Rossell, Heinrichs, Kordsachia, & Labuschagne, 2018) emphasizes the need to consider how the neuropeptide acts elsewhere in the brain. Because oxytocin has diverse pathways and manner of travel in the brain, I was most interested in two group ICA-based studies (Bethlehem et al., 2017; Brodmann, Gruber, & Goya-Maldonado, 2017). Bethlehem et al. (2017) identified that intranasal oxytocin increased FNC between cortical and subcortical regions, while Brodmann et al. (2017) findings suggest that oxytocin may modulate intersection of default and cingulo-opercular networks, via the ventral attention network acting as a "circuit breaker" to reorient attention to salient features of the environment.

Since my review was published, a placebo-controlled, between-subjects study in a large, non-clinical sample of men and women (Xin et al., 2018) found that oxytocin increased functional connectivity strength within the default network, and increased segregation between default subnetworks with salience and dorsal attention networks. This could indicate that intranasal oxytocin promotes attention to emotional and social cues by increasing the competitive organization of large-scale brain networks involved in internal

601 vs. external attention (Xin et al., 2018). However, would intranasal oxytocin show the
602 same effects in a bereaved sample, for whom *internal* social/emotional stimuli (such as
603 thoughts of the deceased) may be very salient?

604 Currently, there are no published resting state fMRI studies that examine oxytocin's
605 effect on dynamic FNC. Schiller, Koenig, and Heinrichs (2019) found that intranasal
606 oxytocin reduced temporal stability of neural networks from spatio-temporal EEG, and
607 that the effects were more pronounced in participants with the type of anxious and
608 dependent attachment styles that may contribute to risk for developing complicated grief;
609 e.g., (K. Shear & Shair, 2005)). A recent preprint found no effect of oxytocin on the
610 frequency of brain temporal state switching, using a novel Bayesian connectivity change
611 point model (Jiang et al., 2020). However, Jiang et al. (2020) did identify a dynamic
612 effective connectivity pattern that was unique to the group treated with intranasal
613 oxytocin ("dynamic effective connectivity" was operationalized by estimating dependency
614 and directionality among all ROIs within each temporal state). Relevant to the current
615 study, the oxytocin group-only pattern featured (1) greater effective connectivity within
616 salience network regions (dACC, anterior and posterior insula) and (2) greater midline
617 default network (precuneus and posterior cingulate) effective connectivity to salience
618 network regions. Effective connectivity *from* the amygdala to other regions was not greater
619 in the oxytocin group, but there was greater effective connectivity *to* the amygdala from
620 salience, reward (ventral tegmental area, striatum), and social cognition (posterior superior
621 temporal sulcus) network regions. They also observed increased effective connectivity from
622 the posterior superior temporal sulcus, posterior cingulate, and posterior insula to the
623 ventral tegmental area and striatum, and bidirectional effective connectivity of both the
624 medial prefrontal and orbitofrontal cortices with the posterior insula – among various other
625 interhemispheric connections.

626 In conclusion, oxytocin has the capacity to influence neural activity in a variety of
627 brain regions, and resolution of grief may be impeded by prolonged salience of the

deceased, through the impact on spontaneous thought in susceptible individuals. Intranasal oxytocin theoretically offers a way to manipulate automatic constraints over internal mentation during resting state, given that oxytocin administration may sensitize participants to motivationally-salient social and emotional stimuli through its effects on large-scale brain networks.

Specific aims and hypotheses

Aim 1 involves only data from the placebo session, whereas Aim 2 involves data from both oxytocin and placebo sessions.

Aim 1. To identify whether static and/or dynamic resting state functional connectivity (FNC/dFNC) differs among widowed older adults who are adjusting well versus those who are adjusting poorly (i.e., complicated grief).

- H1: The complicated grief group will show less variability in spontaneous thought over time, as demonstrated by fewer dFNC state transitions.
- H2: The complicated grief group will show greater automatic constraints on thought content, as shown by greater dwell time in states of default mode-salience network interconnectivity.

Aim 2. To investigate if/how intranasal oxytocin alters static and/or dynamic functional network connectivity (FNC/dFNC) in older adults, and whether effects of oxytocin are moderated by complicated grief symptoms.

- H1: Under oxytocin, the sample as a whole will show increased salience network interconnectivity with other networks, relative to placebo.
- H2: Grief severity (as a continuous variable) will moderate oxytocin effects on FNC/dFNC, with greater influence on participants with higher levels of complicated grief symptoms.

Method

Participants

Participants were 40 community-dwelling older adults between the ages of 55-80 ($M = 69.22$ years, $SD = 6.49$, range = 57-79; see **Table 1**) recruited from the southern Arizona area in 2015-2017, who had experienced the death of their spouse or long-term romantic partner approximately six to 36 months prior to participation ($M = 15.40$ months, $SD = 8.17$). Data reported here were collected as part of a larger neuroimaging study. Recruitment strategies included letters mailed to surviving spouses based on published obituaries, newspaper advertisements, and notices through medical centers, hospices, and retirement communities. Several participants were also recruited via word-of-mouth from enrolled participants (e.g., they chose to share the study information with other members of their grief support group) or referred by community clinicians. Exclusion criteria included inability to comprehend English; standard MRI contraindications; active suicidality, homicidality, or psychotic symptoms; ongoing major health conditions such as cancer; uncontrolled hypertension; and medications likely to impact the oxytocin system (e.g., systemic corticosteroids). All female participants were post-menopausal. Psychotropic medication use was allowed on a case-by-case basis, and limited to participants whose medication regimen and dosing had been stable for at least three months. Participants who were prescribed benzodiazepines on a PRN basis were asked to refrain from taking them on the day of their visit. (Older adults are prescribed psychotropics at higher rates, while being less likely to have an associated mental health diagnosis (Maust, Oslin, & Marcus, 2014), and it is relatively common even for people with “normative” grief to be prescribed antidepressants and/or anxiolytics by a primary care physician).

Enrolled participants were categorized as belonging to either the complicated grief (CG) or non-complicated grief (Non-CG) group based on a clinical cutoff score of 25 or greater on the Inventory of Complicated Grief (ICG; Prigerson et al. (1995)). Stratified

sampling ensured that a full range of ICG scores was represented ($M = 23.35$, $SD = 12.47$, range = 4-51).

An additional three participants were dropped from the study after enrollment but before completing their first MRI session, due to ferromagnetic implants in the skull or oral cavity that were not disclosed during their initial screening ($n = 2$) or incidental radiological findings on their anatomical brain scan ($n = 1$). Two additional participants withdrew or were withdrawn after completing the first MRI session, due to nausea ($n = 1$) or significant back pain-related discomfort in the scanner resulting in excessive motion ($n = 1$). These participants were compensated, provided with appropriate follow-up, and their data were not included in the master dataset. Information on recruitment, enrollment, and completion rates is described in the study CONSORT diagram (**Figure 4**).

Design and Procedures

All aspects of the study were approved by the University of Arizona's Institutional Review Board Human Subjects Protection Program. Participants gave written informed consent and were compensated \$200 for completing the study.

Prospective participants completed a standardized phone screening interview conducted by this author or the other graduate student on the project. After screening, each enrolled participant completed a set of questionnaires via computer, and provided personal photos of their spouse and another loved one to the research team for use in a behavioral task. Each participant attended two research visits approximately seven to ten days apart. At each visit, participants completed pre-scan measures of state emotion and anxiety before self-administering the oxytocin or placebo nasal spray under the researcher's supervision. After a 30-minute serum rise-time period for the oxytocin, participants entered the MRI room and were positioned in the scanner to their comfort. During their scan session, participants received a series of structural and functional MRI sequences for a

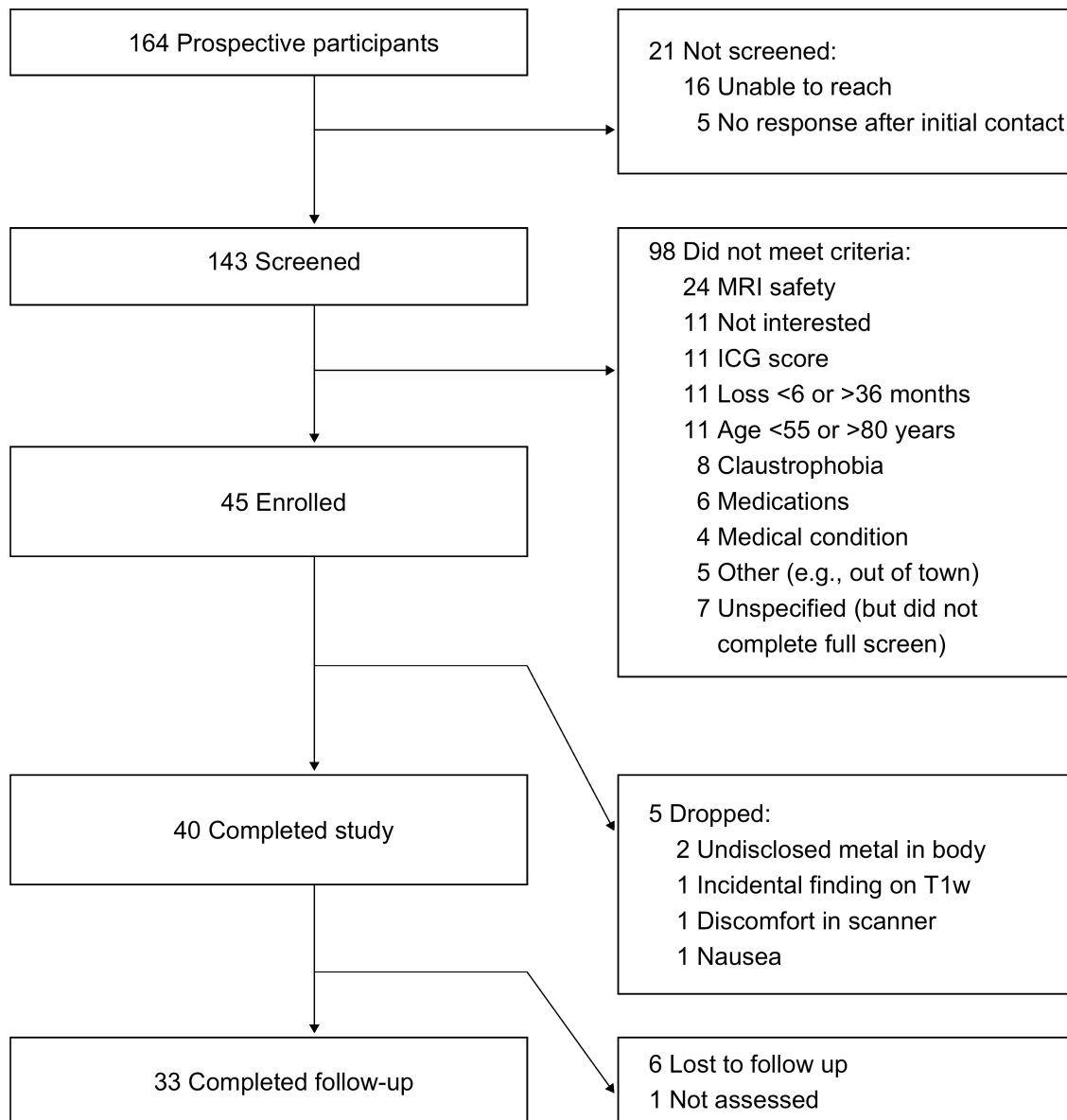


Figure 4. Parent Study CONSORT Diagram

total scan time of approximately 35 minutes. The resting state sequence was always delivered last, preceded by a behavioral task (reported in Arizmendi et al. (n.d.), *under review*) in which participants viewed photos of their deceased partner, a living loved one, generic death-related scenes (e.g., hospital room, casket, gravestone), a stranger, and neutral scenes while making responses using an MR-compatible joystick. After exiting the scanner, participants completed post-scan state measures, were compensated for their time, and, at the second visit, debriefed. The two visits were otherwise identical, apart from the specific nasal spray received. In addition to the above procedures, participants provided biological samples unrelated to the current investigation, including salivary cortisol three times during the visit (baseline, immediately pre-scan, and post-scan) and a genetic sample via buccal swab at the end of their second visit.

Resting State. Resting state paradigms assess brain activity in the absence of explicit task instructions or experimentally-related goals. Consistent with established procedures, participants were asked to stay awake, keep their eyes focused centered on a fixation cross, and to “let [their] thoughts come and go as they normally do” but to refrain from any specific mental activity such as counting, praying, or meditating.

Materials

Intranasal spray (oxytocin/placebo). At each of their two visits, participants received a nasal spray containing either intranasal oxytocin or placebo. A single dose (24 IU; MacDonald et al. (2011)) of synthetic oxytocin (Syntocinon, Novartis, Switzerland) or the placebo (Novartis, Switzerland) was self-administered via six 4-IU puffs into each nostril, alternating nostrils between each puff. The placebo contained all non-active ingredients as the oxytocin spray in order to standardize taste and odor. The order and identity of the spray was counterbalanced across participants and double-blinded. The researcher at the scanner was blind to both the identity of the spray as well as the participant’s grief severity scores.

Intranasal administration bypasses the blood-brain barrier (Quintana, Alvares, Hickie, & Guastella, 2015), with peak cerebrospinal fluid concentrations at approximately 75 minutes post-administration (Striepens et al., 2013). Across participants and sessions, mean time from administration to start of the resting state scan was 68.19 minutes ($SD = 14.17$, range = 43 - 109). There was a significant effect of visit ($t(37) = 3.17$, $p = 0.00$), where time from spray administration to testing state was longer in the first visit ($M = 72.10$, $SD = 15.23$ minutes) than the second ($M = 64.29$, $SD = 11.98$ minutes), due to the fact that it generally took longer to get participants situated comfortably in the MRI at their first visit. However, the difference in timing between first and second visit is likely mitigated by the randomization of the two sprays, as evidenced by the fact that timing did not differ significantly between oxytocin and placebo sessions ($t(37) = -1.56$, $p = 0.13$). There was no significant effect of sex on timing ($t(74) = 0.32$, $p = 0.75$).

Measures

Participants completed a number of self-report measures, including self-reported demographics, health-related variables, length of relationship, and time elapsed since their partner's death. Measures relevant to the current study are the following:

Beck Depression Inventory-II (BDI-II) (Beck, Steer, & Brown, 1996). The BDI-II is a widely-used, 21-item measure of depressive symptoms across emotional, cognitive, behavioral and somatic domains. Higher scores indicate more frequent and/or severe symptoms. Scores of 13 or greater suggest at least a mild level of clinical depression.

Inventory of Complicated Grief (ICG) (Prigerson et al., 1995). The ICG is a 19-item measure of complicated grief symptoms distinct from depression or anxiety and predictive of functional impairment. Items were derived from a sample of spousally-bereaved older adults. Greater scores indicate more frequent and/or severe symptoms. The ICG showed high internal consistency in our sample (Cronbach's alpha =

0.93). The ICG can also be used dichotomously, where scores ≥ 25 indicate a clinically-significant level of complicated grief symptoms.

MRI Data Acquisition and Management

Imaging data were acquired on a Siemens Magnetom Skyra 3T MRI scanner with a 32-channel head coil (Syngo MR E11 software, field strength 2.89) at Banner University Medical Center in Tucson, AZ. A seven-minute structural T1-weighted MPRAGE sequence (TR = 2300ms, TE = 2.3ms, TI = 900ms, flip angle = 8° , matrix size = 256×256 , $0.9 \times 0.9 \times 0.9$ mm voxels, 192 slices) preceded the functional scans. Resting state fMRI data were collected during a six-minute, multi-echo echoplanar imaging sequence of 180 contiguous whole-brain functional volumes (TR = 2000ms, TE = 30ms, flip angle = 90° , matrix = 92×80 , $2.6 \times 2.6 \times 3.5$ mm voxels, orientation = 158, 29 slices). All imaging data for this study was converted from DICOM to NIFTI and organized according to Brain Imaging Data Structure (BIDS; Gorgolewski et al. (2016)) specifications using the batch interface of `dcm2niix` (Li, Morgan, Ashburner, Smith, & Rorden, 2016), as described here: https://sarensseeley.github.io/BIDS-fmriprep-MRIQC.html#making_your_data_bids-compliant.

MRI Data Preprocessing and Analysis

Quality control. I used *MRIQC* 0.14.2, an open-source tool for extracting MRI quality measures (Esteban et al., 2017), to determine which participants should be excluded from further analysis. *MRIQC* provides individual and group reports which can identify outlying subjects on a number of image quality measures (IQMs). Anatomical IQMs include measures assessing on noise (e.g., signal-to-noise ratio, coefficient of joint variation of grey and white matter), measures based on information theory (e.g., foreground-background energy ratio), measures targeting specific artifacts (e.g., bias field location and spread), and other measures (e.g., image blurriness [FWHM], summary

statistics within different regions/tissue types). Functional IQMs include measures for spatial information (e.g., signal-to-noise ratio, FWHM, summary statistics within different regions/tissue types), temporal information (e.g., temporal derivative of timecourses [DVARs]), and specific artifacts (e.g., mean framewise displacement, ghost-to-signal ratio, number of non-steady state volumes, AFNI’s outlier and quality indices). After computing individual IQMs per subject and session, MRIQC produces group reports showing a scatterplot for each IQM. Group T1w and BOLD reports were visually inspected and compared to sample MRIQC reports on larger datasets (<https://poldracklab.github.io/mriqc/>) in order to identify lower-quality images. Based on visual inspection and the MRIQC reports, two participants were excluded from further analysis due to either consistent, substantial movements in excess of 2mm consistently throughout the scan (sub-142), or poor brain coverage during the resting state scan at one session, apparently caused by the subject moving out of FOV in between imaging sequences (sub-147).

Preprocessing. Results included in this manuscript come from preprocessing performed using *fMRIPrep* 1.1.8 (Esteban et al. (2019); Esteban et al. (2018); RRID:SCR_016216), which is based on *Nipype* 1.1.3 (Gorgolewski et al. (2011); Gorgolewski et al. (2018); RRID:SCR_002502). Description of preprocessing pipeline and procedures was automatically generated by *fMRIPrep*.

Anatomical data preprocessing. Two T1-weighted (T1w) images per participant (one per session) were used to generate one individual-level anatomical template per participant using *fMRIPrep*’s `--longitudinal` flag. A few participants had only one usable T1w images due to poor data quality of the anatomical scan at one of their sessions; in these cases, we used just the one T1w image that was of higher quality. All of them were corrected for intensity non-uniformity (INU) using `N4BiasFieldCorrection` (Tustison et al., 2010, ANTs 2.2.0). A T1w-reference map was computed after registration of two T1w images (after INU-correction) using `mri_robust_template` (FreeSurfer 6.0.1,

Reuter, Rosas, & Fischl, 2010). The T1w-reference was then skull-stripped using `antsBrainExtraction.sh` (ANTs 2.2.0), using OASIS as target template. Brain surfaces were reconstructed using `recon-all` (FreeSurfer 6.0.1, RRID:SCR_001847, Dale, Fischl, & Sereno, 1999), and the brain mask estimated previously was refined with a custom variation of the method to reconcile ANTs-derived and FreeSurfer-derived segmentations of the cortical gray-matter of Mindboggle (RRID:SCR_002438, Klein et al., 2017). Spatial normalization to the ICBM 152 Nonlinear Asymmetrical template version 2009c (Fonov, Evans, McKinstry, Almli, & Collins, 2009, RRID:SCR_008796) was performed through nonlinear registration with `antsRegistration` (ANTs 2.2.0, RRID:SCR_004757, Avants, Epstein, Grossman, & Gee, 2008), using brain-extracted versions of both T1w volume and template. Brain tissue segmentation of cerebrospinal fluid (CSF), white-matter (WM) and gray-matter (GM) was performed on the brain-extracted T1w using `fast` (FSL 5.0.9, RRID:SCR_002823, Zhang, Brady, & Smith, 2001).

Functional data preprocessing. For each of the 2 BOLD runs per subject (across sessions), the following preprocessing was performed. First, a reference volume and its skull-stripped version were generated using a custom methodology of *fMRIPrep*. A deformation field to correct for susceptibility distortions was estimated based on *fMRIPrep*'s *fieldmap-less* approach. The deformation field is that resulting from co-registering the BOLD reference to the same-subject T1w-reference with its intensity inverted (Huntenburg, 2014; Wang et al., 2017). Registration is performed with `antsRegistration` (ANTs 2.2.0), and the process regularized by constraining deformation to be nonzero only along the phase-encoding direction, and modulated with an average fieldmap template (Treiber et al., 2016). Based on the estimated susceptibility distortion, an unwarped BOLD reference was calculated for a more accurate co-registration with the anatomical reference. The BOLD reference was then co-registered to the T1w reference using `bbregister` (FreeSurfer) which implements boundary-based registration (Greve & Fischl, 2009). Co-registration was configured with nine degrees of freedom to account for

distortions remaining in the BOLD reference. Head-motion parameters with respect to the BOLD reference (transformation matrices, and six corresponding rotation and translation parameters) are estimated before any spatiotemporal filtering using `mcflirt` (FSL 5.0.9, Jenkinson, Bannister, Brady, & Smith, 2002). BOLD runs were slice-time corrected using `3dTshift` from AFNI (Cox & Hyde, 1997, RRID:SCR_005927). The BOLD time-series (including slice-timing correction when applied) were resampled onto their original, native space by applying a single, composite transform to correct for head-motion and susceptibility distortions. These resampled BOLD time-series will be referred to as *preprocessed BOLD in original space*, or just *preprocessed BOLD*. Automatic removal of motion artifacts using independent component analysis (ICA-AROMA, Pruim, Mennes, et al., 2015) was performed on the *preprocessed BOLD on MNI space* time-series after a spatial smoothing with an isotropic, Gaussian kernel of 6mm FWHM (full-width half-maximum). Corresponding “non-aggressively” denoised runs were produced after such smoothing. Additionally, the “aggressive” noise-regressors were collected and placed in the corresponding confounds file. The BOLD time-series were resampled to MNI152NLin2009cAsym standard space, generating a *preprocessed BOLD run in MNI152NLin2009cAsym space*.

Several noise-related time-series were calculated based on the *preprocessed BOLD*: framewise displacement (FD), DVARS and three region-wise global signals. FD and DVARS are calculated for each functional run, both using their implementations in *Nipype* (following the definitions by Power et al., 2014). The three global signals are extracted within the CSF, the WM, and the whole-brain masks. Additionally, a set of physiological regressors were extracted to allow for component-based noise correction (*CompCor*, Behzadi, Restom, Liau, & Liu, 2007). Principal components are estimated after high-pass filtering the *preprocessed BOLD* time-series (using a discrete cosine filter with 128s cut-off) for the two *CompCor* variants: temporal (tCompCor) and anatomical (aCompCor). Six tCompCor components are then calculated from the top 5% variable voxels within a mask

covering the subcortical regions. This subcortical mask is obtained by heavily eroding the brain mask, which ensures it does not include cortical GM regions. For aCompCor, six components are calculated within the intersection of the aforementioned mask and the union of CSF and WM masks calculated in T1w space, after their projection to the native space of each functional run (using the inverse BOLD-to-T1w transformation). The head-motion estimates calculated in the correction step were also placed within the corresponding confounds file. The BOLD time-series, were resampled to surfaces on the following spaces: *fsaverage5*. All resamplings can be performed with *a single interpolation step* by composing all the pertinent transformations (i.e. head-motion transform matrices, susceptibility distortion correction when available, and co-registrations to anatomical and template spaces). Gridded (volumetric) resamplings were performed using `antsApplyTransforms` (ANTs), configured with Lanczos interpolation to minimize the smoothing effects of other kernels (Lanczos, 1964). Non-gridded (surface) resamplings were performed using `mri_vol2surf` (FreeSurfer).

Many internal operations of *fMRIPrep* use *Nilearn* 0.4.2 (???, RRID:SCR_001362), mostly within the functional processing workflow. For more details of the pipeline, see the section corresponding to workflows in *fMRIPrep*'s documentation.

fMRI Analysis.

Artifact identification and denoising. : As described above, independent components (ICs) classified as noise by ICA-AROMA were removed from the preprocessed BOLD time series in *fMRIPrep*. *ICA-AROMA* improves the reproducibility of resting state networks relative to other motion removal approaches like spike regression and scrubbing, which reduce temporal degrees of freedom (Pruim et al., 2015; Pruim, Mennes, et al., 2015). Although the *ICA-AROMA* classifier is trained specifically to identify motion-related artifacts, it also appeared to correctly classify some other types of noise in the data (i.e., physiological fluctuations, residual slice-timing-related variance that was not accounted for by slice-timing correction). ICASSO estimates from *GIFT* indicated that ICs

derived from the denoised data showed much greater reliability and stability compared to ICs derived from preprocessed outputs that were smoothed only and did not undergo ICA-AROMA denoising. Therefore, the data that underwent non-aggressive denoising via *ICA-AROMA* were used in subsequent analyses.

Following the group ICA using *Group ICA of fMRI Toolbox* (GIFT) 4.0b (Rachakonda, Egolf, Correa, Calhoun, & Neuropsychiatry, 2007) (*see next section*), ICs at the group level were classified as either noise, signal, or undetermined/mixed, based on their spatial distribution, power spectra, and ICASSO stability estimates as described in (Allen et al., 2011).

Noise ICs were characterized by the presence of some or all of the following features: (1) peak activations in non-grey matter, (2) spatial overlap with typical vascular, ventricular, susceptibility, or motion artifacts, and (3) time courses that were dominated by higher-frequency fluctuations as evidenced by spectral peaks above .10Hz and/or a lower ratio of low-to-high frequency power (fALFF).

Classification of non-noise ICs was based on visual inspection of their spatial maps as compared to typical spatial distributions of established large-scale brain networks, aided by correlating IC spatial maps with (1) patterns associated with cognitive terms derived from large-scale meta-analysis (Yarkoni, Poldrack, Nichols, Van Essen, & Wager, 2011) and (2) resting state network templates from the Stanford functional atlas (https://findlab.stanford.edu/functional_ROIs.html). Noise components typically have smaller or negative correlation coefficients with the network templates. Signal components loaded heavily on terms for cognitive functions that would logically be associated with the putative network represented by a given IC.

Group ICA and postprocessing. I used *GIFT* to decompose the imaging data into functional networks using group spatial ICA. Data reduction incorporated both experimental sessions, with “session” (oxytocin or placebo) specified as a repeated measure,

in order to permit the resulting ICs at each session to be directly compared across subjects and sessions. The first three volumes of each scan were dropped to discard non-steady state volumes for any subject/session, leaving 177 volumes for the ICA. Data were first preprocessed by removing the image mean per voxel at each timepoint.

I set the GIFT parameters to extract 45 principal components for the subject-specific data reduction using the expectation maximization algorithm (Roweis, 1998), and 30 components for the group-level data reduction. Subject-specific PCA retains more variance at the individual level compared to a grand-mean approach (Rachakonda et al., 2007). The relatively lower-order decomposition was chosen to avoid overfitting, considering that ICA-AROMA had already removed considerable noise-related variance from individual subject/session scans that would have otherwise been parsed into ICs in the group ICA.

The group ICA was run iteratively ten times using both random initial values and bootstrapping using ICASSO in GIFT (Himberg & Hyvärinen, 2003). ICASSO is an approach to assess the stability and reliability of the ICA estimates (**Figure 5**).

All cluster estimates had a stability index (iq) of 0.89 or above ($M_{iq} = .97$, $SD_{iq} = .02$). Compact and isolated estimate centrotypes indicated that they were reliably identified across iterations, and the clusters corresponding to ICs of interest were generally distinct from other ICs, as demonstrated by non-agglomeration between the estimates as shown in the dendrogram and similarities graph (**Figure 5**).

Spatial maps and time courses for each session and subject were estimated using GICA (Calhoun, Adali, Pearlson, & Pekar, 2001) and scaled to Z-scores. GICA back-reconstructs individual subject spatial maps from the group-level data reduction and ICA estimates, and is shown to be more robust than GICA2 or GICA3 for low model order data (Rachakonda et al., 2007). Group means, standard deviations, and t-maps were calculated for each component over the number of datasets used in the ICA. Subject specific timecourses were detrended (linear, cubic, and quadratic) and despiked using **3dDespike**

(Cox & Hyde, 1997) , then filtered using a fifth-order Butterworth low-pass filter with a high frequency cutoff of 0.15 Hz (Rachakonda et al., 2007). Static functional connectivity (FNC) was derived from the timecourse matrix represented as a 30 x 30 covariance matrix containing correlation values between pairs of ICs (per subject and session).

Dynamic functional connectivity estimation. Time-varying, or dynamic functional connectivity (DFNC) was estimated from the subject ICA timecourses using the approach described in (Allen, Erhardt, Wei, Eichele, & Calhoun, 2012), via the dFNC Toolbox (DFNC v1.0a) available in GIFT. A 22-TR (44 seconds) rectangular window was convolved with a Gaussian $\sigma = 3$ TRs to obtain a tapered window, which was slid in steps of 1 TR for a total of 155 windows per session. Time windows with local maxima in functional connectivity variance (“subject exemplars”) were chosen by subsampling windows/pairs for each subject. k -means clustering was applied to individual subject matrices representing changes in correlation as a function of time. This yielded four cluster centroids, or dynamic “states.” Each state reflects re-occurring patterns of functional connectivity. Number of clusters was based on elbow criteria for different values of k .

A representative DFNC matrix for each state was calculated on each subject by averaging DFNC matrices of the same state. Not all participants displayed all four states. DFNC metrics of state properties (mean dwell time in each state; n transitions between states) were calculated for each subject/session. Meta-state metrics (see (Allen et al., 2012)) were calculated but ultimately not used in final analyses, given that three of the four variables appeared to be correlated with mean framewise displacement ($r = -.21 - -.30$, $p = .06-.10$).

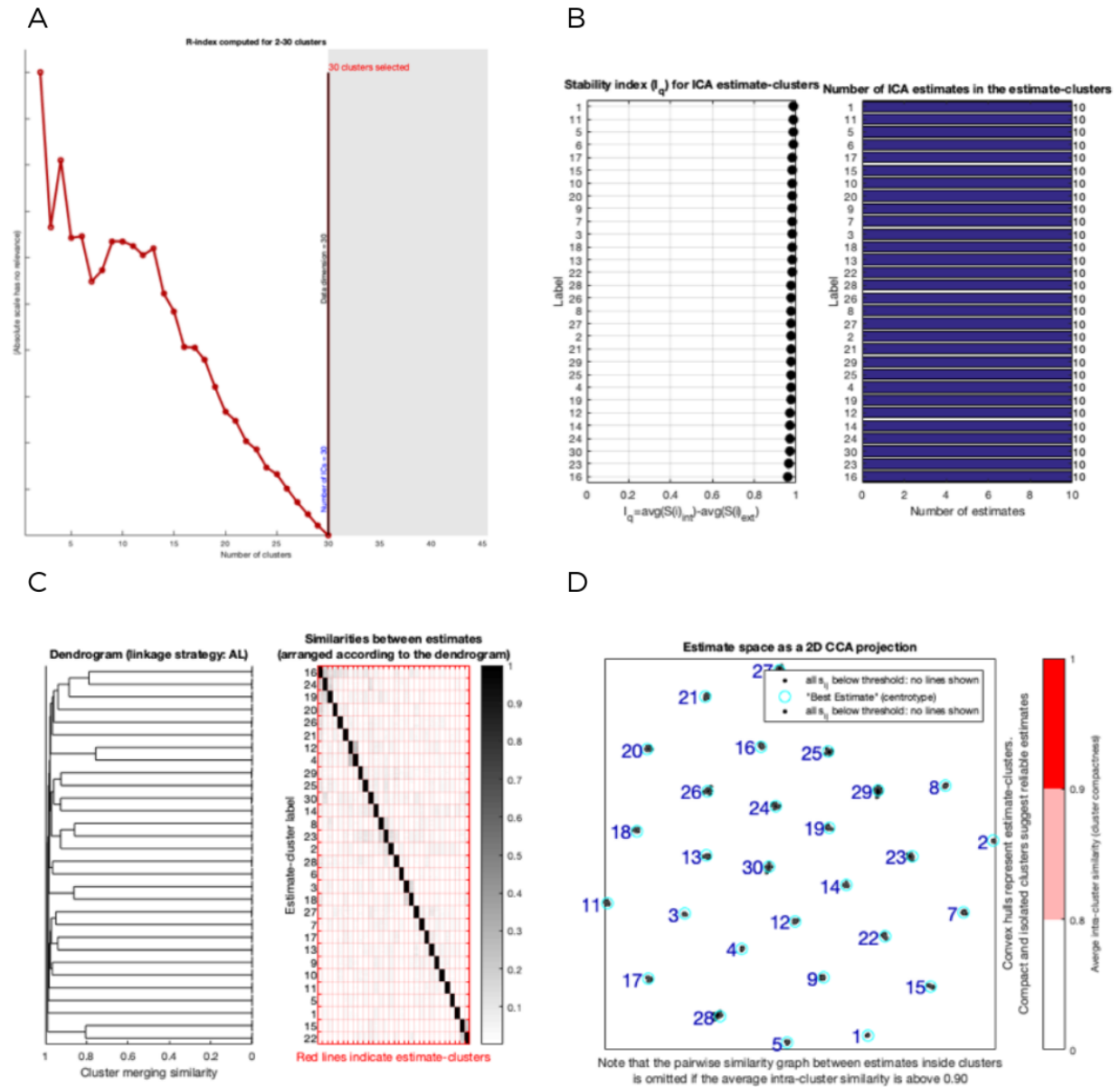


Figure 5. GIFT's ICASSO plots for the group ICA, showing stability, reliability, and distinctiveness of the 30 components. A: R-index computed for clustering results using two through 30 clusters. The clustering result with the minimum R-index value represents the best number of clusters. B: The stability or quality index (i_q), showing high stability (minimum $i_q = .89$, mean $i_q = .97$) across ICA estimates. C: Dendrogram and correlogram showing clustering and similarities between estimates. D: The estimate space as a 2D curvilinear component analysis projection. The blue outline around the black dots represent the cluster "best estimate" or centrotpe, while the black dots represent the single-run estimates. Cluster estimates for each component are compact and isolated from other clusters.

Results

Participant characteristics

The sample ($n = 38$; **Table 1**) included primarily female, retired, non-Hispanic White, participants, 36 of whom had been in heterosexual partnerships. The majority of the sample had received at least a two-year college degree. Most participants had been with their deceased partner for several decades, and participated in the study more than a year after their partner's death. Participants were stratified by their scores on the ICG, with participants scoring 25 or greater being categorized in the complicated grief group (CG, $n = 15$) group and participants scoring under 25 being categorized in the non-complicated grief group (NCG, $n = 23$).

Current or past medical issues in the sample were typical of the population and included hypertension, chronic kidney disease, glaucoma, osteoarthritis, back or joint problems, spinal stenosis, circulation problems (e.g., Reynaud's), autoimmune disorders (fibromyalgia, chronic fatigue, Sjögren's), and remitted cancer (leukemia, breast, prostate, melanoma). One participant reported having experienced a "stress-induced heart attack" following the death of their partner.

Polypharmacy was common, with two-thirds of the sample taking two or more prescription medications and about a third reporting taking four or more. The most commonly-reported prescription medications included antihypertensive agents (e.g., diuretics, angiotensin receptor blockers, ACE inhibitors, beta-blockers), statins, synthetic thyroid hormone, and psychoactive medications (benzodiazepines, antidepressants, anticonvulsants). Participants in the CG group were not more likely to be taking psychoactive medications than the NCG group, and several participants reported being prescribed psychoactives for non-mood or anxiety reasons, such as insomnia and pain.

Characteristic	NCG, N = 23 ¹	CG, N = 15 ¹	p-value ²
Sex			0.073
Female	19 (83%)	8 (53%)	
Male	4 (17%)	7 (47%)	
Age (years)	68.77 (6.46)	69.86 (7.14)	0.52
Relationship length (years)	36.89 (11.06)	38.57 (14.61)	0.68
Time from death (months)	16.63 (8.51)	12.74 (7.47)	0.12
Race			0.39
White	23 (100%)	14 (93%)	
Non-White	0 (0%)	1 (6.7%)	
Ethnicity			0.15
Hispanic or Latino	0 (0%)	2 (13%)	
Employment			0.12
Full time	0 (0%)	3 (20%)	
Part time	3 (13%)	1 (6.7%)	
Unemployed	1 (4.3%)	0 (0%)	
Retired	19 (83%)	11 (73%)	
Psychoactive medications			>0.99
Taking psychoactive(s)	7 (30%)	5 (33%)	
ICG	14.61 (6.42)	35.33 (8.50)	<0.001
BDI	5.83 (4.82)	16.13 (6.14)	<0.001

Table 1.

Participant characteristics. NCG = non-complicated grief; CG = complicated grief.

¹Statistics presented: n (%); mean (SD)

²Statistical tests performed: Fisher's exact test; Wilcoxon rank-sum test

Group ICA

The group ICA yielded 30 components, of which 19 ICs were identified as resting state networks (**Figure 6, Table 2**). Eleven ICs demonstrated noise features, as described in the *Artifact identification and denoising* section above, and were classified as artifacts. Two default network (DN) components were identified; however they did not map clearly onto the DN midline core and medial temporal lobe subnetworks described in the model by (Christoff et al., 2016). Their spatial characteristics did appear broadly consistent with the distinct yet parallel and interwoven “DN_A” and “DN_B” networks recently described by (Buckner & DiNicola, 2019). For clarity, I will refer to the two DN components identified in my data as DN_{retrosplenial} (IC10) and DN_{Core} (IC27). Yet despite differences, there were some similarities to Christoff et al. subnetwork classification DN_{retrosplenial} showed strong functional connectivity with parahippocampal and retrosplenial cortices. As shown in **Figure 7**, DN_{retrosplenial} (IC10) and DN_{Core} (IC27) both demonstrated strong positive correlations with IC13 but were not particularly strongly correlated with each other. IC13 also showed positive correlations with right frontoparietal (IC6), visual (IC2) and auditory (IC14) networks in addition to DN_{retrosplenial} and DN_{Core}. The connectivity pattern supported an interpretation of IC13 as representing a precuneus network involved in episodic memory and other diverse functions, via connections with association cortices (Cavanna & Trimble, 2006).

Note that from here on, the “salience network” components (IC12, IC26) will be referred to as “cingulo-opercular network” components, given that we did not actually know whether activation was a response to salient stimuli, since this was a resting state scan.

Resting State Network	IC #	Peak voxel coordinates (MNI)	Peak voxel location	f/ALFF
DN~A~	10	10, -55, 12	Retrosplenial cortex	8.16
DN~B~	27	-3, -55, 22	Posterior cingulate	12.1
Frontoparietal	6	48, -55, 58	Inferior parietal lobule (R)	7.81
	17	-31, -75, 54	Intraparietal sulcus (L)	8.04
Cingulo-opercular	26	-1, 18, 38	Dorsal anterior cingulate	5.82
	12	-45, 18, -11	Anterior insula (L)	2.65
Precuneus	13	-1, -77, 46	Dorsal precuneus	5.25
Sensorimotor	5	-49, -39, 62	Postcentral gyrus (L)	4.2
	11	-67, -35, 34	Postcentral gyrus/supramarginal gyrus (L)	9.32
	1	-55, -7, 28	Precentral gyrus/postcentral gyrus (L)	7.14
	25	-1, -39, -23	Vermis	3.14
Orbitofrontal/striatal	21	-3, 10, -1	Ventral striatum/mOFC	5.21
Temporal pole	4	-39, 16, -21	Anterior temporal pole (L)	2.08
Visual	23	8, -85, 15	Lingual gyrus	7.88
	8	34, -93, -9	Inferior occipital gyrus (R)	5.39
	2	-9, -75, 12	Cuneus	4.92
Auditory	14	-57, -23, 12	Superior temporal gyrus (L)	5.61
Language	9	-63, -45, 4	Superior temporal gyrus (Wernicke's area) (L)	9.91
Basal ganglia	16	-5, 4, 8	Caudate	2.72

Table 2. Resting state networks. Artifacts: IC #s 3, 7, 15, 18, 19, 20, 22, 24, 28, 29, 30. f/ALFF = low-frequency power (0.01-0.10 Hz) divided by the total power in the detectable frequency range, calculated across subjects/sessions. IC = independent component, L = left, R = right. Unthresholded spatial maps for the 30 components are available on NeuroVault: <https://neurovault.org/collections/BZHIAIYG/>

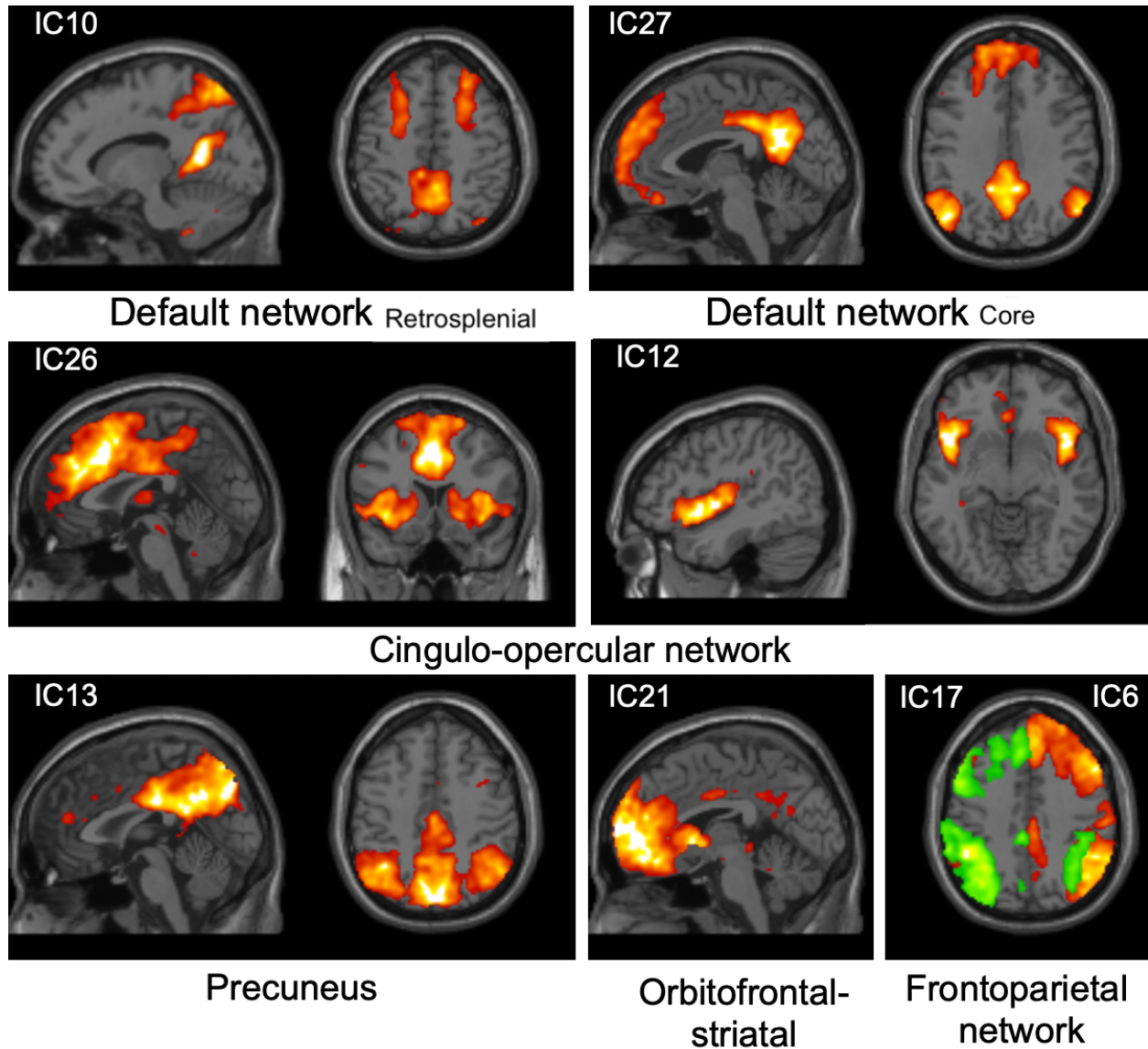


Figure 6. Spatial maps of independent components comprising selected networks, thresholded at $Z = 2$ and displayed on a standard T1 template image.

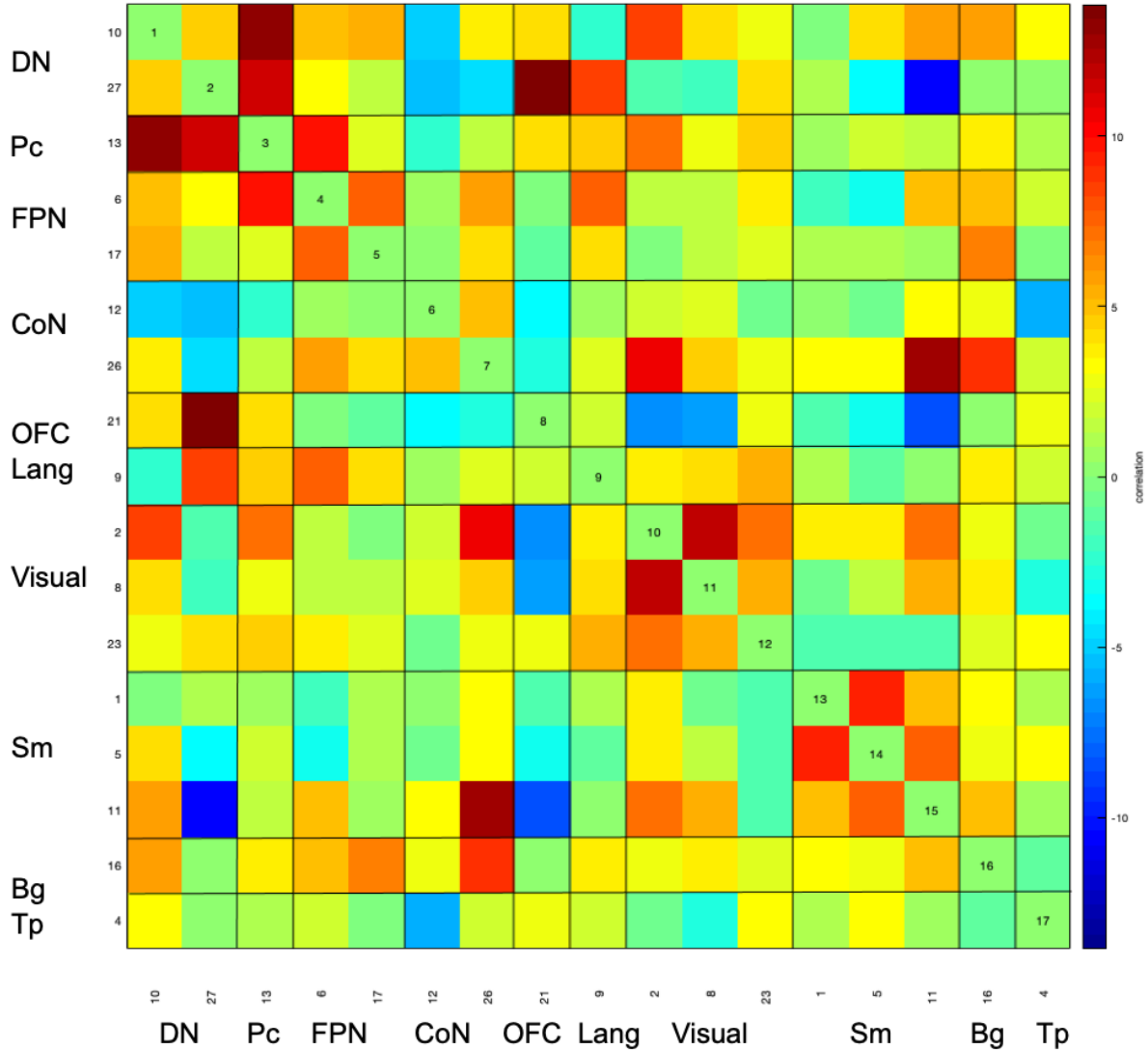


Figure 7. Functional connectivity matrix: Standardized correlation matrix between independent components (collapsing across the placebo and oxytocin sessions and levels of grief severity). DN = default network, Pc = precuneus network, FPN = frontoparietal network, CON = cingulo-opercular network, OFC = orbitofrontal/striatal network, Lang = language network, Visual = visual network, SM = sensorimotor network, Bg = basal ganglia, Tp = temporal pole. Auditory network component (IC14) not shown due to contamination with eye movement in oxytocin session data.

Static FNC

As described above, GIFT generated a 30 x 30 covariance matrix of standardized correlation coefficients, by averaging the timecourse correlation between each of the 30 components from the group ICA (of which 11 were artifacts) and every other component. In this study, I focused on the components relevant to my hypothetical model: DN_{retrosplenial} (IC10), DN_{Core} (IC27), cingulo-opercular network (IC12, IC26), and frontoparietal network (IC6, IC17). Between-component functional connectivity was calculated from Pearson correlations of the IC time courses.

In order to reduce the number of variables and comparisons, I further selected the ICs that were higher in quality and most representative of their large-scale network, for both the static FNC and DFNC analyses. I retained the two DN components (DN_{retrosplenial}, IC10; DN_{Core}, IC27), given that the component spatial maps suggested subnetworks associated with different functions, and these subnetworks corresponded to the parcellation outlined in my theoretical model. DN_{retrosplenial} appeared to map most closely to the medial temporal lobe subnetwork, while DN_{Core} appeared to map most closely to the midline core subnetwork. For the salience network, I chose the cingulo-opercular network component centered on the dACC (CoN_{dACC}, IC26), given that IC12 had more high-frequency noise as evidenced by a lower f/ALFF. For the frontoparietal network, I chose the component centered on the right inferior parietal lobule (IC6), because the group spatial map for IC17 indicated some obvious residual eye movement-related artifact. There did not appear to be a component that clearly corresponded to the dorsal attention network. This left six IC pairs:

Within-network connectivity:

- DN_{retrosplenial} & DN_{Core} (IC10-IC27)

Between-network connectivity:

- $DN_{\text{retrosplenial}}$ & CoN_{dACC} (IC10-IC26)
- $DN_{\text{retrosplenial}}$ & FPN (IC10-IC6)
- DN_{Core} & CoN_{dACC} (IC27-IC26)
- DN_{Core} & FPN (IC27-IC6)
- CoN_{dACC} & FPN (IC26-IC6)

My hypotheses did not predict a particular relationship between $DN_{\text{retrosplenial}}$ and FPN in my model (**Figure 3**) so I excluded that pair, leaving five pairs for analyses.

To test the hypothesized changes in functional connectivity between resting state networks potentially implicated in complicated grief, I used multiple linear regression to predict ICG total scores from static FNC between the model-relevant IC pairs, with separate models for (1) within-network FNC and (2) between-network FNC.

Within-network model. The first model predicted grief severity from within-DN connectivity:

$DN_{\text{retrosplenial}}$ - DN_{Core} functional connectivity did not significantly predict grief severity ($b = 8.99$, $95\%CI = [-4.70 \text{ and } 22.67]$, $SE = 6.75$, $t = 1.33$, $p = 0.19$) - as reflected in the poor overall model fit, $F(1,36) = 1.77$, adjusted $R^2 = 0.02$, $p = 0.19$.

Between-network model. The second model predicted grief severity from between-network connectivity:

Functional connectivity between DN_{Core} and CoN_{dACC} components was a significant predictor of grief severity, $b = 17.02$, $95\%CI = [3.25 \text{ and } 30.79]$, $SE = 6.77$, $t = 2.51$, $p = 0.02$) above and beyond other between-network connectivity. However, the overall model fit was not significant, $F(4,33) = 2.06$, adjusted $R^2 = 0.10$, $p = 0.11$.

To further investigate this result, I tested whether DN_{Core} - CoN_{dACC} functional connectivity would predict grief severity in a model that included other variables that might contribute to grief severity: age, depression, and sex. Age and depression (BDI

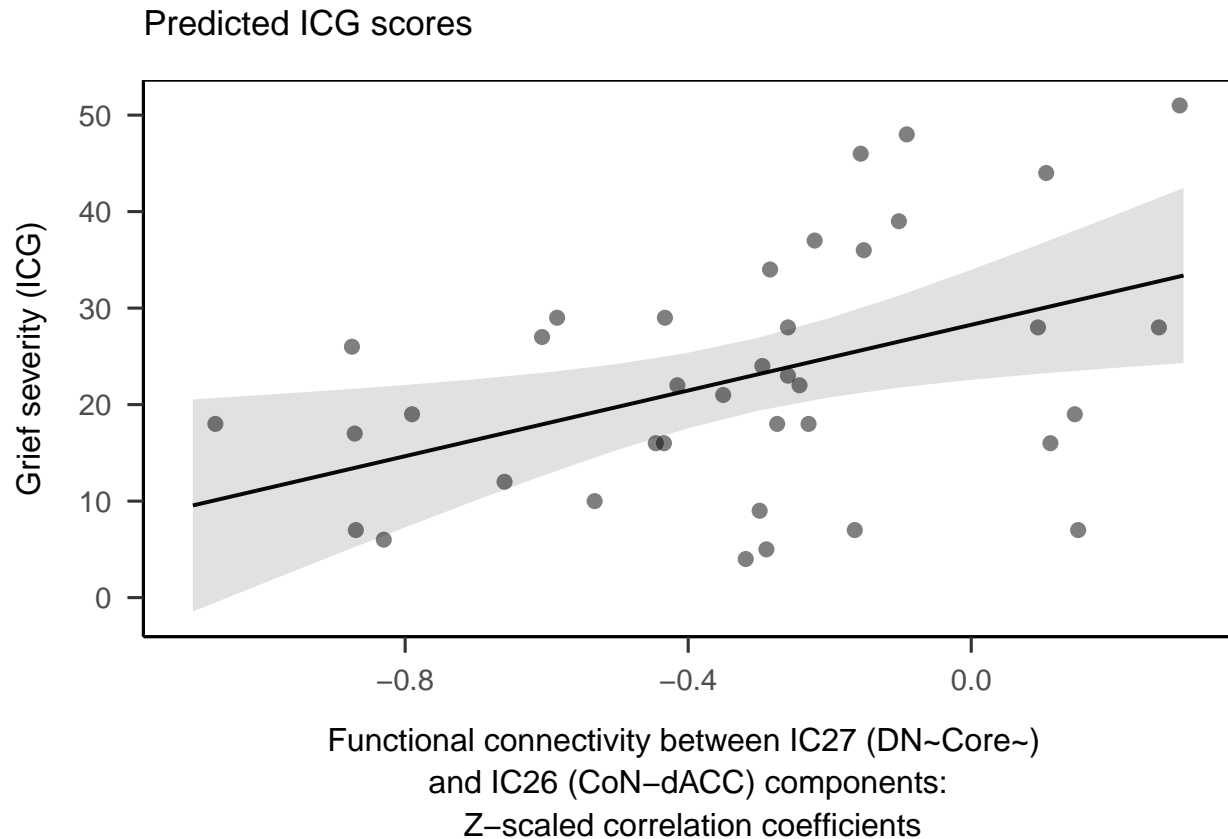


Figure 8. Grief severity scores predicted from default - cingulo-opercular network functional connectivity.

scores) were centered on the sample mean. This model did not include the non-predictive component pairs from the first model.

Functional connectivity between the DN_{Core} and CoN_{dACC} components remained a significant predictor of grief severity when age, sex, and depressive symptoms score were included as covariates in the model ($b = 8.48$, $95\%CI = [0.74 \text{ and } 16.21]$, $SE = 3.800$, $t = 2.23$, $p = 0.03$). Depressive symptoms and sex did significantly predict ICG scores, but age did not. The overall model explained 63% of the variance in grief severity ($F(4,33) = 16.76$, adjusted $R^2 = 0.63$, $p = 0.00$ ($<.001$) (**Figure 8**).

Effects of oxytocin. In order to identify whether intranasal oxytocin affected cingulo-opercular network functional connectivity with other networks implicated in the model (i.e., $DN_{retrosplenial}$, DN_{Core} , FPN), with grief severity as a potential moderator, I ran

three linear mixed models per component pair (estimated using REML and nloptwrap optimizer). All models included a random factor of participant.

- Model 1 included only fixed effects of grief severity and session.
- Model 2 added a fixed effect of depressive symptoms.
- Model 3 added the fixed effects of age in years and sex (as variables that could be expected to influence FNC and/or response to oxytocin).

DN_{Core} - CoN_{dACC} FNC. Grief severity (beta = 0.01, SE = 0.00, 95% CI [0.00, 0.02], $p = 0.033$) had a significant positive effect on FNC between the DN_{Core} and CoN_{dACC} components in Model 1. There was no significant effect of Session (oxytocin/placebo) nor the Grief severity x Session interaction. The model's total explanatory power (fixed + random effects) was substantial (conditional $R^2 = 0.47$), with about 10% of the variance explained by the fixed effects alone. 41% of the variance was explained by between-person differences ($ICC = .41$). Adding the fixed effects of depression severity (Model 2) or the other covariates (Model 3) negated any significant effect of grief severity on DN_{Core} - CoN_{dACC} FNC (**Table 3**) when data from oxytocin and placebo sessions were combined (unlike the results with just the placebo data).

	Model 1				Model 2				Model 3			
Coefficient	Estimate	SE	95% CI	p	Estimate	SE	95% CI	p	Estimate	SE	95% CI	p
Intercept	-0.27	0.05	-0.37 - -0.18	<0.001	-0.27	0.05	-0.37 - -0.17	<0.001	-0.27	0.06	-0.39 - -0.16	<0.001
ICG	0.01	0.00	0.00 - 0.02	0.033	0.01	0.01	-0.00 - 0.02	0.208	0.01	0.01	-0.01 - 0.02	0.296
Session	0.07	0.04	-0.02 - 0.16	0.116	0.07	0.04	-0.02 - 0.16	0.116	0.07	0.04	-0.02 - 0.16	0.116
ICG x Session	-0.00	0.00	-0.01 - 0.00	0.410	-0.00	0.00	-0.01 - 0.00	0.410	-0.00	0.00	-0.01 - 0.00	0.410
BDI					0.00	0.01	-0.02 - 0.02	0.739	0.00	0.01	-0.02 - 0.02	0.755
Age (years)									0.00	0.01	-0.01 - 0.02	0.861
Sex									0.00	0.09	-0.18 - 0.18	0.999
Random Effects	<i>1</i>	<i>2</i>	<i>3</i>									
σ^2	0.08	0.08	0.08									
τ_{00}	0.05 ID	0.06 ID	0.06 ID									
ICC	0.41	0.42	0.45									
N	38 ID	38 ID	38 ID									
Observations	76	76	76									
Marginal R2 / Conditional R2	0.099 / 0.472	0.099 / 0.482	0.096 / 0.501									

Table 3. Multilevel model results with and without covariates: DN_{Core} - CoN_{dACC} FNC

$DN_{retrosplenial}$ - CoN_{dACC} FNC. Intranasal oxytocin had a significant positive effect on $DN_{retrosplenial}$ - CoN_{dACC} FNC, beta = 0.07, SE = 0.03, 95% CI [0.02, 0.12], p = 0.008 (**Figure 9**). Grief severity had no significant effect on functional connectivity between the $DN_{retrosplenial}$ and CoN_{dACC} components in Model 1, either alone (beta = 0.00, SE = 0.00, 95% CI [0.00, 0.01], p = 0.294) or in interaction with Session. The same general pattern of results was observed when depressive symptoms and other covariates were added as fixed factors (**Table 4**), with marginally significant effects of grief severity and depressive symptoms once BDI score was added in Model 2. The first model's total explanatory power (i.e., fixed + random effects) was substantial (conditional $R^2 = 0.56$). However, less than 10% of the variance was explained by the fixed effects alone (marginal $R^2 = .06$). Adding depressive symptoms, age, and sex as covariates increased the variance explained by the fixed effects alone by about 10% (Model 3 marginal $R^2 = 0.15$). About half of the variance in $DN_{retrosplenial}$ - CoN_{dACC} FNC was explained by between-person differences (Model 1 ICC = .53).

	Model 1				Model 2				Model 3			
<i>Coefficient</i>	<i>Estimate</i>	<i>SE</i>	<i>CI</i>	<i>p</i>	<i>Estimate</i>	<i>SE</i>	<i>CI</i>	<i>p</i>	<i>Estimate</i>	<i>SE</i>	<i>CI</i>	<i>p</i>
Intercept	0.12	0.03	0.05 – 0.19	0.001	0.12	0.03	0.05 – 0.18	<0.001	0.11	0.04	0.04 – 0.19	0.003
ICG	0.00	0.00	-0.00 – 0.01	0.294	0.01	0.00	0.00 – 0.02	0.039	0.01	0.00	0.00 – 0.02	0.043
Session	0.07	0.03	0.02 – 0.12	0.008	0.07	0.03	0.02 – 0.12	0.008	0.07	0.03	0.02 – 0.12	0.008
ICG x Session	-0.00	0.00	-0.00 – 0.00	0.769	-0.00	0.00	-0.00 – 0.00	0.769	-0.00	0.00	-0.00 – 0.00	0.769
BDI					-0.01	0.01	-0.02 – 0.00	0.067	-0.01	0.01	-0.03 – 0.00	0.063
Age (years)									-0.01	0.01	-0.02 – 0.00	0.206
Sex									-0.02	0.06	-0.13 – 0.10	0.792
Random Effects												
σ^2	0.03	0.03	0.03									
τ_{00}	0.03 ID	0.03 ID	0.03 ID									
ICC	0.53	0.51	0.51									
N	38 ID	38 ID	38 ID									
Observations	76	76	76									
Marginal R2 / Conditional R2	0.063 / 0.558	0.121 / 0.565	0.147 / 0.580									

Table 4. Multilevel model results with and without covariates: $DN_{retrosplenial}$ - CoN_{dACC} FNC

FPN - CoN_{dACC} FNC. Grief severity had a very small positive effect on FPN - CoN_{dACC} FNC, beta = 0.01, SE = 0.00, 95% CI [0.00, 0.01], p = 0.26. Session had no significant effect on functional connectivity between the FPN and CoN_{dACC} components in Model 1, either alone (beta = -0.06, SE = 0.04, 95% CI [-0.14, 0.02], p = 0.115) or in interaction with grief severity. The same general pattern of results was observed when

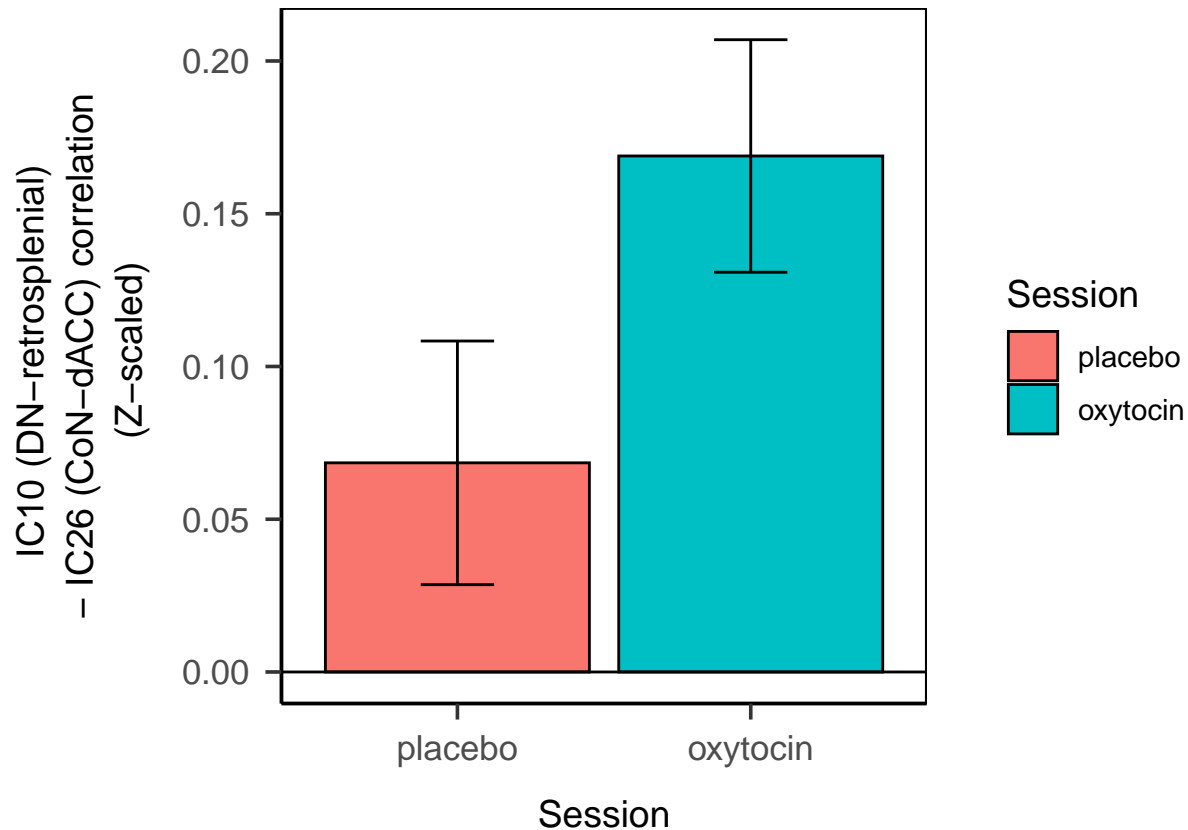


Figure 9. Intranasal oxytocin increased FNC between default and cingulo-opercular network components.

depressive symptoms were added as fixed factor, but adding age and sex reduced the effect of grief severity to a non-statistically-significant level (**Table 5**). Total explanatory power (fixed + random effects) in these models was less than in the other component models (conditional $R^2 = 0.33 - 0.40$), with approximately 12% of the variance explained by the fixed effects alone. About a quarter of the variance in FPN - CoN_{dACC} FNC was explained by between-person differences (Model 1 ICC = .24).

Within-DN FNC. Neither grief severity nor session had a significant effect on within-DN FNC, with only 3% of the model's explanatory power due to effects of the fixed factors (marginal $R^2 = 0.03$, increasing to 0.08 when all covariates were included in Model 3). There was a moderate effect of between-person variation (ICC = 0.23) (**Table 6**).

	Model 1				Model 2				Model 3			
<i>Coefficient</i>	<i>Estimate</i>	<i>SE</i>	<i>CI</i>	<i>p</i>	<i>Estimate</i>	<i>SE</i>	<i>CI</i>	<i>p</i>	<i>Estimate</i>	<i>SE</i>	<i>CI</i>	<i>p</i>
Intercept	0.19	0.04	0.12 – 0.26	<0.001	0.19	0.04	0.12 – 0.26	<0.001	0.20	0.04	0.11 – 0.28	<0.001
ICG	0.01	0.00	0.00 – 0.01	0.026	0.01	0.00	0.00 – 0.02	0.026	0.01	0.00	-0.00 – 0.02	0.074
Session	-0.06	0.04	-0.14 – 0.02	0.115	-0.06	0.04	-0.14 – 0.02	0.115	-0.06	0.04	-0.14 – 0.02	0.115
ICG x Session	0.00	0.00	-0.00 – 0.01	0.140	0.00	0.00	-0.00 – 0.01	0.140	0.00	0.00	-0.00 – 0.01	0.140
BDI					-0.01	0.01	-0.02 – 0.01	0.361	-0.01	0.01	-0.02 – 0.01	0.434
Age (years)									-0.00	0.01	-0.01 – 0.01	0.957
Sex									0.01	0.07	-0.12 – 0.15	0.859
Random Effects												
σ^2	0.06	0.06	0.06									
τ_{00}	0.02 ID	0.02 ID	0.02 ID									
ICC	0.24	0.24	0.27									
N	38 ID	38 ID	38 ID									
Observations	76	76	76									
Marginal R2 / Conditional R2	0.115 / 0.327	0.125 / 0.337	0.122 / 0.358									

Table 5. Multilevel model results with and without covariates: FPN - CoN dACC FNC

Dynamic FNC

On average, participants transitioned between states approximately eight times ($SD = 3.4$) over the course of the six-minute resting state sequence. The transition probability matrix indicated that participants were much more likely to remain in a particular state across time than to transition from a given state to a different state, as indicated by probability values $>.80$ on the diagonal but $<.20$ elsewhere in the matrix.

One-sample t tests for dynamics (vs. null) compared the median DFNC correlations in each of the four centroids to the null (**Figure 10**).

Centroid 1 (42%, or 4955 occurrences) showed relatively stable functional connectivity across component pairs, indicating that the degree of correlation between a component pair tended not to change much over time. The one-sample t test result indicated that in State 1, functional connectivity between CoN-dACC and R FPN components was significantly more variable compared to the centroid median.

Centroid 2 (17%, or 2025 occurrences) was characterized by large positive fluctuations across all component pairs, with functional connectivity between DN_{Core} and CoN_{dACC} being relatively more stable. The one-sample t test result indicated that in State 2, both $DN_{retrosplenial}$ and CoN_{dACC} showed greater positive variability in functional connectivity between with other three components compared to the centroid median.

Centroid 3 (22%, or 2557 occurrences) was characterized by relatively stable

Coefficient	Model 1				Model 2				Model 3			
	Estimate	SE	CI	p	Estimate	SE	CI	p	Estimate	SE	CI	p
Intercept	0.14	0.04	0.07 – 0.22	<0.001	0.14	0.04	0.07 – 0.22	<0.001	0.16	0.04	0.08 – 0.25	<0.001
ICG	0.00	0.00	-0.00 – 0.01	0.175	0.00	0.00	-0.00 – 0.01	0.388	0.00	0.00	-0.01 – 0.01	0.883
Session	0.02	0.04	-0.07 – 0.10	0.694	0.02	0.04	-0.07 – 0.10	0.694	0.02	0.04	-0.07 – 0.10	0.694
ICG x Session	-0.00	0.00	-0.01 – 0.01	0.664	-0.00	0.00	-0.01 – 0.01	0.664	-0.00	0.00	-0.01 – 0.01	0.664
BDI					0.00	0.01	-0.01 – 0.02	0.902	0.00	0.01	-0.01 – 0.02	0.625
Age (years)									0.01	0.01	-0.00 – 0.02	0.140
Sex									0.07	0.07	-0.07 – 0.20	0.329
Random Effects												
σ^2	0.07	0.07	0.07									
τ_{00}	0.02 ID	0.02 ID	0.02 ID									
ICC	0.23	0.25	0.23									
N	38 ID	38 ID	38 ID									
Observations	76	76	76									
Marginal R2 / Conditional R2	0.033 / 0.257	0.032 / 0.270	0.083 / 0.291									

Table 6. Multilevel model results with and without covariates: DN retrosplenial - DN Core FNC

functional connectivity between DN_{retrosplenial} and the other three components. DN_{Core} showed large negative fluctuations with CoN_{dACC} and R FPN components. CoN-dACC showed positive fluctuations with the ~R FPN.~ The one-sample t test result indicated large negative fluctuations in functional connectivity between R FPN - DN_{Core}, and large positive fluctuations between R FPN - CoN-dACC. and functional connectivity in these pairs was significantly more variable than the centroid median.

Centroid 4 (19%, or 2243 occurrences) was characterized by relatively stable functional connectivity between DN_{retrosplenial} and the other three components and large negative fluctuations in connectivity between DN_{Core} and CoN-dACC. However, in Centroid 4, functional connectivity between CoN-dACC and R FPN showed negative rather than positive fluctuations, while the DN_{Core} - R FPN pair showed positive fluctuations. The one-sample t test result indicated large negative fluctuations in DN_{Core} functional connectivity with both R FPN and CoN-dACC components, and functional connectivity in these pairs was significantly more variable than the centroid median.

Effects of oxytocin. I initially used the same analytic approach as with sFNC (linear mixed model using `lme4` with fixed effects of grief severity and session, and “participant” as a random effect). However, model fits for both mean dwell time and n transitions were singular, indicating that some dimensions of the variance-covariance matrix had been estimated as exactly zero. Complex mixed-effect models (i.e., those with a

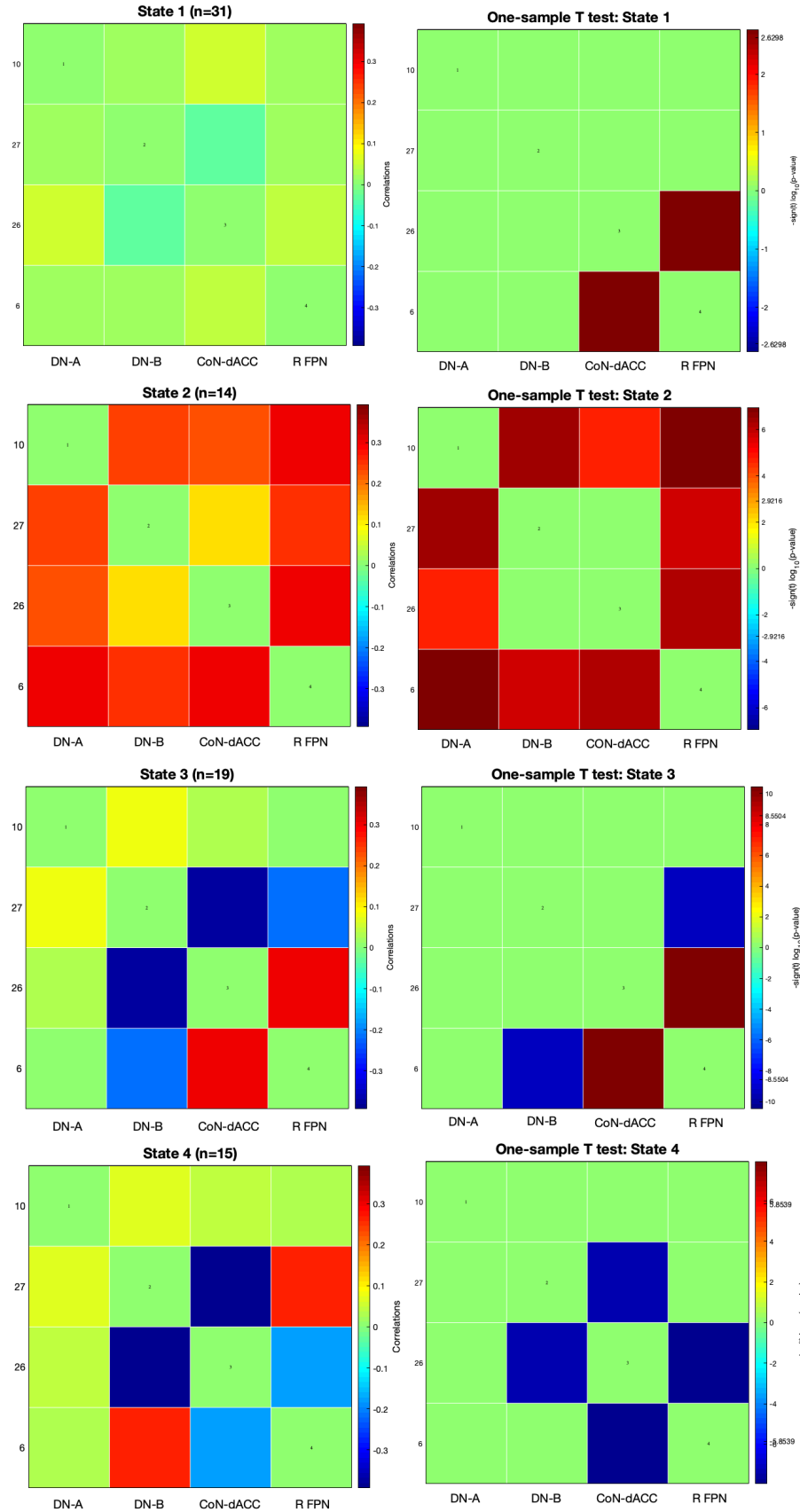


Figure 10. States identified in DFNC analyses. Note: One-sample t tests are performed on the median of DFNC correlations, using a minimum threshold of 10 windows and an FDR-corrected p.

large number of variance-covariance parameters) frequently result in singular fits, so the singular fit suggested that that I should re-run the models either without the random effect of participant or use a repeated-measures ANOVA. I opted for the latter over a regular linear regression in order to model dependency in the data resulting from multiple observations within a single participant.

Dwell time. “Dwell time” represents the mean time (n windows) that a participant remained in a given state before switching to another state. In the placebo session, participants spent an average of 19.52 ($SD = 15.86$) consecutive windows in State 1, 10.45 ($SD = 13.58$) consecutive windows in State 2, 15.74 ($SD = 12.64$) consecutive windows in State 3, and 12 ($SD = 13.38$) consecutive windows in State 4. In the oxytocin session, participants spent an average of 18.04 ($SD = 14.71$) consecutive windows in State 1, 11.99 ($SD = 15.29$) consecutive windows in State 2, 11.87 ($SD = 9.26$) consecutive windows in State 3, and 14.23 ($SD = 25.95$) consecutive windows in State 4.

I \log_{10} -transformed the dwell time variable because visual inspection of the data showed that dwell time was highly negatively skewed and kurtotic, and there were several outliers that could have driven any observed effects (skew = 3.40, kurtosis = 21.78). I added a constant of 1 to the dwell time variable in order not to have zero values for the log transformation. The n transitions variable was approximately normally distributed (skew = 0.31, kurtosis = 0.11).

The first RM-ANOVA included dwell time as a dependent variable, a between-subjects effect of grief severity, and within-subjects effects of state (#1, 2, 3, or 4) and session (placebo; oxytocin). Neither grief severity ($F(1, 35) = 0.74$, $MSE = 0.10$, $p = .396$, $\hat{\eta}_G^2 = .001$), state ($F(2.49, 87.18) = 6.77$, $MSE = 0.41$, $p = .001$, $\hat{\eta}_G^2 = .095$), nor session ($F(1, 35) = 1.72$, $MSE = 0.11$, $p = .198$, $\hat{\eta}_G^2 = .003$) predicted mean dwell time. However, there was an interaction between grief severity and state, $F(2.49, 87.18) = 6.65$, $MSE = 0.41$, $p = .001$, $\hat{\eta}_G^2 = .093$. This result held when using group (NCG vs. CG) rather than the continuous measure of grief severity for the purposes of interpreting the

Table 7. *Dynamic functional connectivity: Dwell time by Group, Session, and State*

Effect	F	df_1^{GG}	df_2^{GG}	MSE	p	$\hat{\eta}_G^2$
Group	1.21	1	35	0.10	.280	.002
Session	1.21	1	35	0.11	.280	.002
State	5.88	2.46	86.00	0.44	.002	.086
Group x Session	0.59	1	35	0.11	.448	.001
Group x State	3.87	2.46	86.00	0.44	.018	.059
Session x State	0.28	2.89	101.16	0.22	.831	.003
Group x Session x State	1.32	2.89	101.16	0.22	.272	.012

Note. Results of a repeated-measures ANOVA: higher grief severity was associated with more time spent in a state characterized by large positive fluctuations across default, cingulo-opercular, and frontoparietal network components (particularly component pairs involving the retrosplenial default network [IC10] and dACC cingulo-opercular network [IC26]). ICG = Inventory of Complicated Grief.

1178 interaction (**Table 7**). Pairwise comparisons for **group|state** interaction indicated that
 1179 participants with higher ICG scores spent more time in State 2 than participants with
 1180 lower ICG scores, ($\beta = 8.36$, $SE = 3.89$, $t(35) = 2.15$, $p = .039$ (averaged over levels of
 1181 Session) (**Figure 11**).

1182 **Number of state transitions.** The second RM-ANOVA included n transitions as
 1183 a dependent variable, between-subjects effect of grief severity, and within-subjects effect of
 1184 session (placebo; oxytocin).

1185 There were no effects of complicated grief severity or session on number of transitions
 1186 participants displayed across their scan (**Table 8**).

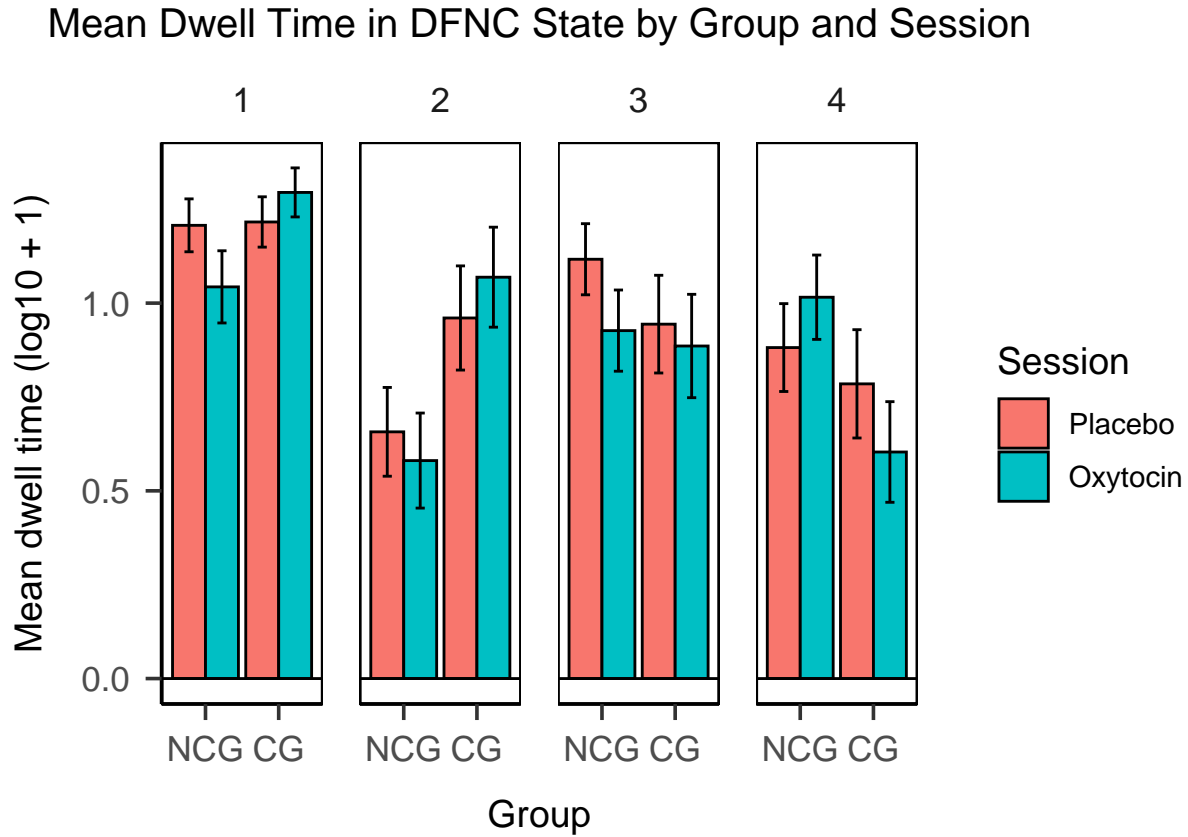


Figure 11. Mean dwell time in each DFNC state by group and session.

Table 8. *Dynamic functional connectivity: n transitions by complicated grief severity and session*

Effect	F	df_1^{GG}	df_2^{GG}	MSE	p	$\hat{\eta}_G^2$
ICG	0.53	1	36	12.95	.472	.008
Session	0.00	1	36	10.41	.972	.000
ICG x Session	1.24	1	36	10.41	.274	.015

Note. Results of a repeated-measures ANOVA: neither complicated grief severity nor oxytocin (vs. placebo) appeared to significantly affect the number of times that a participant transitioned between states over the resting state scan.

Discussion

Summary

The present study aimed to identify effects of complicated grief symptoms on large-scale brain network activity during resting state, using a data-driven approach (group ICA) for network detection. Overall, findings suggest differences in both static and time-varying, or dynamic, resting state functional connectivity, in widowed older adults experiencing higher versus lower levels of complicated grief symptoms. Results partially support my hypothesized model of how the default, cingulo-opercular/salience, and frontoparietal/executive networks may interact in a person in complicated grief (Figure 2), suggesting that brain network interactions could be associated with common internal mentation processes in people with complicated grief.

Resting state static and dynamic functional connectivity measures are associated with complicated grief symptom severity. In Aim 1, I sought to identify whether static and/or dynamic FNC in five selected independent component pairs was predictive of complicated grief symptom severity. Linear regression indicated that only static FNC between the midline core default network component and the cingulo-opercular component having its peak in the dACC was a significant predictor of complicated grief symptoms. The relationship remained statistically significant when age, sex, and depressive symptoms were added as covariates to the model. Specifically, older adults with higher complicated grief symptoms generally showed less negative (closer to zero) static FNC between default_{core} and cingulo-opercular_{dACC} network components. FNC values that are closer to zero, rather than negative, could indicate less functional segregation between default and cingulo-opercular network subsystems that are typically anticorrelated. Internal mentation may pose more of a problem for a bereaved person if it is less segregated from brain subsystems that might tag distressing emotional content as being highly relevant and requiring action. In absence of direct measures of thought content

during the resting state scan, this conclusion is speculative. However, the dynamic FNC results support the conclusion of less functional segregation between large-scale networks in complicated grief. Participants on the whole showed four “states”, corresponding to different repeated patterns of interconnectivity across time between model-relevant network components. Complicated grief severity was associated with greater time spent in the state featuring significant positive default_{retrosplenial} interconnectivity with the default_{core}, cingulo-opercular_{dACC}, and right frontoparietal components, as well as between cingulo-opercular_{dACC} and right frontoparietal components. The pattern of positive inter- and intra-network connectivity suggests that people with higher levels of complicated grief symptoms spent more time in a state of lower modularity, and may support my hypothesis that people with higher complicated grief would spend more time in a state with greater salience network involvement, particularly with the default network. However, contrary to my hypothesis that people with higher levels of complicated grief symptoms would display lower variability in mental states during the resting state scan as indicated by fewer state transitions, complicated grief severity was not associated with number of transitions between states.

Complicated grief severity does not influence resting state functional connectivity response to intranasal oxytocin. In Aim 2, I sought to identify how intranasal oxytocin influenced static and dynamic FNC in bereaved older adults. I hypothesized that for the sample as a whole, oxytocin would increase salience network interconnectivity with default_{core} and frontoparietal networks, and that complicated grief severity would moderate this effect. Contrary to my prediction based on previous behavioral findings of a group-specific increase in reaction times in the oxytocin session (Arizmendi et al., under review), there was no statistically-significant interaction between complicated grief symptom severity and session (oxytocin vs. placebo) for either static or dynamic FNC variables.

Of the component/network pairs under investigation in this study, intranasal

oxytocin only significantly increased static FNC between IC10 (default_{retrosplenial}) and IC26 (cingulo-opercular_{dACC}). The small effect of oxytocin remained statistically significant after controlling for age, sex, and depressive symptoms, but fixed effects alone explained only 15% of the variance in static FNC, with over half being explained by between-person differences not captured in the fixed effects. This suggests that unaccounted-for individual differences played a large role. Complicated grief severity emerged as a marginally-significant predictor after controlling for depressive symptoms but was clearly not a major determinant of default_{retrosplenial}—cingulo-opercular_{dACC} FNC under oxytocin as evidenced by the lack of any significant interaction effect.

For dynamic FNC, there was no significant effect of intranasal oxytocin on either dwell time or number of transitions. Visualization of the data suggested that oxytocin may have increased the magnitude of differences between complicated and non-complicated grief group participants in three out of four states' dwell time, but it should be noted that the three-way interaction for state by complicated grief severity by session was not statistically significant whether complicated grief severity was treated as a continuous or dichotomous variable. Taken together with Arizmendi et al. (n.d.) findings from the same sample, these resting state data might indicate that tasks like the one that preceded resting state are a more precise probe of complicated grief-related phenomena. Non-significant or fairly small effects of intranasal oxytocin on FNC in general could also be due to the older adult sample. For example, intranasal oxytocin significantly altered amygdala-PFC resting state FNC in younger but not older adults, likely due to age-related hormonal decreases (Ebner et al., 2016). It is also possible that the resting state sequence was not well-timed relative to intranasal oxytocin effects. There is some limited evidence for CSF levels peaking 75 minutes after a 24-IU dose (Striepens et al., 2013); alternatively, changes in regional cerebral blood flow as a result of 40-IU dose were observed from 25 to 78 minutes post-administration, peaking at 39-51 minutes (Paloyelis et al., 2016), though both of these studies involved males only (and mostly younger males).

In summary, widowed older adults with higher complicated grief symptoms spent more time in a state of lower modularity among large-scale brain networks during resting state, but did not transition between states less frequently. Intranasal oxytocin provoked a small increase in static functional connectivity between default_{retrosplenial}—cingulo-opercular_{dACC} components but oxytocin did not differentially impact participants with higher complicated grief symptoms.

Implications

It is difficult to know what mental processes are reflected by the low modularity state, but a previous study in children found that time spent in a state of positive correlations among default, salience, and central executive networks was associated with how often participants reported thinking about other people during resting state (Marusak et al., 2017). Participants in my dissertation completed a task involving photos of a stranger, their deceased spouse, and a living close loved one immediately before resting state scan. Task stimuli could have activated mental representations of others, particularly for those with higher complicated grief severity. This interpretation might fit with Schneek et al. (2019) finding that bereaved adults with an avoidant grieving style show sustained yet ineffective monitoring for mental representations of the deceased, via a frontotemporoparietal network linked to selective attention to the deceased. Recent parcellations indicate separable frontoparietal subnetworks, with subnetwork FPN_A being more closely coupled with the default network (vs. dorsal attention network) and likely involved in regulating internal thoughts and emotions (Dixon et al., 2018). Thus, right frontoparietal network involvement with default and cingulo-opercular networks seen in State 2 in this study might reflect efforts to monitor and guide internal thought. Without subjective reports of thought content during resting state, this is speculative, but it would be consistent with my hypothesis that complicated grief involves aspects of both automatic (intrusions) and deliberate (cognitive avoidance via rumination or suppression) constraints

over ongoing thought. Participants with higher grief severity scores more frequently mentioned their deceased spouse relative to other categories (e.g., living loved ones' photos, focus/effort on the task, sensory details, metacognitive thoughts) when asked in post-scan questions about what they were “thinking, feeling, and doing” during the task ($r = .44$, $p = .006$). The degree to which they mentioned their spouse vs. other topics was uncorrelated with either static default_{core}—cingulo-opercular_{dACC} FNC ($r = .07$, $p = .694$) or dwell time in State 2 ($r = .28$, $p = .10$). Therefore, I did not continue with planned but exploratory analyses testing whether spouse-related thought during the task mediated observed associations between resting state functional connectivity and complicated grief severity. The “spouse focus” variable derived from free-text post-scan reports is probably a poor index of participants' subjective experience during resting state. Mentions of the spouse were heterogeneous in content and valence, with some participants expressing sentiments of longing, depression, and disbelief, while others reported that the photos brought back happy memories and gratitude for their shared life. Others did not mention their spouse at all in their response. It is unlikely that this rough and noisy measurement based only on presence or absence of self-reported thinking about the deceased spouse during the task was a good index of complicated grief-relevant mental activity during resting state. That said, the network spatial maps that I labeled as DN and cingulo-opercular/salience network in this study show similarities to a recent fMRI ALE meta-analysis (Makovac, Fagioli, Rae, Critchley, & Ottaviani, 2020), which implicated activation in posterior and medial cingulate, anterior insula, thalamus, and mPFC areas in transdiagnostic perseverative thought, with dACC and precuneus activation distinguishing between control and clinical groups (Makovac et al., 2020).

The oxytocin-linked increase in default_{retrosplenial} – cingulo-opercular_{dACC} static FNC in this study is consistent with (Xin et al., 2018) ICA-based work that showed greater static FNC during in the oxytocin group between components identified as SN_{ACC} and ventral posterior DN, with the unthresholded spatial map for the latter closely resembling

our DN_{retrosplenial} component. Increased default_{retrosplenial} – cingulo-opercular_{dACC} static FNC could reflect the manner in which intranasal oxytocin reconfigures large-scale brain networks to facilitate socio-emotional information processing even in the absence of immediate social stimuli, like during resting state as described in my systematic review (Seeley et al., 2018). Both the retrosplenial cortex and anterior cingulate are brain structures in which OXTR mRNA is highly expressed (Quintana et al., 2019) and through which oxytocin and vasopressin (which interacts with the oxytocin system) receptor activation facilitates social cognition, learning, and behavior in humans and other species (Johnson & Young, 2017). For example, in prairie voles, infusing the ACC with an oxytocin receptor agonist reduces ACC activation and consolation behavior toward a stressed cagemate (Burkett et al., 2016), and changes in functional connectivity between the ACC and mPFC, hippocampus, retrosplenial cortex, and ventral tegmental area have been observed after pair bonding (López-Gutiérrez et al., 2019). It would be interesting to look at intranasal oxytocin and/or complicated grief symptom severity effects on the OFC/nucleus accumbens resting state network (IC21) that was unexpectedly identified through gICA, given the apparent specificity of nucleus accumbens oxytocin receptor density for pair-bonding (Walum & Young, 2018).

Limitations

Results of the study should be interpreted in the context of several limitations pertaining to methods, study design, and sample.

My model and hypotheses focused on the salience network, yet I categorized the putatively salience-related components in this study as part of the cingulo-opercular network (after receiving the helpful suggestion that it would be more accurate to define this network in terms of its anatomy since its function during resting state was unknown). Although the terms “salience network” and “cingulo-opercular network” are often used interchangeably, and both appear to be largely anchored in the dorsal ACC and anterior

insula, some researchers have argued that these are in fact distinct, though closely-located networks that serve different functions, with the salience network featuring greater paralimbic connectivity involved in bottom-up stimulus capture, whereas the cingulo-opercular network is involved in attentional switching and maintenance to facilitate cognitive control via frontoparietal network connectivity (Power et al., 2011).

Both structural and functional brain connectivity measures have been critiqued as being highly sensitive to motion and physiological artifacts that can introduce spurious fluctuations. I attempted to mitigate this possibility through my preprocessing and analysis choices, such as using ICA-AROMA (Pruim et al., 2015; Pruim, Mennes, et al., 2015), which has been shown to perform better than standard motion parameter regression, and involves less data loss than volume censoring (Parkes, Fulcher, Yücel, & Fornito, 2018).

There is considerable flexibility in fMRI processing and analysis. The GIFT toolbox in particular requires users to choose and input a number of parameters during different steps of analysis that may influence outcome. I ended up reprocessing/analyzing the group ICA data several times as I discovered that the default setting or the specific parameter I had initially selected was not optimal for my data. Reassuringly, the group ICA results appeared to yield very similar results, identifying roughly the same components and general pattern of average intercorrelations. The dFNC results were more varied according to the number and specific components that were examined. One reason for this is that estimation appears to be influenced by parameters such as sliding window length and cut-off frequency (Leonardi & Van De Ville, 2015). Although some studies describe sliding window methods as being non-optimal (Lindquist, Xu, Nebel, & Caffo, 2014), the tapered sliding window approach used in this study appears to work equally well at window lengths of 30 seconds or above (Xie et al., 2019). Additionally, most previous dFNC studies include all non-artifact independent components. This can provide more insight into what a particular state might reflect (in terms of cognition) but also appeared to increase the number of dFNC outcome variables that were correlated with mean framewise

displacement in my data. Therefore, I decided to focus only on the four components in my model ($DN_{\text{Retrosplenial}}$, DN_{core} , CoN_{dACC} , right FPN) because I suspected that including the other components was also introducing noise, based on some of their spatial maps and/or frequency distributions. However, it is possible that I made the incorrect choice and a dFNC analysis comprising all component timecourses would be more accurate or informative. For example, Liégeois et al. (2019) suggest that dFNC measures obtained from internetwork connections across all networks, rather than between or within network pairs, explains more variance in task-based behavioral phenotypes (though self-report phenotypes, such as loneliness, generally were equally well explained by static and dynamic FNC, which is relevant to this study's focus on self-reported complicated grief symptoms rather than behaviors).

Dynamic (time-varying) functional connectivity measures may suffer from undesirably low test-retest reliability (Choe et al., 2017; Zhang, Baum, Adduru, Biswal, & Michael, 2018), which is particularly relevant in the context of our repeated-measures study design. However, cortical networks, particular default and frontoparietal, do seem to be more reliable than others, particularly subcortical networks (Noble, Scheinost, & Constable, 2019). Overall, there are many outstanding questions and controversies in the field around methodological, statistical, and biological considerations in studying time-varying functional connectivity as it relates to the brain as a dynamic system (see the comprehensive overview by Lurie et al. (2020)), so my dFNC analyses in particular should be considered preliminary; suggestive rather than conclusive.

Data on participants' thoughts during resting state would have helped investigate whether observed differences were related to differences in the specific types of thought that people were engaging in during the scan. I theorized that viewing images of the deceased in the task immediately preceding resting state might activate maladaptive internal mentation typical of complicated grief in those more susceptible to engaging with those types of thoughts. However, it is equally possible that this did not occur.

Finally, there is reason to believe that these findings may not generalize to all bereaved people. The sample consisted primarily of White older adults who had experienced the death of a spouse or long-term romantic partner. The almost exclusively non-Hispanic White sample was not representative of the racial and ethnic demographics of widows in the US. For example, Black women may experience widowhood at approximately twice the rate of non-Hispanic White women (Angel, Jiménez, & Angel, 2007). The omission of their experiences in much of the bereavement literature (Granek & Peleg-Sagy, 2017) is a major restriction on our knowledge, which the present study does nothing to address. While the 72% female sample reflected the roughly 3:1 female:male ratio in the US population of widowed older adults, the issue of the small number of men in the sample was compounded by the fact that most scored above the clinical threshold on the Inventory of Complicated Grief. Age and sex both appear to influence both response to intranasal oxytocin (Ebner et al., 2016; Jiang et al., 2020) and functional connectivity (e.g., (Bluhm et al., 2008; Damoiseaux, 2017; Peper, Heuvel, Mandl, Pol, & Honk, 2011). Further, oxytocin may modulate social reward-related activity in the mesolimbic dopamine system at different doses in males vs. females (Borland, Aiani, et al., 2019; Borland et al., 2019). Therefore, results may not generalize to younger bereaved people, and results that appear specific to complicated grief could be confounded by the sex imbalance in the sample. Indeed, entering age and sex (in conjunction with depressive symptoms) as covariates did change certain results. Lastly, the small sample size ($n = 38$) prevented me from examining covariates other than age, sex, and depression (selected a priori), as I was concerned about overfitting the models by including a large number of predictors, and the study was not powered to examine multi-way interactions between main effects of interest and covariates.

Future directions

Given that the data presented here are cross-sectional and were acquired only after the death of the spouse, it is not possible to identify whether differences in static and

dynamic FNC represent trait vulnerabilities that precede the death and potentially predispose a person to engage in more maladaptive internal mentation that in turn exacerbates grief severity. An alternative possibility is that observed FNC differences reflect the instantiation of processes involved in poorer adaptation – a consequence or correlate, rather than a cause of complicated grief. Further, are the observed differences in FNC present in all bereaved people during experiences of more intense grief, or are they unique to complicated grief? Comparing FNC in bereaved people both during the acute grief phase (i.e., within 6 months of the death) and at 12 months or later. Identifying whether FNC looks the same for all people in the acute phase vs. those who are struggling to adapt after a year (the timepoint at which most grief disorders can be diagnosed) could shed some light on debates as to whether complicated grief/grief disorders represent quantitatively (normative grief symptoms that remain too intense for too long) or qualitatively distinct phenomena.

Of note, I observed marked variation between participants in grey/white matter structural integrity on their T1-MPRAGE scans: some had a surprising degree (given their lack of cognitive impairment) of grey matter atrophy, ventricular enlargement, and/or white matter lesions. It is possible that compensatory functional connectivity changes occurred in response to structural changes that were not assessed. Complicated grief symptoms have been associated with lower total brain volume in a large population-based sample (Saavedra Pérez et al., 2015). As well, older adults in a large population-based study who reported greater loneliness showed lower amygdala and hippocampal grey matter volume (Düzel et al., 2019). However, studies that specifically investigated hippocampal structure in bereaved and non-bereaved Chinese parents found that bereavement status, but not poor adaptation to the death of their only child (as measured by PTSD symptoms), was associated with smaller left hippocampal volume (Luo et al., 2017, 2016) – though these were conducted with much a smaller sample. Large-scale prospective, longitudinal studies might seek to identify structural and functional changes in

the brain associated with different trajectories of adaptation to the death of a spouse, and how bereavement-related changes might interact with normal aging processes in older adults. This could help us determine how psychosocial stressors like the death of a spouse, social isolation, and loneliness could potentially exacerbate negative physical and mental effects of aging. For example, studies in non-bereaved people show general age-related declines in network efficiency and modularity associated with cognitive impairment (Song et al., 2014), older adults with complicated grief have been found to have overall cognitive and processing speed deficits (Saavedra Pérez et al., 2015), and widowed older adults showed greater age-related memory decline compared to older adults whose spouse was still alive (Aartsen, Van Tilburg, Smits, Comijs, & Knipscheer, 2005).

Intranasal oxytocin had minimal effect in the present study. The fact that FNC between networks involved in salience and self-referential processing supports (albeit weakly) the idea that oxytocin does influence these networks. However, oxytocin still remains a viable mechanism in complicated grief. There may be some clues from prairie vole models, where we can more directly manipulate neuropeptide activity. For example, when voles were allowed to recover from a stressor in the presence of their partner, having their partner around elicited central release of oxytocin and buffered physiological and behavioral stress reactions. These effects were not observed in voles that recovered alone. When voles were treated with an oxytocin receptor agonist, there was no buffering effect of the partner's presence (Smith & Wang, 2014)). Humans also show a strong social buffering effect. One of the difficult aspects of complicated grief is that (as one of the participants in this study described), they can be surrounded by caring family and friends, and yet, nothing seems to even slightly touch the anguish of being separated from their partner. In contrast, participants who appeared to have adapted better frequently described how other relationships had strengthened since the death. Also relevant to complicated grief, Amadei et al. (2017) showed that prairie voles with greater connectivity in a mPFC-nucleus accumbens circuit demonstrated affiliative behavior (huddling) toward their partner

sooner, and pair-bond formation was accelerated when this circuit had previously been experimentally manipulated.

Conclusion

This study illustrates differences in both static and dynamic resting state functional connectivity between older adults with higher vs. lower complicated grief symptom severity. Taken together, results suggest that complicated grief symptoms are associated with reduced inter-network segregation/modularity, particularly for posterior default and anterior cingulate/salience network regions. However, network interactions were not necessarily less variable over time. Static functional connectivity between posterior default and salience network areas was greater under intranasal oxytocin, similar to an earlier group ICA study with younger non-bereaved individuals (Xin et al., 2018), but complicated grief severity did not moderate the effect of oxytocin. Findings support the hypothesis that interactions between large-scale brain networks are altered in complicated grief. Future studies should seek to establish whether functional connectivity differences in bereaved adults with higher complicated grief severity actually reflects differences in content or form of internal thought in bereaved people.

R packages/versions used

1496
 1497 R (Version 3.6.1; R Core Team, 2019) and the R-packages *afex* (Version 0.23.0;
 1498 Singmann, Bolker, Westfall, & Aust, 2019), *apaTables* (Version 2.0.5; Stanley, 2018),
 1499 *bookdown* (Version 0.17; Xie, 2016), *carData* (Version 3.0.2; J. Fox et al., 2018), *citr*
 1500 (Version 0.3.2; Aust, 2019), *corrplot2017* (Wei & Simko, 2017), *dplyr* (Version 0.8.5;
 1501 Wickham, François, Henry, & Müller, 2020), *effects* (Version 4.1.1; J. Fox & Weisberg,
 1502 2018; Fox, 2003; Fox & Hong, 2009), *emmeans* (Version 1.3.4; Lenth, 2019), *forcats*
 1503 (Version 0.4.0; Wickham, 2019a), *ggplot2* (Version 3.3.0; Wickham, 2016), *ggsignif* (Version
 1504 0.6.0; Ahlmann-Eltze, 2019), *gt* (Version 0.1.0; Iannone, Cheng, & Schloerke, 2020; Sjoberg,
 1505 Hannum, Whiting, & Zabor, 2020), *gtsummary* (Version 1.2.6; Sjoberg et al., 2020), *knitr*
 1506 (Version 1.28; Xie, 2015), *lme4* (Version 1.1.21; Bates, Mächler, Bolker, & Walker, 2015),
 1507 *lmerTest* (Version 3.1.0; Kuznetsova, Brockhoff, & Christensen, 2017), *MASS* (Version
 1508 7.3.51.4; Venables & Ripley, 2002), *Matrix* (Version 1.2.17; Bates & Maechler, 2019),
 1509 *mvtnorm* (Version 1.0.10; Genz & Bretz, 2009), *papaja* (Version 0.1.0.9942; Aust & Barth,
 1510 2020), *psych* (Version 1.8.12; Revelle, 2018), *purrr* (Version 0.3.3; Henry & Wickham,
 1511 2019), *readr* (Version 1.3.1; Wickham, Hester, & Francois, 2018), *reghelper* (Version 0.3.4;
 1512 Hughes, 2018), *sandwich* (Version 2.5.1; Zeileis, 2004, 2006), *sjmisc* (Version 2.8.3; Lüdecke,
 1513 2018), *sjPlot* (Version 2.8.3; Lüdecke, 2020), *stringr* (Version 1.4.0; Wickham, 2019b), *tibble*
 1514 (Version 2.1.3; Müller & Wickham, 2019), *tidyr* (Version 1.0.0; Wickham & Henry, 2019),
 1515 and *tidyverse* (Version 1.2.1; Wickham, 2017)

References

- Aartsen, M. J., Van Tilburg, T., Smits, C. H., Comijs, H. C., & Knipscheer, K. C. (2005). Does widowhood affect memory performance of older persons? *Psychological Medicine*, 35(2), 217–226. <https://doi.org/10.1017/S0033291704002831>
- Agnati, L. F., Guidolin, D., Guescini, M., Genedani, S., & Fuxe, K. (2010). Understanding wiring and volume transmission. <https://doi.org/10.1016/j.brainresrev.2010.03.003>
- Agnati, L. F., Zoli, M., Strömberg, I., & Fuxe, K. (1995). Inter-cellular communication in the brain: Wiring versus volume transmission. [https://doi.org/10.1016/0306-4522\(95\)00308-6](https://doi.org/10.1016/0306-4522(95)00308-6)
- Ahlmann-Eltze, C. (2019). *Ggsignif: Significance brackets for 'ggplot2'*. Retrieved from <https://CRAN.R-project.org/package=ggsignif>
- Allen, E. A., Erhardt, E. B., Damaraju, E., Gruner, W., Segall, J. M., Silva, R. F., ... Calhoun, V. D. (2011). A Baseline for the Multivariate Comparison of Resting-State Networks. *Frontiers in Systems Neuroscience*. <https://doi.org/10.3389/fnsys.2011.00002>
- Allen, E. A., Erhardt, E. B., Wei, Y., Eichele, T., & Calhoun, V. D. (2012). Capturing inter-subject variability with group independent component analysis of fMRI data: A simulation study. *NeuroImage*. <https://doi.org/10.1016/j.neuroimage.2011.10.010>
- Amadei, E. A., Johnson, Z. V., Jun Kwon, Y., Shpiner, A. C., Saravanan, V., Mays, W. D., ... Liu, R. C. (2017). Dynamic corticostriatal activity biases social bonding in monogamous female prairie voles. *Nature*. <https://doi.org/10.1038/nature22381>
- American Psychiatric Association. (2013). *Diagnostic and Statistical Manual of Mental Disorders*. American Psychiatric Association. <https://doi.org/10.1176/appi.books.9780890425596>
- Angel, J. L., Jiménez, M. A., & Angel, R. J. (2007). The economic consequences of

widowhood for older minority women. *Gerontologist*.

<https://doi.org/10.1093/geront/47.2.224>

Arizmendi, B., Seeley, S., Allen, J., Killgore, W., Andrews-Hanna, J., & O'Connor, M. (n.d.). *Feeling a pull to be close: The effect of oxytocin on approach and avoidance in complicated grief*.

Aust, F. (2019). *Citr: 'RStudio' add-in to insert markdown citations*. Retrieved from <https://CRAN.R-project.org/package=citr>

Aust, F., & Barth, M. (2020). *papaja: Create APA manuscripts with R Markdown*. Retrieved from <https://github.com/crsh/papaja>

Avants, B. B., Epstein, C. L., Grossman, M., & Gee, J. C. (2008). Symmetric diffeomorphic image registration with cross-correlation: Evaluating automated labeling of elderly and neurodegenerative brain. *Medical Image Analysis*, 12(1), 26–41. <https://doi.org/10.1016/j.media.2007.06.004>

Barrett, C. E., Arambula, S. E., & Young, L. J. (2015). The oxytocin system promotes resilience to the effects of neonatal isolation on adult social attachment in female prairie voles. *Translational Psychiatry*, 5(7), e606–e606. <https://doi.org/10.1038/tp.2015.73>

Barrett, L. F., & Satpute, A. B. (2013). Large-scale brain networks in affective and social neuroscience: towards an integrative functional architecture of the brain. *Current Opinion in Neurobiology*, 23(3), 361–372. <https://doi.org/10.1016/j.conb.2012.12.012>

Bartz, J. A., Zaki, J., Bolger, N., & Ochsner, K. N. (2011). Social effects of oxytocin in humans: Context and person matter. <https://doi.org/10.1016/j.tics.2011.05.002>

Bartz, J. A., Zaki, J., Ochsner, K. N., Bolger, N., Kolevzon, A., Ludwig, N., & Lydon, J. E. (2010). Effects of oxytocin on recollections of maternal care and closeness. *Proceedings of the National Academy of Sciences of the United States of America*.

<https://doi.org/10.1073/pnas.1012669107>

Bates, D., & Maechler, M. (2019). *Matrix: Sparse and dense matrix classes and methods*. Retrieved from <https://CRAN.R-project.org/package=Matrix>

Bates, D., Mächler, M., Bolker, B., & Walker, S. (2015). Fitting linear mixed-effects models using lme4. *Journal of Statistical Software*, 67(1), 1–48.

<https://doi.org/10.18637/jss.v067.i01>

Beaty, R. E., Benedek, M., Silvia, P. J., & Schacter, D. L. (2016). Creative Cognition and Brain Network Dynamics. <https://doi.org/10.1016/j.tics.2015.10.004>

Beaty, R. E., Chen, Q., Christensen, A. P., Qiu, J., Silvia, P. J., & Schacter, D. L. (2018). Brain networks of the imaginative mind: Dynamic functional connectivity of default and cognitive control networks relates to openness to experience. *Human Brain Mapping*. <https://doi.org/10.1002/hbm.23884>

Beck, A., Steer, R., & Brown, G. (1996). *Beck Depression Inventory-II (BDI-II)*.

Behzadi, Y., Restom, K., Liau, J., & Liu, T. T. (2007). A component based noise correction method ({CompCor}) for {BOLD} and perfusion based fMRI. *NeuroImage*, 37(1), 90–101. <https://doi.org/10.1016/j.neuroimage.2007.04.042>

Bellet, B. W., Jones, P. J., Neimeyer, R. A., & McNally, R. J. (2018). Bereavement Outcomes as Causal Systems: A Network Analysis of the Co-Occurrence of Complicated Grief and Posttraumatic Growth. *Clinical Psychological Science*, 6(6), 797–809. <https://doi.org/10.1177/2167702618777454>

Bellet, B. W., LeBlanc, N. J., Nizzi, M.-c., Carter, M. L., Does, F. H. S. van der, Peters, J., ... McNally, R. J. (2020). Identity confusion in complicated grief: A closer look. *Journal of Abnormal Psychology*, 129(4), 397–407. <https://doi.org/10.1037/abn0000520>

Bethlehem, R. A. I., Honk, J. van, Auyeung, B., Baron-Cohen, S., R.A.I., B., J., van H., ... S., B.-C. (2013). Oxytocin, brain physiology, and functional connectivity: A review

of intranasal oxytocin fMRI studies. *Psychoneuroendocrinology*, 38(7), 962–974.

<https://doi.org/10.1016/j.psyneuen.2012.10.011>

Bethlehem, R. A. I., Lombardo, M. V., Lai, M.-C., Auyeung, B., Crockford, S. K., Deakin, J., ... Baron-Cohen, S. (2017). Intranasal oxytocin enhances intrinsic corticostriatal functional connectivity in women. *Translational Psychiatry*, 7(4), e1099.

<https://doi.org/10.1038/tp.2017.72>

Bluhm, R. L., Osuch, E. A., Lanius, R. A., Boksman, K., Neufeld, R. W., Théberge, J., & Williamson, P. (2008). Default mode network connectivity: Effects of age, sex, and analytic approach. *NeuroReport*. <https://doi.org/10.1097/WNR.0b013e328300ebbf>

Boddez, Y. (2018). The presence of your absence: A conditioning theory of grief. *Behaviour Research and Therapy*, 106, 18–27. <https://doi.org/10.1016/j.brat.2018.04.006>

Boelen, P. A., Hout, M. A. van den, & Bout, J. van den. (2006). A Cognitive-Behavioral Conceptualization of Complicated Grief. *Clinical Psychology: Science and Practice*, 13(2), 109–128. <https://doi.org/10.1111/j.1468-2850.2006.00013.x>

Boelen, P. A., Huntjens, R. J., Deursen, D. S. van, & Hout, M. A. van den. (2010). Autobiographical memory specificity and symptoms of complicated grief, depression, and posttraumatic stress disorder following loss. *Journal of Behavior Therapy and Experimental Psychiatry*, 41(4), 331–337. <https://doi.org/10.1016/j.jbtep.2010.03.003>

Boelen, P. A., Keijsers, L., & Van Den Hout, M. A. (2012). The role of self-concept clarity in prolonged grief disorder. *Journal of Nervous and Mental Disease*. <https://doi.org/10.1097/NMD.0b013e31823e577f>

Boelen, P. A., & Lensvelt-Mulders, G. J. L. M. (2005). Psychometric Properties of the Grief Cognitions Questionnaire (GCQ). *Journal of Psychopathology and Behavioral Assessment*, 27(4), 291–303. <https://doi.org/10.1007/s10862-005-2409-5>

Boelen, P. A., Van Den Bout, J., & De Keijser, J. (2003). Traumatic grief as a

disorder distinct from bereavement-related depression and anxiety: A replication study with bereaved mental health care patients. *American Journal of Psychiatry*, 160(7), 1339–1341. <https://doi.org/10.1176/appi.ajp.160.7.1339>

Borland, J. M., Aiani, L. M., Norvelle, A., Grantham, K. N., O’Laughlin, K., Terranova, J. I., ... Albers, H. E. (2019). Sex-dependent regulation of social reward by oxytocin receptors in the ventral tegmental area. *Neuropsychopharmacology*. <https://doi.org/10.1038/s41386-018-0262-y>

Borland, J. M., Rilling, J. K., Frantz, K. J., & Albers, H. E. (2019). Sex-dependent regulation of social reward by oxytocin: an inverted U hypothesis. Nature Publishing Group. <https://doi.org/10.1038/s41386-018-0129-2>

Bosch, O. J., & Young, L. J. (2018). Oxytocin and social relationships: From attachment to bond disruption. In *Current topics in behavioral neurosciences*. https://doi.org/10.1007/7854_2017_10

Brodmann, K., Gruber, O., & Goya-Maldonado, R. (2017). Intranasal Oxytocin Selectively Modulates Large-Scale Brain Networks in Humans. *Brain Connectivity*, 7(7), 454–463. <https://doi.org/10.1089/brain.2017.0528>

Buckner, R. L., & DiNicola, L. M. (2019). The brain’s default network: updated anatomy, physiology and evolving insights. *Nature Reviews Neuroscience*, 20(10), 593–608. <https://doi.org/10.1038/s41583-019-0212-7>

Bui, E., Hellberg, S. N., Hoepfner, S. S., Rosencrans, P., Young, A., Ross, R. A., ... Simon, N. M. (2019). Circulating levels of oxytocin may be elevated in complicated grief: a pilot study. *European Journal of Psychotraumatology*. <https://doi.org/10.1080/20008198.2019.1646603>

Calhoun, V. D., Adali, T., Pearlson, G. D., & Pekar, J. J. (2001). A method for making group inferences from functional MRI data using independent component analysis. *Human Brain Mapping*, 14(3), 140–151. <https://doi.org/10.1002/hbm.1048>

Calhoun, V. D., Miller, R., Pearlson, G., & Adalı, T. (2014). The Chronnectome: Time-Varying Connectivity Networks as the Next Frontier in fMRI Data Discovery. *Neuron*, 84(2), 262–274. <https://doi.org/10.1016/j.neuron.2014.10.015>

Carver, C. S., & Scheier, M. F. (2000). Autonomy and self-regulation. *Psychological Inquiry*.

Cavanna, A. E., & Trimble, M. R. (2006). The precuneus: A review of its functional anatomy and behavioural correlates. Oxford University Press. <https://doi.org/10.1093/brain/awl004>

Chiang, S., Vankov, E. R., Yeh, H. J., Guindani, M., Vannucci, M., Haneef, Z., & Stern, J. M. (2018). Temporal and spectral characteristics of dynamic functional connectivity between resting-state networks reveal information beyond static connectivity. *PLoS ONE*. <https://doi.org/10.1371/journal.pone.0190220>

Choe, A. S., Nebel, M. B., Barber, A. D., Cohen, J. R., Xu, Y., Pekar, J. J., ... Lindquist, M. A. (2017). Comparing test-retest reliability of dynamic functional connectivity methods. *NeuroImage*, 158, 155–175. <https://doi.org/10.1016/J.NEUROIMAGE.2017.07.005>

Christoff, K., Irving, Z. C., Fox, K. C. R., Spreng, R. N., & Andrews-Hanna, J. R. (2016). Mind-wandering as spontaneous thought: a dynamic framework. *Nature Reviews Neuroscience*, 17(11), 718–731. <https://doi.org/10.1038/nrn.2016.113>

Cox, R. W., & Hyde, J. S. (1997). Software tools for analysis and visualization of fMRI data. *NMR in Biomedicine*, 10(4-5), 171–178. [https://doi.org/10.1002/\(SICI\)1099-1492\(199706/08\)10:4/5<171::AID-NBM453>3.0.CO;2-L](https://doi.org/10.1002/(SICI)1099-1492(199706/08)10:4/5<171::AID-NBM453>3.0.CO;2-L)

Dale, A. M., Fischl, B., & Sereno, M. I. (1999). Cortical Surface-Based Analysis: I. Segmentation and Surface Reconstruction. *NeuroImage*, 9(2), 179–194. <https://doi.org/10.1006/nimg.1998.0395>

Damoiseaux, J. S. (2017). Effects of aging on functional and structural brain connectivity. *NeuroImage*. <https://doi.org/10.1016/j.neuroimage.2017.01.077>

Demirtaş, M., Tornador, C., Falcón, C., López-Solà, M., Hernández-Ribas, R., Pujol, J., ... Deco, G. (2016). Dynamic functional connectivity reveals altered variability in functional connectivity among patients with major depressive disorder. *Human Brain Mapping, 37*(8), 2918–2930. <https://doi.org/10.1002/hbm.23215>

Dixon, M. L., De La Vega, A., Mills, C., Andrews-Hanna, J., Spreng, R. N., Cole, M. W., & Christoff, K. (2018). Heterogeneity within the frontoparietal control network and its relationship to the default and dorsal attention networks. *Proceedings of the National Academy of Sciences, 115*(7), E1598–E1607. <https://doi.org/10.1073/pnas.1715766115>

Düzel, S., Drewelies, J., Gerstorf, D., Demuth, I., Steinhagen-Thiessen, E., Lindenberger, U., & Kühn, S. (2019). Structural Brain Correlates of Loneliness among Older Adults. *Scientific Reports*. <https://doi.org/10.1038/s41598-019-49888-2>

Ebner, N. C., Chen, H., Porges, E., Lin, T., Fischer, H., Feifel, D., & Cohen, R. A. (2016). Oxytocin's effect on resting-state functional connectivity varies by age and sex. *Psychoneuroendocrinology, 69*, 50–59. <https://doi.org/10.1016/j.psyneuen.2016.03.013>

Eckstein, M., Scheele, D., Weber, K., Stoffel-Wagner, B., Maier, W., & Hurlemann, R. (2014). Oxytocin facilitates the sensation of social stress. *Human Brain Mapping*. <https://doi.org/10.1002/hbm.22508>

Ehring, T., & Watkins, E. R. (2008). Repetitive Negative Thinking as a Transdiagnostic Process. *International Journal of Cognitive Therapy, 1*(3), 192–205. <https://doi.org/10.1680/ijct.2008.1.3.192>

Eisma, M. C., Lang, T. A. de, & Boelen, P. A. (2020). How thinking hurts: Rumination, worry, and avoidance processes in adjustment to bereavement. *Clinical Psychology and Psychotherapy*. <https://doi.org/10.1002/cpp.2440>

Eisma, M. C., Schut, H. A., Stroebe, M. S., Boelen, P. A., Van Den Bout, J., & Stroebe, W. (2015). Adaptive and maladaptive rumination after loss: A three-wave longitudinal study. *British Journal of Clinical Psychology*.
<https://doi.org/10.1111/bjc.12067>

Eisma, M. C., & Stroebe, M. S. (2017). Rumination following bereavement: an overview. *Bereavement Care*, 36(2), 58–64.
<https://doi.org/10.1080/02682621.2017.1349291>

Esteban, O., Birman, D., Schaer, M., Koyejo, O. O., Poldrack, R. A., & Gorgolewski, K. J. (2017). MRIQC: Advancing the automatic prediction of image quality in MRI from unseen sites. *PLOS ONE*, 12(9), e0184661. <https://doi.org/10.1371/journal.pone.0184661>

Esteban, O., Blair, R., Markiewicz, C. J., Berleant, S. L., Moodie, C., Ma, F., ... Gorgolewski, K. J. (2018). fMRIPrep. *Software*. <https://doi.org/10.5281/zenodo.852659>

Esteban, O., Markiewicz, C. J., Blair, R. W., Moodie, C. A., Isik, A. I., Erramuzpe, A., ... Gorgolewski, K. J. (2019). fMRIPrep: a robust preprocessing pipeline for functional MRI. *Nature Methods*, 16(1), 111–116. <https://doi.org/10.1038/s41592-018-0235-4>

Etkin, A., Büchel, C., & Gross, J. J. (2015). The neural bases of emotion regulation. <https://doi.org/10.1038/nrn4044>

Farahani, F. V., Karwowski, W., & Lighthall, N. R. (2019). Application of graph theory for identifying connectivity patterns in human brain networks: A systematic review. <https://doi.org/10.3389/fnins.2019.00585>

Fonov, V. S., Evans, A. C., McKinstry, R. C., Almli, C. R., & Collins, D. L. (2009). Unbiased nonlinear average age-appropriate brain templates from birth to adulthood. *NeuroImage*, 47, Supple, S102. [https://doi.org/10.1016/S1053-8119\(09\)70884-5](https://doi.org/10.1016/S1053-8119(09)70884-5)

Fonzo, G. A., & Etkin, A. (2017). Affective neuroimaging in generalized anxiety disorder: an integrated review. *Dialogues in Clinical Neuroscience*, 19(2), 169–179.

- 1717 Retrieved from <http://www.ncbi.nlm.nih.gov/pubmed/28867941>
1718 <http://www.pubmedcentral.nih.gov/articlerender.fcgi?artid=PMC5573561>
- 1719 Fox, J. (2003). Effect displays in R for generalised linear models. *Journal of*
1720 *Statistical Software*, 8(15), 1–27. Retrieved from <http://www.jstatsoft.org/v08/i15/>
- 1721 Fox, J., & Hong, J. (2009). Effect displays in R for multinomial and
1722 proportional-odds logit models: Extensions to the effects package. *Journal of Statistical*
1723 *Software*, 32(1), 1–24. Retrieved from <http://www.jstatsoft.org/v32/i01/>
- 1724 Fox, J., & Weisberg, S. (2018). Visualizing fit and lack of fit in complex regression
1725 models with predictor effect plots and partial residuals. *Journal of Statistical Software*,
1726 87(9), 1–27. <https://doi.org/10.18637/jss.v087.i09>
- 1727 Fox, J., Weisberg, S., & Price, B. (2018). *CarData: Companion to applied regression*
1728 *data sets*. Retrieved from <https://CRAN.R-project.org/package=carData>
- 1729 Freed, P. (2007). Sadness and Loss: Toward a Neurobiopsychosocial Model.
1730 *American Journal of Psychiatry*, 164(1), 28. <https://doi.org/10.1176/appi.ajp.164.1.28>
- 1731 Freed, P. J., Yanagihara, T. K., Hirsch, J., & Mann, J. J. (2009). Neural Mechanisms
1732 of Grief Regulation. *Biological Psychiatry*, 66(1), 33–40.
1733 <https://doi.org/10.1016/j.biopsych.2009.01.019>
- 1734 Genz, A., & Bretz, F. (2009). *Computation of multivariate normal and t probabilities*.
1735 Heidelberg: Springer-Verlag.
- 1736 Gimpl, G., & Fahrenholz, F. (2001). The oxytocin receptor system: Structure,
1737 function, and regulation. <https://doi.org/10.1152/physrev.2001.81.2.629>
- 1738 Golden, A. M., Dagleish, T., & Mackintosh, B. (2007). Levels of specificity of
1739 autobiographical memories and of biographical memories of the deceased in bereaved
1740 individuals with and without complicated grief. *Journal of Abnormal Psychology*.
1741 <https://doi.org/10.1037/0021-843X.116.4.786>

Golden, A. M. J., & Dalgleish, T. (2010). Is prolonged grief distinct from bereavement-related posttraumatic stress? *Psychiatry Research*, 178(2), 336–341. <https://doi.org/10.1016/j.psychres.2009.08.021>

Gorgolewski, K., Burns, C. D., Madison, C., Clark, D., Halchenko, Y. O., Waskom, M. L., & Ghosh, S. (2011). Nipype: a flexible, lightweight and extensible neuroimaging data processing framework in Python. *Frontiers in Neuroinformatics*, 5, 13. <https://doi.org/10.3389/fninf.2011.00013>

Gorgolewski, K. J., Auer, T., Calhoun, V. D., Craddock, R. C., Das, S., Duff, E. P., ... Poldrack, R. A. (2016). The brain imaging data structure, a format for organizing and describing outputs of neuroimaging experiments. *Scientific Data*, 3, 160044. <https://doi.org/10.1038/sdata.2016.44>

Gorgolewski, K. J., Esteban, O., Markiewicz, C. J., Ziegler, E., Ellis, D. G., Notter, M. P., ... Ghosh, S. (2018). Nipype. *Software*. <https://doi.org/10.5281/zenodo.596855>

Grace, S. A., Rossell, S. L., Heinrichs, M., Kordsachia, C., & Labuschagne, I. (2018). Oxytocin and brain activity in humans: A systematic review and coordinate-based meta-analysis of functional MRI studies. <https://doi.org/10.1016/j.psyneuen.2018.05.031>

Granek, L., & Peleg-Sagy, T. (2017). The use of pathological grief outcomes in bereavement studies on African Americans. *Transcultural Psychiatry*. <https://doi.org/10.1177/1363461517708121>

Greve, D. N., & Fischl, B. (2009). Accurate and robust brain image alignment using boundary-based registration. *NeuroImage*, 48(1), 63–72. <https://doi.org/10.1016/j.neuroimage.2009.06.060>

Henry, L., & Wickham, H. (2019). *Purrr: Functional programming tools*. Retrieved from <https://CRAN.R-project.org/package=purrr>

Himberg, J., & Hyvärinen, A. (2003). ICASSO: Software for investigating the

reliability of ICA estimates by clustering and visualization. In *Neural networks for signal processing - proceedings of the ieee workshop*. <https://doi.org/10.1109/NNSP.2003.1318025>

Houwen, K. van der, Stroebe, M., Schut, H., Stroebe, W., & Bout, J. van den. (2010). Mediating processes in bereavement: The role of rumination, threatening grief interpretations, and deliberate grief avoidance. *Social Science & Medicine*, 71(9), 1669–1676. <https://doi.org/10.1016/j.socscimed.2010.06.047>

Huang, F.-Y., Hsu, A.-L., Hsu, L.-M., Tsai, J.-S., Huang, C.-M., Chao, Y.-P., ... Wu, C. W. (2019). Mindfulness Improves Emotion Regulation and Executive Control on Bereaved Individuals: An fMRI Study. *Frontiers in Human Neuroscience*. <https://doi.org/10.3389/fnhum.2018.00541>

Hughes, J. (2018). *Reghelper: Helper functions for regression analysis*. Retrieved from <https://CRAN.R-project.org/package=reghelper>

Huntenburg, J. M. (2014). *Evaluating nonlinear coregistration of {BOLD} {EPI} and T1w images* (Master's Thesis). Freie Universität, Berlin. Retrieved from <http://hdl.handle.net/11858/00-001M-0000-002B-1CB5-A>

Hurlemann, R., & Scheele, D. (2016). Dissecting the Role of Oxytocin in the Formation and Loss of Social Relationships. *Biological Psychiatry*, 79(3), 185–193. <https://doi.org/10.1016/j.biopsych.2015.05.013>

Iannone, R., Cheng, J., & Schloerke, B. (2020). *Gt: Easily create presentation-ready display tables*. Retrieved from <https://github.com/rstudio/gt>

Jenkinson, M., Bannister, P., Brady, M., & Smith, S. (2002). Improved Optimization for the Robust and Accurate Linear Registration and Motion Correction of Brain Images. *NeuroImage*, 17(2), 825–841. <https://doi.org/10.1006/nimg.2002.1132>

Jiang, X., Geng, Y., Zhao, Z., Zhou, F., Zhao, W., Yang, S., ... Kendrick, K. M. (2020). Intrinsic , dynamic and effective connectivity among large-scale brain networks

modulated by oxytocin. *bioRxiv*. <https://doi.org/10.1101/2020.04.22.055038>

Jin, C., Jia, H., Lanka, P., Rangaprakash, D., Li, L., Liu, T., ... Deshpande, G. (2017). Dynamic brain connectivity is a better predictor of PTSD than static connectivity. *Human Brain Mapping*. <https://doi.org/10.1002/hbm.23676>

Johnson, Z. V., & Young, L. J. (2017). Oxytocin and vasopressin neural networks: Implications for social behavioral diversity and translational neuroscience. *Neuroscience and Biobehavioral Reviews*, 76(Pt A), 87–98. <https://doi.org/10.1016/j.neubiorev.2017.01.034>

Kaiser, R. H., Andrews-Hanna, J. R., Wager, T. D., & Pizzagalli, D. A. (2015). Large-scale network dysfunction in major depressive disorder: A meta-analysis of resting-state functional connectivity. *JAMA Psychiatry*, 72(6), 603–611. <https://doi.org/10.1001/jamapsychiatry.2015.0071>

Kaiser, R. H., Whitfield-Gabrieli, S., Dillon, D. G., Goer, F., Beltzer, M., Minkel, J., ... Pizzagalli, D. A. (2016). Dynamic Resting-State Functional Connectivity in Major Depression. *Neuropsychopharmacology*, 41(7), 1822–1830. <https://doi.org/10.1038/npp.2015.352>

Kaplan, D. B., & Berkman, B. J. (2018). Effects of Life Transitions on the Elderly. *Merck Manual*.

Karapanagiotidis, T., Vidaurre, D., Quinn, A. J., Vatansever, D., Poerio, G. L., Jefferies, E., ... Smallwood, J. (2018). Neural dynamics at rest associated with patterns of ongoing thought. *bioRxiv*. <https://doi.org/10.1101/454371>

Kersting, A., Brähler, E., Glaesmer, H., & Wagner, B. (2011). Prevalence of complicated grief in a representative population-based sample. *Journal of Affective Disorders*. <https://doi.org/10.1016/j.jad.2010.11.032>

Klein, A., Ghosh, S. S., Bao, F. S., Giard, J., Häme, Y., Stavsky, E., ... Keshavan, A.

(2017). Mindboggling morphometry of human brains. *PLOS Computational Biology*, 13(2), e1005350. <https://doi.org/10.1371/journal.pcbi.1005350>

Kragel, P. A., & LaBar, K. S. (2016). Decoding the Nature of Emotion in the Brain. <https://doi.org/10.1016/j.tics.2016.03.011>

Kucyi, A., Tambini, A., Sadaghiani, S., Keilholz, S., & Cohen, J. R. (2018). Spontaneous cognitive processes and the behavioral validation of time-varying brain connectivity. *Network Neuroscience*, 1–57. https://doi.org/10.1162/NETN_a_00037

Kuznetsova, A., Brockhoff, P. B., & Christensen, R. H. B. (2017). lmerTest package: Tests in linear mixed effects models. *Journal of Statistical Software*, 82(13), 1–26. <https://doi.org/10.18637/jss.v082.i13>

Lanczos, C. (1964). Evaluation of Noisy Data. *Journal of the Society for Industrial and Applied Mathematics Series B Numerical Analysis*, 1(1), 76–85. <https://doi.org/10.1137/0701007>

Latham, A. E., & Prigerson, H. G. (2004). Suicidality and Bereavement: Complicated Grief as Psychiatric Disorder Presenting Greatest Risk for Suicidality. *Suicide and Life-Threatening Behavior*, 34(4).

Lenth, R. (2019). *Emmeans: Estimated marginal means, aka least-squares means*. Retrieved from <https://CRAN.R-project.org/package=emmeans>

Leonardi, N., & Van De Ville, D. (2015). On spurious and real fluctuations of dynamic functional connectivity during rest. <https://doi.org/10.1016/j.neuroimage.2014.09.007>

LeRoy, A. S., Gabert, T., Garcini, L., Murdock, K. W., Heijnen, C., & Fagundes, C. (2020). Attachment orientations and loss adjustment among bereaved spouses. *Psychoneuroendocrinology*, 112(February 2019), 104401. <https://doi.org/10.1016/j.psyneuen.2019.104401>

LeRoy, A. S., Knee, C. R., Derrick, J. L., & Fagundes, C. P. (2019). Implications for Reward Processing in Differential Responses to Loss: Impacts on Attachment Hierarchy Reorganization. *Personality and Social Psychology Review*, 23(4), 391–405.

<https://doi.org/10.1177/1088868319853895>

Li, X., Morgan, P. S., Ashburner, J., Smith, J., & Rorden, C. (2016). The first step for neuroimaging data analysis: DICOM to NIfTI conversion. *Journal of Neuroscience Methods*.

<https://doi.org/10.1016/j.jneumeth.2016.03.001>

Liégeois, R., Li, J., Kong, R., Orban, C., Van De Ville, D., Ge, T., ... Yeo, B. T. (2019). Resting brain dynamics at different timescales capture distinct aspects of human behavior. *Nature Communications*, 10(1), 2317.

<https://doi.org/10.1038/s41467-019-10317-7>

Lindquist, M. A., Xu, Y., Nebel, M. B., & Caffo, B. S. (2014). Evaluating dynamic bivariate correlations in resting-state fMRI: A comparison study and a new approach.

NeuroImage. <https://doi.org/10.1016/j.neuroimage.2014.06.052>

Liu, J. J., Taillefer, S. E., Tassone, A., & Vickers, K. (2019). The importance of bereavement cognitions on grief symptoms: Applications of cognitive processing therapy.

Death Studies, 1–11. <https://doi.org/10.1080/07481187.2019.1671537>

Liu, W., Liu, H., Wei, D., Sun, J., Yang, J., Meng, J., ... Qiu, J. (2015). Abnormal degree centrality of functional hubs associated with negative coping in older Chinese adults who lost their only child. *Biological Psychology*, 112, 46–55.

<https://doi.org/10.1016/j.biopsycho.2015.09.005>

Liu, Y., Sheng, F., Woodcock, K. A., & Han, S. (2013). Oxytocin effects on neural correlates of self-referential processing. *Biological Psychology*.

<https://doi.org/10.1016/j.biopsycho.2013.08.003>

Liu, Y., Wu, B., Wang, X., Li, W., Zhang, T., Wu, X., & Han, S. (2017). Oxytocin effects on self-referential processing: Behavioral and neuroimaging evidence. *Social*

Cognitive and Affective Neuroscience. <https://doi.org/10.1093/scan/nsx116>

Lobb, E. A., Kristjanson, L. J., Aoun, S. M., Monterosso, L., Halkett, G. K. B., & Davies, A. (2010). Predictors of Complicated Grief: A Systematic Review of Empirical Studies. *Death Studies*, 34(8), 673–698. <https://doi.org/10.1080/07481187.2010.496686>

López-Gutiérrez, M. F., Ortiz, J. J., Camacho, F. J., Young, L. J., Paredes, R. G., Diaz, N. F., ... Alcauter, S. (2019). Social bonding induces changes in brain functional connectivity in male and female monogamous voles: a longitudinal fMRI study. *bioRxiv*. <https://doi.org/10.1101/752345>

Ludwig, M., & Leng, G. (2006). Dendritic peptide release and peptide-dependent behaviours. *Nature Reviews Neuroscience*, 7(2), 126–136. <https://doi.org/10.1038/nrn1845>

Lundorff, M., Holmgren, H., Zachariae, R., Farver-Vestergaard, I., & O'Connor, M. (2017). Prevalence of prolonged grief disorder in adult bereavement: A systematic review and meta-analysis. *Journal of Affective Disorders*, 212, 138–149. <https://doi.org/10.1016/j.jad.2017.01.030>

Luo, Y., Liu, Y., Qin, Y., Zhang, X., Ma, T., Wu, W., ... Cao, Z. (2017). The atrophy and laterality of the hippocampal subfields in parents with or without posttraumatic stress disorder who lost their only child in China. *Neurological Sciences*. <https://doi.org/10.1007/s10072-017-2952-3>

Luo, Y., Shan, H., Liu, Y., Wu, L., Zhang, X., Ma, T., ... Cao, Z. (2016). Decreased left hippocampal volumes in parents with or without posttraumatic stress disorder who lost their only child in China. *Journal of Affective Disorders*. <https://doi.org/10.1016/j.jad.2016.03.003>

Lurie, D. J., Kessler, D., Bassett, D. S., Betzel, R. F., Breakspear, M., Kheilholz, S., ... Calhoun, V. D. (2020). Questions and controversies in the study of time-varying functional connectivity in resting fMRI. *Network Neuroscience*, 4(1), 30–69. https://doi.org/10.1162/netn_a_00116

- 1894 Lüdecke, D. (2018). Sjmisc: Data and variable transformation functions. *Journal of*
1895 *Open Source Software*, 3(26), 754. <https://doi.org/10.21105/joss.00754>
- 1896 Lüdecke, D. (2020). *SjPlot: Data visualization for statistics in social science*.
1897 <https://doi.org/10.5281/zenodo.1308157>
- 1898 Maccallum, F., & Bryant, R. A. (2010). Impaired autobiographical memory in
1899 complicated grief. *Behaviour Research and Therapy*.
1900 <https://doi.org/10.1016/j.brat.2009.12.006>
- 1901 Maccallum, F., & Bryant, R. A. (2013). A Cognitive Attachment Model of prolonged
1902 grief: Integrating attachments, memory, and identity. *Clinical Psychology Review*, 33(6),
1903 713–727. <https://doi.org/10.1016/j.cpr.2013.05.001>
- 1904 MacCallum, F., & Bryant, R. A. (2011). Imagining the future in Complicated Grief.
1905 <https://doi.org/10.1002/da.20866>
- 1906 MacDonald, E., Dadds, M. R., Brennan, J. L., Williams, K., Levy, F., & Cauchi, A.
1907 J. (2011). A review of safety, side-effects and subjective reactions to intranasal oxytocin in
1908 human research. *Psychoneuroendocrinology*, 36(8), 1114–1126.
1909 <https://doi.org/10.1016/j.psychneuen.2011.02.015>
- 1910 Maciejewski, P. K., Maercker, A., Boelen, P. A., & Prigerson, H. G. (2016).
1911 “Prolonged grief disorder” and “persistent complex bereavement disorder”, but not
1912 “complicated grief”, are one and the same diagnostic entity: an analysis of data from the
1913 Yale Bereavement Study. *World Psychiatry*, 15(3), 266–275.
1914 <https://doi.org/10.1002/wps.20348>
- 1915 Makovac, E., Fagioli, S., Rae, C. L., Critchley, H. D., & Ottaviani, C. (2020). Can’t
1916 get it off my brain: Meta-analysis of neuroimaging studies on perseverative cognition.
1917 *Psychiatry Research: Neuroimaging*, 295, 111020.
1918 <https://doi.org/10.1016/j.psychresns.2019.111020>

1919 Malgaroli, M., Maccallum, F., & Bonanno, G. A. (2018). Symptoms of persistent
1920 complex bereavement disorder, depression, and PTSD in a conjugally bereaved sample: A
1921 network analysis. *Psychological Medicine*. <https://doi.org/10.1017/S0033291718001769>

1922 Marlin, B. J., & Froemke, R. C. (2017). Oxytocin modulation of neural circuits for
1923 social behavior. <https://doi.org/10.1002/dneu.22452>

1924 Marusak, H. A., Calhoun, V. D., Brown, S., Crespo, L. M., Sala-Hamrick, K., Gotlib,
1925 I. H., & Thomason, M. E. (2017). Dynamic functional connectivity of neurocognitive
1926 networks in children. *Human Brain Mapping*. <https://doi.org/10.1002/hbm.23346>

1927 Marusak, H. A., Elrahal, F., Peters, C. A., Kundu, P., Lombardo, M. V., Calhoun, V.
1928 D., ... Rabinak, C. A. (2018). Mindfulness and dynamic functional neural connectivity in
1929 children and adolescents. *Behavioural Brain Research*.
1930 <https://doi.org/10.1016/j.bbr.2017.09.010>

1931 Maust, D. T., Oslin, D. W., & Marcus, S. C. (2014). Effect of age on the profile of
1932 psychotropic users: Results from the 2010 National Ambulatory Medical Care Survey.
1933 *Journal of the American Geriatrics Society*, 62(2), 358–364.
1934 <https://doi.org/10.1111/jgs.12640>

1935 McEvoy, P. M., Moulds, M. L., & Mahoney, A. E. (2013). Mechanisms driving pre-
1936 and post-stressor repetitive negative thinking: Metacognitions, cognitive avoidance, and
1937 thought control. *Journal of Behavior Therapy and Experimental Psychiatry*.
1938 <https://doi.org/10.1016/j.jbtep.2012.07.011>

1939 McLaughlin, K. A., & Nolen-Hoeksema, S. (2011). Rumination as a transdiagnostic
1940 factor in depression and anxiety. *Behaviour Research and Therapy*, 49(3), 186–193.
1941 <https://doi.org/10.1016/j.brat.2010.12.006>

1942 Mennin, D. S., & Fresco, D. M. (2013). What, Me Worry and Ruminate About
1943 DSM-5 and RDoC? The Importance of Targeting Negative Self-Referential Processing.
1944 *Clinical Psychology: Science and Practice*, 20(3), 258–267.

<https://doi.org/10.1111/cpsp.12038>

Menon, V. (2011). Large-scale brain networks and psychopathology: a unifying triple network model. *Trends in Cognitive Sciences*, 15(10), 483–506.

<https://doi.org/10.1016/J.TICS.2011.08.003>

Mikulincer, M., & Shaver, P. R. (2014). An attachment perspective on bereavement. In *Handbook of bereavement research and practice: Advances in theory and intervention*.

<https://doi.org/10.1037/14498-005>

Müller, K., & Wickham, H. (2019). *Tibble: Simple data frames*. Retrieved from <https://CRAN.R-project.org/package=tibble>

Najafi, M., McMenamin, B. W., Simon, J. Z., & Pessoa, L. (2016). Overlapping communities reveal rich structure in large-scale brain networks during rest and task conditions. *NeuroImage*, 135, 92–106. <https://doi.org/10.1016/j.neuroimage.2016.04.054>

Neimeyer, R. A. (2016). Meaning Reconstruction in the Wake of Loss: Evolution of a Research Program. *Behaviour Change*. <https://doi.org/10.1017/bec.2016.4>

Nicotera, I., Oliviero Rossi, C., Liveri, V. T., & Calandra, P. (2014). Decoupling of Dynamic Processes in Surfactant-Based Liquid Mixtures: The Case of Lithium-Containing Bis(2-ethylhexyl)phosphoric Acid/Bis(2-ethylhexyl)amine Systems. *Langmuir*, 30(28), 8336–8341. <https://doi.org/10.1021/la501744u>

Noble, S., Scheinost, D., & Constable, R. T. (2019). A decade of test-retest reliability of functional connectivity: A systematic review and meta-analysis. *NeuroImage*. <https://doi.org/10.1016/j.neuroimage.2019.116157>

O'Connor, M.-F., & Sussman, T. J. (2014). Developing the Yearning in Situations of Loss Scale: Convergent and Discriminant Validity for Bereavement, Romantic Breakup, and Homesickness. *Death Studies*, 38(7), 450–458. <https://doi.org/10.1080/07481187.2013.782928>

- 1970 O'Connor, M.-F., Wellisch, D. K., Stanton, A. L., Eisenberger, N. I., Irwin, M. R., &
1971 Lieberman, M. D. (2008). Craving love? Enduring grief activates brain's reward center.
1972 *NeuroImage*, 42(2), 969–972. <https://doi.org/10.1016/j.neuroimage.2008.04.256>
- 1973 Paloyelis, Y., Doyle, O. M., Zelaya, F. O., Maltezos, S., Williams, S. C., Fotopoulou,
1974 A., & Howard, M. A. (2016). A Spatiotemporal Profile of In Vivo Cerebral Blood Flow
1975 Changes Following Intranasal Oxytocin in Humans. *Biological Psychiatry*, 79(8), 693–705.
1976 <https://doi.org/10.1016/j.biopsych.2014.10.005>
- 1977 Parkes, L., Fulcher, B., Yücel, M., & Fornito, A. (2018). An evaluation of the efficacy,
1978 reliability, and sensitivity of motion correction strategies for resting-state functional MRI.
1979 *NeuroImage*, 171, 415–436. <https://doi.org/10.1016/j.neuroimage.2017.12.073>
- 1980 Peper, J. S., Heuvel, M. P. van den, Mandl, R. C., Pol, H. E., & Honk, J. van.
1981 (2011). Sex steroids and connectivity in the human brain: A review of neuroimaging
1982 studies. <https://doi.org/10.1016/j.psyneuen.2011.05.004>
- 1983 Pessoa, L., & McMenamin, B. (2017). Dynamic Networks in the Emotional Brain.
1984 <https://doi.org/10.1177/1073858416671936>
- 1985 Pohl, T. T., Young, L. J., & Bosch, O. J. (2018). Lost connections: Oxytocin and the
1986 neural, physiological, and behavioral consequences of disrupted relationships. *International*
1987 *Journal of Psychophysiology*. <https://doi.org/10.1016/j.ijpsycho.2017.12.011>
- 1988 Power, J. D., Cohen, A. L., Nelson, S. M., Wig, G. S., Barnes, K. A., Church, J. A.,
1989 ... Petersen, S. E. (2011). Functional Network Organization of the Human Brain. *Neuron*.
1990 <https://doi.org/10.1016/j.neuron.2011.09.006>
- 1991 Power, J. D., Mitra, A., Laumann, T. O., Snyder, A. Z., Schlaggar, B. L., & Petersen,
1992 S. E. (2014). Methods to detect, characterize, and remove motion artifact in resting state
1993 fMRI. *NeuroImage*, 84(Supplement C), 320–341.
1994 <https://doi.org/10.1016/j.neuroimage.2013.08.048>

- 1995 Prigerson, H. G., & Maciejewski, P. K. (2017). Rebuilding Consensus on Valid
1996 Criteria for Disordered Grief. *JAMA Psychiatry*, 74(5), 435.
1997 <https://doi.org/10.1001/jamapsychiatry.2017.0293>
- 1998 Prigerson, H. G., Maciejewski, P. K., Reynolds, C. F., Bierhals, A. J., Newsom, J. T.,
1999 Fasiczka, A., ... Miller, M. (1995). Inventory of complicated grief: A scale to measure
2000 maladaptive symptoms of loss. *Psychiatry Research*, 59(1-2), 65–79.
2001 [https://doi.org/10.1016/0165-1781\(95\)02757-2](https://doi.org/10.1016/0165-1781(95)02757-2)
- 2002 Prigerson, H. G. O., & Jacobs, S. C. (1999). Traumatic Grief as a Distinct Disorder:
2003 A Rationale, Consensus Criteria, and a Preliminary Empirical Test. In *Handbook of*
2004 *bereavement research: Consequences, coping, and care* (pp. 613–645). Washington:
2005 American Psychological Association. <https://doi.org/10.1037/10436-026>
- 2006 Pruim, R. H., Mennes, M., Buitelaar, J. K., & Beckmann, C. F. (2015). Evaluation of
2007 ICA-AROMA and alternative strategies for motion artifact removal in resting state fMRI.
2008 *NeuroImage*. <https://doi.org/10.1016/j.neuroimage.2015.02.063>
- 2009 Pruim, R. H., Mennes, M., Rooij, D. van, Llera, A., Buitelaar, J. K., & Beckmann, C.
2010 F. (2015). ICA-AROMA: A robust ICA-based strategy for removing motion artifacts from
2011 fMRI data. *NeuroImage*. <https://doi.org/10.1016/j.neuroimage.2015.02.064>
- 2012 Quintana, D. S., Alvares, G. A., Hickie, I. B., & Guastella, A. J. (2015). Do delivery
2013 routes of intranasally administered oxytocin account for observed effects on social cognition
2014 and behavior? A two-level model. *Neuroscience & Biobehavioral Reviews*, 49, 182–192.
2015 <https://doi.org/10.1016/j.neubiorev.2014.12.011>
- 2016 Quintana, D. S., Rokicki, J., Meer, D. van der, Alnæs, D., Kaufmann, T.,
2017 Córdova-Palomera, A., ... Westlye, L. T. (2019). Oxytocin pathway gene networks in the
2018 human brain. *Nature Communications*. <https://doi.org/10.1038/s41467-019-08503-8>
- 2019 Rachakonda, S., Egolf, E., Correa, N., Calhoun, V., & Neuropsychiatry, O. (2007).
2020 Group ICA of fMRI Toolbox (GIFT) Manual.

R Core Team. (2019). *R: A language and environment for statistical computing*. Vienna, Austria: R Foundation for Statistical Computing. Retrieved from <https://www.R-project.org/>

Reuter, M., Rosas, H. D., & Fischl, B. (2010). Highly accurate inverse consistent registration: A robust approach. *NeuroImage*, 53(4), 1181–1196. <https://doi.org/10.1016/j.neuroimage.2010.07.020>

Revelle, W. (2018). *Psych: Procedures for psychological, psychometric, and personality research*. Evanston, Illinois: Northwestern University. Retrieved from <https://CRAN.R-project.org/package=psych>

Reynolds, C. F., Cozza, S. J., & Shear, M. K. (2017). Clinically Relevant Diagnostic Criteria for a Persistent Impairing Grief Disorder. *JAMA Psychiatry*, 74(5), 433. <https://doi.org/10.1001/jamapsychiatry.2017.0290>

Robinaugh, D. J., LeBlanc, N. J., Vuletich, H. A., & McNally, R. J. (2014). Network analysis of persistent complex bereavement disorder in conjugally bereaved adults. *Journal of Abnormal Psychology*, 123(3), 510–522. <https://doi.org/10.1037/abn0000002>

Robinaugh, D. J., Mauro, C., Bui, E., Stone, L., Shah, R., Wang, Y., ... Simon, N. M. (2016). Yearning and Its Measurement in Complicated Grief. *Journal of Loss and Trauma*, 21(5), 410–420. <https://doi.org/10.1080/15325024.2015.1110447>

Robinaugh, D. J., & McNally, R. J. (2013). Remembering the past and envisioning the future in bereaved adults with and without complicated grief. *Clinical Psychological Science*. <https://doi.org/10.1177/2167702613476027>

Roweis, S. (1998). EM algorithms for PCA and SPCA. In *Advances in neural information processing systems*.

Saavedra Pérez, H. C., Ikram, M. A., Direk, N., Prigerson, H. G., Freak-Poli, R., Verhaaren, B. F. J., ... Tiemeier, H. (2015). Cognition, structural brain changes and

complicated grief. A population-based study. *Psychological Medicine*, 45(07), 1389–1399.
<https://doi.org/10.1017/S0033291714002499>

Sadino, J. M., & Donaldson, Z. R. (2018). Prairie Voles as a Model for
Understanding the Genetic and Epigenetic Regulation of Attachment Behaviors.
<https://doi.org/10.1021/acschemneuro.7b00475>

Schiele, M. A., Costa, B., Abelli, M., Martini, C., Baldwin, D. S., Domschke, K., &
Pini, S. (2018). Oxytocin receptor gene variation, behavioural inhibition, and adult
separation anxiety: Role in complicated grief. *The World Journal of Biological Psychiatry*,
19(6), 471–479. <https://doi.org/10.1080/15622975.2018.1430374>

Schiller, B., Koenig, T., & Heinrichs, M. (2019). Oxytocin modulates the temporal
dynamics of resting EEG networks. *Scientific Reports*, 9(1), 13418.
<https://doi.org/10.1038/s41598-019-49636-6>

Schneck, N., Haufe, S., Tu, T., Bonanno, G. A., Ochsner, K. N., Sajda, P., & Mann,
J. J. (2017). Tracking Deceased-Related Thinking With Neural Pattern Decoding of a
Cortical-Basal Ganglia Circuit. *Biological Psychiatry: Cognitive Neuroscience and
Neuroimaging*, 2(5), 421–429. <https://doi.org/10.1016/j.bpsc.2017.02.004>

Schneck, N., Tu, T., Haufe, S., Bonanno, G. A., Galfalvy, H., Ochsner, K. N., ...
Sajda, P. (2019). Ongoing monitoring of mindwandering in avoidant grief through
cortico-basal-ganglia interactions. *Social Cognitive and Affective Neuroscience*, 14(2),
163–172. <https://doi.org/10.1093/scan/nsy114>

Schneck, N., Tu, T., Michel, C. A., Bonanno, G. A., Sajda, P., & Mann, J. J. (2018).
Attentional Bias to Reminders of the Deceased as Compared With a Living Attachment in
Grieving. *Biological Psychiatry: Cognitive Neuroscience and Neuroimaging*, 3(2), 107–115.
<https://doi.org/10.1016/j.bpsc.2017.08.003>

Schut, Margaret Stroebe, H. (1999). The dual process model of coping with
bereavement: Rationale and description. *Death Studies*, 23(3), 197–224.

<https://doi.org/10.1080/074811899201046>

Scribner, J. L., Vance, E., Protter, D. S. W., Saslow, E., Cameron, R., Klein, E., ...
Donaldson, Z. R. (2019). A neuronal signature for monogamous reunion. *bioRxiv*.
<https://doi.org/10.1101/675959>

Seeley, S. H., Chou, Y.-h., & O'Connor, M.-F. (2018). Intranasal oxytocin and
OXTR genotype effects on resting state functional connectivity: A systematic review.
Neuroscience & Biobehavioral Reviews, 95, 17–32.
<https://doi.org/10.1016/j.neubiorev.2018.09.011>

Sha, Z., Wager, T. D., Mechelli, A., & He, Y. (2019). Common Dysfunction of
Large-Scale Neurocognitive Networks Across Psychiatric Disorders. *Biological Psychiatry*,
85(5), 379–388. <https://doi.org/10.1016/j.biopsych.2018.11.011>

Shamay-Tsoory, S. G., & Abu-Akel, A. (2016). The Social Salience Hypothesis of
Oxytocin. *Biological Psychiatry*, 79(3), 194–202.
<https://doi.org/10.1016/j.biopsych.2015.07.020>

Shear, K., Frank, E., Houck, P. R., & Reynolds, C. F. (2005). Treatment of
Complicated Grief. *JAMA*, 293(21), 2601. <https://doi.org/10.1001/jama.293.21.2601>

Shear, K., & Shair, H. (2005). Attachment, loss, and complicated grief.
Developmental Psychobiology, 47(3), 253–267. <https://doi.org/10.1002/dev.20091>

Shear, M. K., Simon, N., Wall, M., Zisook, S., Neimeyer, R., Duan, N., ... Keshaviah,
A. (2011). Complicated grief and related bereavement issues for DSM-5.
<https://doi.org/10.1002/da.20780>

Shear, M. K., Wang, Y., Skritskaya, N., Duan, N., Mauro, C., & Ghesquiere, A.
(2014). Treatment of Complicated Grief in Elderly Persons. *JAMA Psychiatry*, 71(11),
1287. <https://doi.org/10.1001/jamapsychiatry.2014.1242>

Singmann, H., Bolker, B., Westfall, J., & Aust, F. (2019). *Afex: Analysis of factorial*

- 2097 *experiments*. Retrieved from <https://CRAN.R-project.org/package=afex>
- 2098 Sjoberg, D. D., Hannum, M., Whiting, K., & Zabor, E. C. (2020). *Gtsummary:*
2099 *Presentation-ready data summary and analytic result tables*. Retrieved from
2100 <https://CRAN.R-project.org/package=gtsummary>
- 2101 Skritskaya, N. A., Mauro, C., Olonoff, M., Qiu, X., Duncan, S., Wang, Y., ... Shear,
2102 M. K. (2017). Measuring Maladaptive Cognitions in Complicated Grief: Introducing the
2103 Typical Beliefs Questionnaire. *The American Journal of Geriatric Psychiatry*, 25(5),
2104 541–550. <https://doi.org/10.1016/j.jagp.2016.09.003>
- 2105 Smith, A. S., & Wang, Z. (2014). Hypothalamic oxytocin mediates social buffering of
2106 the stress response. *Biological Psychiatry*. <https://doi.org/10.1016/j.biopsych.2013.09.017>
- 2107 Soltanian-Zadeh, S., Hossein-Zadeh, G.-A., Shahbabaie, A., & Ekhtiari, H. (2016).
2108 Investigating the relationship between subjective drug craving and temporal dynamics of
2109 the default mode network, executive control network, and salience network in
2110 methamphetamine dependents using rsfMRI. In B. Gimi & A. Krol (Eds.) (Vol. 9788, p.
2111 978826). International Society for Optics; Photonics. <https://doi.org/10.1117/12.2217214>
- 2112 Song, J., Birn, R. M., Boly, M., Meier, T. B., Nair, V. A., Meyerand, M. E., &
2113 Prabhakaran, V. (2014). Age-related reorganizational changes in modularity and
2114 functional connectivity of human brain networks. *Brain Connectivity*.
2115 <https://doi.org/10.1089/brain.2014.0286>
- 2116 Sporns, O. (2011). The human connectome: A complex network.
2117 <https://doi.org/10.1111/j.1749-6632.2010.05888.x>
- 2118 Sripada, C., Angstadt, M., Kessler, D., Phan, K. L., Liberzon, I., Evans, G. W., ...
2119 Swain, J. E. (2014). Volitional regulation of emotions produces distributed alterations in
2120 connectivity between visual, attention control, and default networks. *NeuroImage*.
2121 <https://doi.org/10.1016/j.neuroimage.2013.11.006>

2122 Stanley, D. (2018). *ApaTables: Create american psychological association (apa) style*
2123 *tables*. Retrieved from <https://CRAN.R-project.org/package=apaTables>

2124 Striepens, N., Kendrick, K. M., Hanking, V., Landgraf, R., Wüllner, U., Maier, W., &
2125 Hurlemann, R. (2013). Elevated cerebrospinal fluid and blood concentrations of oxytocin
2126 following its intranasal administration in humans. *Scientific Reports*, 3.
2127 <https://doi.org/10.1038/srep03440>

2128 Stroebe, M., Schut, H., & Boerner, K. (2010). Continuing bonds in adaptation to
2129 bereavement: Toward theoretical integration. <https://doi.org/10.1016/j.cpr.2009.11.007>

2130 Tedeschi, R. G., & Calhoun, L. G. (2004). Posttraumatic Growth: Conceptual
2131 foundations and empirical evidence. https://doi.org/10.1207/s15327965pli1501_01

2132 Topper, M., Emmelkamp, P. M., & Ehring, T. (2010). Improving prevention of
2133 depression and anxiety disorders: Repetitive negative thinking as a promising target.
2134 *Applied and Preventive Psychology*, 14(1-4), 57–71.
2135 <https://doi.org/10.1016/j.appsy.2012.03.001>

2136 Treiber, J. M., White, N. S., Steed, T. C., Bartsch, H., Holland, D., Farid, N., ...
2137 Chen, C. C. (2016). Characterization and Correction of Geometric Distortions in 814
2138 Diffusion Weighted Images. *PLOS ONE*, 11(3), e0152472.
2139 <https://doi.org/10.1371/journal.pone.0152472>

2140 Tustison, N. J., Avants, B. B., Cook, P. A., Zheng, Y., Egan, A., Yushkevich, P. A.,
2141 & Gee, J. C. (2010). N4ITK: Improved N3 Bias Correction. *IEEE Transactions on Medical*
2142 *Imaging*, 29(6), 1310–1320. <https://doi.org/10.1109/TMI.2010.2046908>

2143 US Census Bureau. (n.d.). America's Families and Living Arrangements: 2016.
2144 Retrieved from <https://www.census.gov/data/tables/2016/demo/families/cps-2016.html>

2145 Venables, W. N., & Ripley, B. D. (2002). *Modern applied statistics with s* (Fourth).
2146 New York: Springer. Retrieved from <http://www.stats.ox.ac.uk/pub/MASS4>

Walum, H., & Young, L. J. (2018). The neural mechanisms and circuitry of the pair bond. <https://doi.org/10.1038/s41583-018-0072-6>

Wang, S., Peterson, D. J., Gatenby, J. C., Li, W., Grabowski, T. J., & Madhyastha, T. M. (2017). Evaluation of Field Map and Nonlinear Registration Methods for Correction of Susceptibility Artifacts in Diffusion {MRI}. *Frontiers in Neuroinformatics*, 11. <https://doi.org/10.3389/fninf.2017.00017>

Wei, T., & Simko, V. (2017). *R package "corrplot": Visualization of a correlation matrix*. Retrieved from <https://github.com/taiyun/corrplot>

Wenn, J., O'Connor, M., Breen, L. J., & Rees, C. S. (2019). Exploratory study of metacognitive beliefs about coping processes in prolonged grief symptomatology. *Death Studies*, 43(3), 143–153. <https://doi.org/10.1080/07481187.2018.1440032>

Wickham, H. (2016). *Ggplot2: Elegant graphics for data analysis*. Springer-Verlag New York. Retrieved from <https://ggplot2.tidyverse.org>

Wickham, H. (2017). *Tidyverse: Easily install and load the 'tidyverse'*. Retrieved from <https://CRAN.R-project.org/package=tidyverse>

Wickham, H. (2019a). *Forcats: Tools for working with categorical variables (factors)*. Retrieved from <https://CRAN.R-project.org/package=forcats>

Wickham, H. (2019b). *Stringr: Simple, consistent wrappers for common string operations*. Retrieved from <https://CRAN.R-project.org/package=stringr>

Wickham, H., François, R., Henry, L., & Müller, K. (2020). *Dplyr: A grammar of data manipulation*. Retrieved from <https://CRAN.R-project.org/package=dplyr>

Wickham, H., & Henry, L. (2019). *Tidyr: Tidy messy data*. Retrieved from <https://CRAN.R-project.org/package=tidyr>

Wickham, H., Hester, J., & Francois, R. (2018). *Readr: Read rectangular text data*. Retrieved from <https://CRAN.R-project.org/package=readr>

Williams, J. L., Hardt, M. M., Henschel, A. V., & Eddinger, J. R. (2019).
Experiential avoidance moderates the association between motivational sensitivity and
prolonged grief but not posttraumatic stress symptoms. *Psychiatry Research*, 273, 336–342.
<https://doi.org/10.1016/J.PSYCHRES.2019.01.020>

Wrosch, C., Scheier, M. F., Miller, G. E., Schulz, R., & Carver, C. S. (2003).
Adaptive Self-Regulation of Unattainable Goals: Goal Disengagement, Goal
Reengagement, and Subjective Well-Being. *Personality and Social Psychology Bulletin*,
29(12), 1494–1508. <https://doi.org/10.1177/0146167203256921>

Xie, H., Zheng, C. Y., Handwerker, D. A., Bandettini, P. A., Calhoun, V. D., Mitra,
S., & Gonzalez-Castillo, J. (2019). Efficacy of different dynamic functional connectivity
methods to capture cognitively relevant information. *NeuroImage*.
<https://doi.org/10.1016/j.neuroimage.2018.12.037>

Xie, Y. (2015). *Dynamic documents with R and knitr* (2nd ed.). Boca Raton, Florida:
Chapman; Hall/CRC. Retrieved from <https://yihui.org/knitr/>

Xie, Y. (2016). *Bookdown: Authoring books and technical documents with R*
markdown. Boca Raton, Florida: Chapman; Hall/CRC. Retrieved from
<https://github.com/rstudio/bookdown>

Xin, F., Zhou, F., Zhou, X., Ma, X., Geng, Y., Zhao, W., ... Becker, B. (2018).
Oxytocin Modulates the Intrinsic Dynamics Between Attention-Related Large-Scale
Networks. *Cerebral Cortex*. <https://doi.org/10.1093/cercor/bhy295>

Xiu, D., Chow, A. Y., & Tang, S. (2020). Predictive factors for differential changes in
grief symptoms following group bereavement intervention for Chinese widowed older
adults. *Clinical Psychology and Psychotherapy*. <https://doi.org/10.1002/cpp.2425>

Yarkoni, T., Poldrack, R. A., Nichols, T. E., Van Essen, D. C., & Wager, T. D.
(2011). Large-scale automated synthesis of human functional neuroimaging data. *Nature*
Methods. <https://doi.org/10.1038/nmeth.1635>

- 2198 Yi, X., Gao, J., Wu, C., Bai, D., Li, Y., Tang, N., & Liu, X. (2018). Prevalence and
2199 risk factors of prolonged grief disorder among bereaved survivors seven years after the
2200 Wenchuan earthquake in China: A cross-sectional study. *International Journal of Nursing*
2201 *Sciences*. <https://doi.org/10.1016/j.ijnss.2018.04.001>
- 2202 Yuan, H., Phillips, R., Wong, C. K., Zotev, V., Misaki, M., Wurfel, B., ... Bodurka, J.
2203 (2018). Tracking resting state connectivity dynamics in veterans with PTSD. *NeuroImage:*
2204 *Clinical*. <https://doi.org/10.1016/j.nicl.2018.04.014>
- 2205 Zeileis, A. (2004). Econometric computing with HC and HAC covariance matrix
2206 estimators. *Journal of Statistical Software*, 11(10), 1–17.
2207 <https://doi.org/10.18637/jss.v011.i10>
- 2208 Zeileis, A. (2006). Object-oriented computation of sandwich estimators. *Journal of*
2209 *Statistical Software*, 16(9), 1–16. <https://doi.org/10.18637/jss.v016.i09>
- 2210 Zhang, C., Baum, S. A., Adduru, V. R., Biswal, B. B., & Michael, A. M. (2018).
2211 Test-retest reliability of dynamic functional connectivity in resting state fMRI.
2212 *NeuroImage*, 183, 907–918. <https://doi.org/10.1016/j.neuroimage.2018.08.021>
- 2213 Zhang, J., Cheng, W., Liu, Z., Zhang, K., Lei, X., Yao, Y., ... Feng, J. (2016). Neural,
2214 electrophysiological and anatomical basis of brain-network variability and its characteristic
2215 changes in mental disorders. *Brain*. <https://doi.org/10.1093/brain/aww143>
- 2216 Zhang, Y., Brady, M., & Smith, S. (2001). Segmentation of brain {MR} images
2217 through a hidden Markov random field model and the expectation-maximization algorithm.
2218 *IEEE Transactions on Medical Imaging*, 20(1), 45–57. <https://doi.org/10.1109/42.906424>